1. Report No. FHWA/TX-15/0-6744-2	2. Government Accession No.	3. Recipient's Catalog No.
4. Title and Subtitle HMA SHEAR RESISTANCE, PERMANENT DEFORMATION, AND RUTTING TESTS FOR TEXAS MIXES: FINAL YEAR-2 REPORT		5. Report Date Published: November 2014
		6. Performing Organization Code
7. Author(s) Lubinda F. Walubita, Abu NM Faruk, Sang I. Lee, Dung Nguyen, Raenita Hassan, and Tom Scullion		8. Performing Organization Report No. Report 0-6744-2
9. Performing Organization Name and Address Texas A&M Transportation Institute College Station, Texas 77843-3135		10. Work Unit No. (TRAIS)
		11. Contract or Grant No. Project 0-6744
12. Sponsoring Agency Name and Address Texas Department of Transportation Research and Technology Implementation Office 125 E. 11th Street Austin, Texas 78701-2483		13. Type of Report and Period Covered Technical Report: September 2012–August 2014
		14. Sponsoring Agency Code

16. Abstract

Traditionally run at one test temperature (122°F), the Hamburg wheel tracking test (HWTT) has a proven history of identifying hot mix asphalt (HMA) mixes that are moisture susceptible and/or prone to rutting. However, with the record summer temperatures of the recent years, several shear and rutting failures have occurred with HMA mixes that had passed the HWTT in the laboratory. For the most part, failures occurred in high shear locations, particularly with slow-moving traffic at controlled intersections (accelerating/decelerating), stop-go sections, elevated temperatures, heavy/high traffic loading, and where lower PG asphalt-binder grades have been used.

This two-year study was undertaken to improve the performance of the existing laboratory rutting-shear tests including the HWTT in simulating the field rutting conditions of the HMA and exploring new supplementary and/or surrogate HMA rutting/shear tests. In particular, a potential surrogate test should be able to discriminate HMA mixture performance for application in high shear stress areas (i.e., intersections) as well as discern temperature thresholds at which a given HMA mix, with a given PG asphalt-binder grade, becomes unstable and more prone to rutting and/or shear failure.

In line with these objectives, this final project report documents the research work completed in this study. Several of the existing HMA rutting-shear tests were comprehensively evaluated with special focus on the HWTT. Researchers propose several enhancements to the HWTT protocol that are expected to improve its overall performance in predicting HMA rutting susceptibility. Additionally, a new supplementary HMA shear test, namely the simple punching shear test (SPST) was developed that showed good potential to be considered as a surrogate to the HWTT.

17. Key Words HMA, Rutting, Shear, Permanent Deformation (PD), Stress, Strain, Shear Strength, Modulus, HWTT, Flow Number (FN), Dynamic Modulus (DM), Repeated Load Permanent Deformation (RLPD), Simple Punching Shear Test (SPST), Finite Element (FE)		18. Distribution Statement No restrictions. This document is available to the public through NTIS: National Technical Information Service Alexandria, Virginia 22312 http://www.ntis.gov	
19. Security Classif.(of this report) Unclassified	20. Security Classif.(of this page) Unclassified	21. No. of Pages 178	22. Price

HMA SHEAR RESISTANCE, PERMANENT DEFORMATION, AND RUTTING TESTS FOR TEXAS MIXES: FINAL YEAR-2 REPORT

By

Lubinda F. Walubita
Research Scientist
Texas A&M Transportation Institute

Abu NM Faruk
Research Associate
Texas A&M Transportation Institute

Sang Ick Lee
Assistant Transportation Researcher
Texas A&M Transportation Institute

Dung Nguyen
Student Worker I
Texas A&M Transportation Institute

Raenita Hassan
Student Worker II
Texas A&M Transportation Institute

and

Tom Scullion
Senior Research Engineer
Texas A&M Transportation Institute

DISCLAIMER

The contents of this report reflect the views of the authors, who are responsible for the facts and the accuracy of the data presented herein. The contents do not necessarily reflect the official view or policies of the Federal Highway Administration (FHWA) or the Texas Department of Transportation (TxDOT). This report does not constitute a standard, specification, or regulation, nor is it intended for construction, bidding, or permit purposes. The United States Government and the State of Texas do not endorse products or manufacturers. Trade or manufacturers' names appear herein solely because they are considered essential to the object of this report. The researcher in charge was Lubinda F. Walubita.

ACKNOWLEDGMENTS

TABLE OF CONTENTS

LIST OF FIGURES

LIST OF TABLES

LIST OF NOTATIONS AND SYMBOLS

2-D	Two-dimensional
3-D	Three-dimensional
AADTT	Average annual daily truck traffic
AASHTO	American Association of State Highway and Transportation Officials
AC	Asphalt-binder content
AMPT	Asphalt mixture performance tester
APA	Asphalt Pavement Analyzer
AR	Asphalt-rubber
APT	Accelerated pavement testing
ASTM	American Society for Testing and Materials
AV	Air voids
Avg	Average
ANOVA	Analysis of variance
CAM	Crack attenuating mixtures
COV	Coefficient of variation
CTB	Cement treated base
DOT	Department of Transportation
DM	Dynamic modulus
DR	Discriminatory ratio
FE	Finite element
fps	Foot per second (foot/sec = ft/s; where 1 fps $\cong$ 0.68 mph)
fps^2	Foot per second squared (foot/sec^2 = ft/s^2)
FN	Flow number
FSTCH	Frequency sweep test at constant height
FTW	Fort Worth District of Texas
HMA	Hot mix asphalt
HSD	Honestly significant difference
HWTT	Hamburg wheel tracking test
Hwy	Highway

IDT	Indirect tension
Lab (lab)	Laboratory (laboratory)
LTB	Lime treated base
LVDT	Linear variable displacement transducer
L-D	Load-displacement
Max	Maximum
M-E	Mechanistic-empirical
MTS	Material testing system
OAC	Optimum asphalt-binder content
OGFC	Open graded friction course
PD	Permanent deformation
PFC	Permeable (porous) friction course
PG	Performance grade
PM	Plant-mix
PVMNT	Pavement
RAP	Reclaimed asphalt pavement
RLPD	Repeated load permanent deformation test
RAS	Recycled asphalt shingles
SGC	Superpave gyratory compactor
SMA	Stone mastic (matrix) asphalt
SSE	Shear strain energy
SPST	Simple punching shear test
SPST-DL	Simple punching shear test in dynamic loading mode
SPST-ML	Simple punching shear test in monotonic loading mode
TGC	Texas Gyratory Compactor
TTI	Texas A&M Transportation Institute
TxDOT	Texas Department of Transportation
UTM (UTM-25)	Universal Testing Machine
WMA	Warm mix asphalt

CHAPTER 1   INTRODUCTION

In Texas, rutting or permanent deformation (PD) continues to be a flexible pavement failure mode of concern, particularly under heavy traffic loading under severe shear stress conditions. For assessing this rutting/PD susceptibility of hot mix asphalt (HMA) in the laboratory, currently several testing methods, e.g., Hamburg wheel tracking test (HWTT), repeated load permanent deformation test (RLPD), dynamic modulus (DM) test, are used. Among these laboratory tests, the HWTT routinely used by TxDOT, run at a single test temperature of 122°F in a water bath under TxDOT test procedure Tex-242-F, has a proven history of identifying HMA mixes that are prone to rutting and/or are susceptible to moisture damage (stripping) (TxDOT, 2009). However, with the record summer temperatures of recent years, several rutting failures have occurred with HMA mixes that had passed the HWTT in the laboratory. These failures occurred mostly in high shear locations, in particular with slow-moving (accelerating/decelerating) traffic at controlled intersections, in areas of sustained elevated temperatures, heavy/high traffic loading, and/or where lower performance grade (PG) asphalt-binder grades have been used.

In the recent years where summer pavement temperatures have been over 110°F, several TxDOT districts including Bryan have experienced severe HMA rutting and shear failures for mixes at or near the surface (i.e., SMA, CAM), particularly at intersections; yet these mixes had satisfactorily passed the HWTT in the lab. Figure 1-1 through Figure 1-3 show some examples of severe summer surface rutting, mostly at intersections.
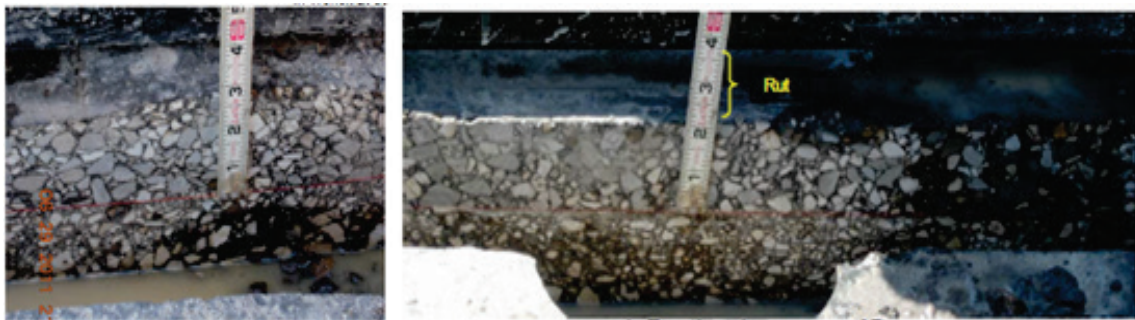
Figure 1-1. Forensic Evaluations on US 79 (Bryan District) due to Premature SMA Rutting (about 1.2 inch Surface Rutting).

Figure 1-2. Severe Surface Rutting on US 96 in Beaumont District (over 1.5 inch Rut Depth).

Figure 1-3. Surface Rutting on Anderson Street in Bryan District (over 0.5 inch Surface Rutting).

The SMA in Figure 1-1, for instance, had a measured rut depth of only 9.7 mm after 20,000 HWTT load passes at 122°F in the laboratory. Clearly, there is a need to revisit the HWTT and its associated Tex-242-F test procedure or explore other supplementary tests (TxDOT, 2009).

To address some of these problems, researchers identified a need to develop supplementary HMA shear resistance and rutting/ PD tests to run parallel with the HWTT that can be applicable for both laboratory molded and field core specimens.

RESEARCH OBJECTIVES

Based on the foregoing information and as a supplement to the HWTT, TxDOT initiated this two-year research study to develop a simple and more discriminating shear resistance and rutting/PD test to supplement the current Tex-242-F test procedure. At a minimum such a test protocol was expected to have the following characteristic features:

- Potential application for routine HMA mix design and screening of HMA mixes to be placed in high shear stress areas (i.e., intersections) as well as being an indicator of the critical temperatures at which a given HMA mix, with a given PG asphalt-binder grade, becomes unstable and more prone to rutting and/or shear failure.
- Practical, cost-effective, reasonable test duration and easy implementation by TxDOT.
- Easy sample preparation with potential to test both lab-prepared and field cores.
- Acceptable level of variation and test reliability.
- Potential to simulate and/or correlate with field rutting performance.

RESEARCH METHODOLOGY AND WORK PLANS

Improper HMA mix selection due to poor laboratory screening can lead to costly premature pavement failures. Thus, tying laboratory testing to field performance is very critical to ensure optimal performance and minimization of maintenance/rehab costs. For rutting, this is particularly critical in areas of elevated temperatures (or in summer), heavy, high-volume, slow-moving traffic with associated longer pavement loading times, and/or where lower PG binder grades are used (for cost optimization purposes, etc.).

To achieve the technical objectives of the study, the research methodology was devised to focus on three key areas, namely:

- Should the HWTT criteria be modified for mixes to be used in these critical locations?
- Can practical supplementary HMA shear resistance and rutting/PD tests be developed to address these problems? Inevitably, such new test protocols should be applicable for both laboratory molded and field core specimens.
- Can the laboratory test data analysis methods be enhanced to produce test outputs that can potentially help the designer at these critical locations?

At a minimum, the scope of work to address these aspects, over a two-year period, included the following key activities:

1. Data search and literature review.
2. Computational modeling and shear stress-strain analysis.
3. Evaluation of the existing rutting/PD tests such as the RLPD, FN, DM, etc., for possible improvements and modifications, relative to the HWTT method.
4. Comprehensive evaluation and possible modification of the HWTT method and the Tex-242-F test procedure.
5. Development of new HMA rutting-shear tests.
6. Sensitivity and statistical analyses of the test methods.
7. Correlation with field data and development of test procedures/specifications.
8. Test demonstration with a case study.

While this final report is tailored to provide a complete documentation of all the work accomplished during the whole two-year study period, primary focus will be on activities 4 through 8. The first three activities were extensively covered in the previous year-one Technical Report 0-6744-1 (Walubita et al., 2013). However, extensive additional work was done on computational modeling and shear stress-strain analysis (activity 2) during year two of this study, and the findings are presented in this final report.

REPORT CONTENTS AND ORGANIZATIONAL LAYOUT

This report consists of 10 chapters, including this one (Chapter 1) that provides the background, research objectives, methodology, and scope of work. The rest of the chapters are organized as follows:

- Chapter 2:   Experimental Design Plan and HMA Mixes Evaluated.
- Chapter 3:   The HWTT Method and Tex-242-F Test Procedure.
- Chapter 4:   The SPST Method – Conceptual Development.
- Chapter 5:   Sensitivity Evaluation – SPST and HWTT.
- Chapter 6:   Laboratory Test Correlations – SPST versus HWTT, FN, RLPD, and DM.
- Chapter 7:   FE 3-D Computational Modeling and Stress-Strain Analysis.

-
-
-

Some appendices of important data are also included at the end of the report. A CD containing video demonstration of the newly developed test methods and data analysis templates is also included as an integral part of this report.

SUMMARY

In this introductory chapter, the background and the research objectives of this project were discussed. The research methodology and scope of work were then described, followed by a summary of the project work plans. The chapter ended with a description of the report contents and the organizational layout.

CHAPTER 2   EXPERIMENTAL DESIGN PLAN AND HMA MIXES

Seven HMA mix types (Type B, C, D, F, CAM, SMA, and PFC) with over 15 different mix designs were evaluated and are discussed in this chapter. The experimental design including the test plan, HMA specimen fabrication, and air void (AV) measurements are also discussed. Researchers provide a summary of key points at the end of the chapter.

MATERIALS AND HMA MIX DESIGNS

In developing the experimental design plan, the research team considered various aspects in terms of the materials and HMA mix designs. At a minimum, the following important aspects were considered:

- Evaluate at least two commonly used Texas dense-graded mixes, with known poor and good field rutting performance, respectively, preferably a Type B (typically good rut-resistant) and CAM (poor rut-resistant) mix.
- Evaluate at least three asphalt-binder contents: optimum and optimum ± 0.5 percent.
- Evaluate at least three asphalt-binder types.
- Evaluate at least three commonly used Texas aggregate types.
- Include SMA and PFC mixes in the testing matrix.

HMA MIX TYPES

Based on the above experimental design plan, the researchers used seven HMA mix types (Type B, C, D, F, CAM, SMA, and PFC) with over 15 different mix designs, which are discussed in this report. Table 2-1 lists these mixes and includes the material type, material sources, and asphalt-binder content (AC). Where applicable, names of highways where the mix had recently been used are also indicated in the table. Detailed mix-design data for some select HMA mixes can also be found in Appendix A of this report.

In terms of usage, the selected mixes cover a reasonable geographical and climatic span of Texas, which includes the dry-cold, dry-warm, wet-cold, wet-warm, and moderate climatic regions; see Figure 2-1. HMA samples of these mixes were molded from both plant-mix and raw materials in the laboratory.

Table 2-1. Materials and Mix-Design Characteristics.

#	Mix Type	District Source	Hwy Used	Asphalt-Binder	Aggregate	Binder Content (AC)
1	Type B	Waco	IH 35	PG 64-22	Limestone + 30% RAP	4.6%
2	Type B	FTW	APT	PG 64-22	Bridgeport Rock + 30% RAP	4.2%
3	Type C	Laredo	Loop 480	PG 64-22, PG 70-22, PG 76-22	Crushed Gravel + 20% RAP	5.0%
4	Type C	Laredo	US 83	PG 64-28	Limestone + 17% RAP	4.6%
5	Type C	Bryan	SH 21	PG 64-22	Limestone + 17% RAP	4.8%
6	Type D	Houston	FM 2100	PG 64-22	Limestone/Dolomite + RAP/RAS	5.3%
7	Type D	Paris	US 277	PG 64-22	Limestone/Dolomite + 17% RAP	5.4%
8	Type D	Atlanta	US 59	PG 64-22, PG 70-22, PG 76-22	Quartzite + 20% RAP	4.7, 5.2, 5.7%
9	Type D	Chico	-	PG 64-22, PG 70-22, PG 76-22	Limestone	4.5, 5.0, 5.5%
10	Type D	Amarillo	US 54	PG 64-22	Limestone + 15% RAP + 5% RAS	6.1, 6.6, 7.1%
11	Type D	FTW	APT	PG 64-22	Bridgeport Rock	4.8%
12	Type F	Paris	US 271	PG 76-22	Sandstone	6.8%
13	CAM	Paris	SH 121	PG 64-22	Igneous/Limestone	7.0%
14	SMA	Waco	IH 35	PG 76-22	Limestone/Dolomite	6.0%
15	PFC	Paris	US 271	PG 76-22	Sandstone	6.7%
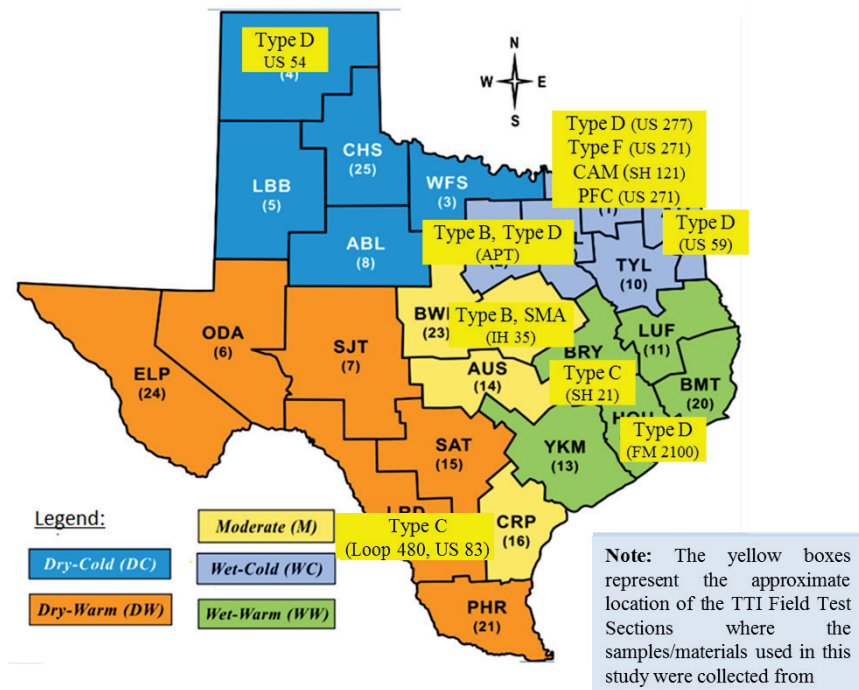
Figure 2-1. Geographical Location of Some of the HMA Mixes Used in This Study.

HMA SPECIMEN FABRICATION

In this study, HMA specimens were prepared/obtained based on the following three procedures:

- Drilled/extracted field cores (APT Type B) from the APT site.
- Prepared in the laboratory from raw materials (Loop 480 Type C, US 59 Type D, Chico Type D, and US 54 Type D).
- Prepared in the laboratory from plant-mix materials (all except APT Type B, Chico Type D, and US 54 Type D).

For the lab-molded specimens that came directly from raw materials, researchers used the HMA specimen preparation procedure consistent with the TxDOT standard specifications Tex-205-F and Tex-241-F, respectively (TxDOT, 2009). The basic procedure involved the following steps: aggregate batching, asphalt-aggregate mixing, short-term oven aging, compaction, cutting, and, finally, volumetric analysis to determine the AV. For the mixes where the asphalt-binder type (PG) was varied, researchers used the Texas gyratory compactor (TGC) method to determine the optimum asphalt-binder content (OAC) (TxDOT, 2009).

For HMA specimens prepared from plant-mix materials, the materials were sampled in accordance with the Tex-222-F procedure and then compacted following the Tex-241-F test procedure (TxDOT, 2009). Table 2-2 summarizes the HMA mixing and compaction temperatures.

Table 2-2. HMA Mixing and Compaction Temperatures.

#	Asphalt Binder Performance Grade (PG)	Mixing Temperature	Compaction Temperature
1	PG 76-22	325°F (163°C)	300°F (149°C)
2	PG 70-22	300°F (149°C)	275°F (135°C)
3	PG 64-22	290°F (143°C)	250°F (121°C)

Aggregate Batching

For fabricating the lab-molded samples directly from raw materials, the aggregates (including recycled materials, where applicable) were batched according to the mix-design sheets

(Tex-204-F) based on the Tex-205-F test procedure (TxDOT, 2005). The procedure was carefully followed so that it was consistent with the TxDOT standard specification Tex-205-F. Calculated amounts of dry aggregates for each sieve size were added to the pan, along with mineral filler and hydrated lime (where applicable), and were mixed thoroughly. The mixed aggregates were left in the oven at an appropriate mixing temperature.

Mixing and Sample Molding

Once the aggregates reached the required mixing temperature for raw materials, they were removed and placed in the mixing bowl along with the heated recycled asphalt pavement (RAP) material. Required amounts of asphalt-binder were added and were thoroughly mixed using a mechanical mixer. The mixture was placed into the oven at an appropriate compaction temperature for short-term oven aging.

HMA short-term oven aging for both lab-molded samples and plant-mix materials lasted for 2 hours at the compaction temperature consistent with the American Association of State Highway and Transportation Officials AASHTO PP2 aging procedure for Superpave mix performance testing (AASHTO, 1999). Short-term oven aging simulates the time between HMA mixing, transportation, and placement up to the time of in situ compaction in the field.

All the HMA specimens (both from plant-mix materials and raw materials) were compacted and molded using the standard Superpave gyratory compactor (SGC) according to Tex-241-F (TxDOT, 2009). All the HMA specimens were compacted to a target AV content of 7 ± 1 percent (TxDOT, 2004). All the HMA samples for HWTT and the simple punching shear test (SPST) were compacted to a height of 2.5 inches in a 6.0-inch diameter mold. For DM, FN, and RLPD testing, the HMA samples were molded to a height of 6.7 inches in the same 6.0-inch diameter molds. Thereafter, the samples were cored/cut to final test specimen dimensions measuring 6.0 inches in height by 4.0 inches in diameter.

Cutting of Specimens and AV Measurements

After molding the samples following the aforementioned procedures, the researchers used a single blade saw to obtain HWTT specimens based on the required specimen dimensions. However, for the SPST method introduced in this study, no sample cutting was necessary since the required specimen geometry is directly obtained from SGC compaction. After cutting the

HWTT specimens, researchers completed volumetric analysis based on fundamental water displacement principles as specified in ASTM D2726 to determine the exact AV content of each test specimen. HMA specimens that failed to meet AV specification (i.e., 7 ± 1 percent) were discarded.

Throughout the study, all the lab-molded specimens, from both raw and plant-mix materials, were tested within five days of molding. As discussed in subsequent chapters, this method is partly to ensure consistency and to minimize the possible effects of oxidative aging on the HMA specimens. For each mix type and mix-design variable, three replicate specimens were tested per test type per test condition. A coefficient of variation (COV) of 30 percent (i.e., COV $\leq$ 30 percent) was used as a threshold measure of repeatability and variability in the test data (Walubita et al., 2013).

SUMMARY

This chapter provided a presentation of the materials and mix designs used in this study. In total, seven HMA mix types (Type B, C, D, F, CAM, SMA, and PFC) with over 15 different mix designs were evaluated. The experimental design plan including the HMA specimen fabrication, short-term oven aging, and specimen cutting were also discussed.

CHAPTER 3 THE HWTT METHOD AND TEX-242-F TEST PROCEDURE

One of the primary goals of this project was to identify and suggest modifications to the current HWTT practice so as to better simulate the field rutting performances of the HMA. The test is run in a water bath set to 122°F (50°C) with 158-lb vertical wheel load at a speed of 50 ± 2 load passes per minute, the HWTT (Tex-242-F) has a proven history of successfully identifying and screening HMA mixes that are prone to rutting and/or are susceptible to moisture damage (stripping). However, with the record summer temperatures of recent years, several rutting failures have occurred with HMA mixes that previously had passed the HWTT in the laboratory. After a preliminary study, these researchers hypothesized that some of these field rutting problems might have been related to the following HWTT challenges and limitations:

- The current HWTT output parameters and failure criteria are based on end-of-test rutting performance and do not take into account the rutting path-history throughout the duration of the test.
- The current HWTT is run at a single test temperature (122°F) that may not be reflective of the current high summer temperature trend that often results in high pavement temperatures over 122°F, sustained for multiple hours each day, sometimes for weeks on end.
- The current HWTT is run at a single wheel speed (50 ± 2 passes/minute) that may not be reflective of some critical field conditions with slow-moving traffic at intersections.
- The current HWTT test procedure (Tex-242-F) does not specify a sitting time frame of the laboratory-molded samples (i.e., the time between sample preparation and actual testing), leaving the samples susceptible to misleading HWTT results due to inconsistent and differential sample aging.
- The test (Tex-242-F) is traditionally run at a single high air void level (i.e., 7 ± 1 percent AV) or 93 ± 1 percent density in the lab, whereas HMA mixes are often placed at a target density range of 96 to 98 percent (4 to 2 percent AV) in the field.

In an attempt to optimize the HWTT potential in identifying the critical HMA rutting/shear properties and screening mixes in the laboratory in terms of their field rutting resistance, a comprehensive sensitivity evaluation of the critical steps of the Tex-242-F test

13

procedure was conducted. As documented in this chapter, this evaluation of the current Tex-242-F (HWTT) test procedure included the following key aspects:

- Evaluation and formulation of an alternative HWTT data analysis procedure.
- Step by step sensitivity evaluation of HWTT loading configurations and the test conditions in an attempt to modify them to better simulate the field loading conditions.

The details of the study findings are discussed in this chapter.

HWTT ALTERNATE DATA ANALYSIS APPROACH

According to the Tex-242-F test procedure, the current HWTT criteria for screening mixes are based on two test outcomes, namely:

1. Maximum rut depth, Rut_{max} : HWTT rutting after 20,000 load-passes or 12.5 mm (whichever comes first).
2. Number of passes to failure, N_d : Number of load passes to reach 12.5 mm of rutting or 20,000 (whichever is smaller).

Both of these parameters are based on HMA rutting performance at the end of the test and do not consider the shape of the rutting response curve or the rutting path-history throughout the duration of the test. However, it is theoretically argued that rutting is most critical at the early life of a pavement; therefore, considering the rutting path-history throughout the duration of the HWTT should give a good indication of a mix's susceptibility to early-life rutting. Figure 3-1 presents a schematic representation of this concept.
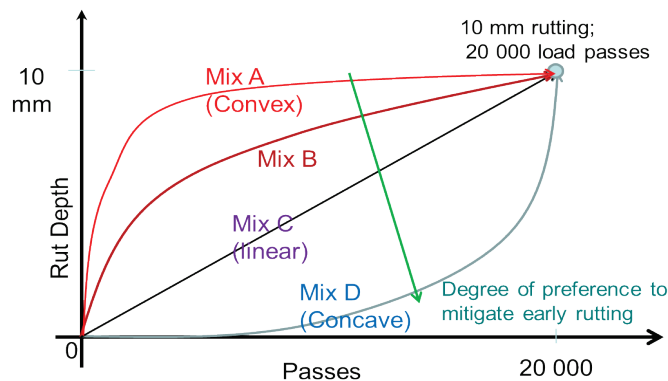
Figure 3-1. Considering the HWTT Rutting Path-History in HWTT Data Analysis.

Figure 3-1 presents HWTT *rut depth* versus *load passes* curves for four hypothetical mixes, Mixes A, B, C, and D. According to the current HWTT test procedure (Tex-242-F), all four mixes rank similarly with 10 mm rutting after 20,000 load passes. However, the rutting paths, denoted by the shape of the curves for the four mixes, are markedly different. The hypothetical Mix A has a convex shape of the HWTT rutting curve, indicating susceptibility of early-life rutting, whereas, the hypothetical Mix D has a concave rutting curve, which might be the preferred mix to mitigate early-life rutting in the field. Indeed, this hypothesis is confirmed through the comparison of field and HWTT rutting performances of two mixes, namely a Type D mix used on US 59 and a Type C mix used on Loop 480 as observed in Figure 3-2.
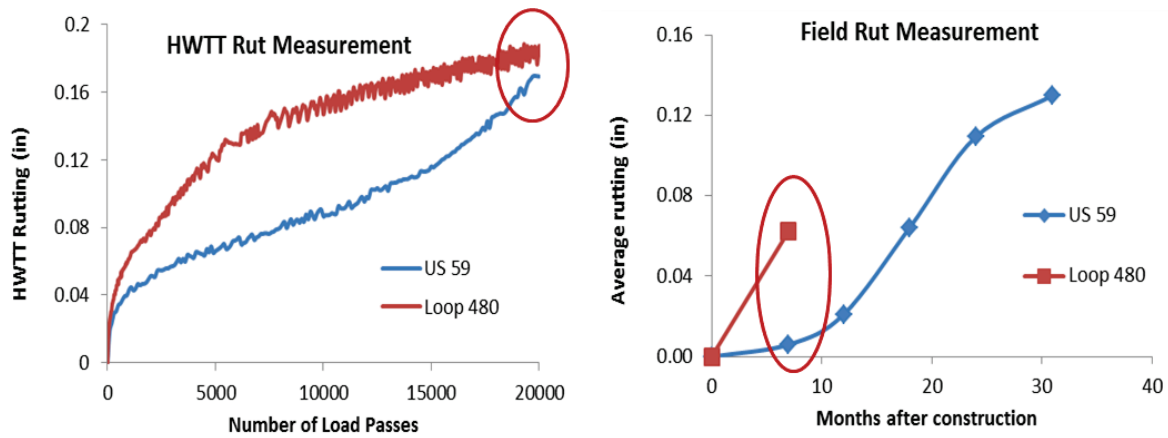
Figure 3-2. Comparing HWTT Rutting Path-History with Early-Life Field Rutting.

For the two mixes presented in Figure 3-2, the HWTT rut depth after 20,000 load passes are fairly similar (0.17 and 0.19 inches for US 59 and Loop 480, respectively). Not discounting the differences in traffic loading, environment, and pavement (PVMNT) structure, the Loop 480 mix has experienced more field rutting than US 59 after the same 7-month period of service life. Thus, it is evident that consideration of the rutting curve shape from the HWTT output can give a critical indication of a mix's susceptibility to early-life rutting in the field. In this study, the researchers have considered three parameters to characterize the curve, namely:

- The area under the rutting curve, Δ.

- The normalized rutting area, Rut_Δ.

- The shape factor, SF.

    Figure 3-3 describes these parameters graphically.
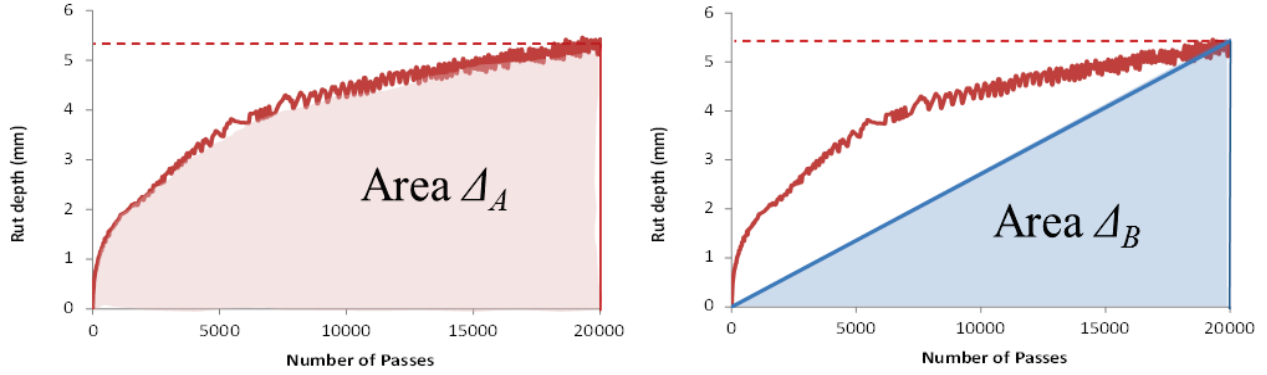
Figure 3-3. HWTT Alternate Data Analysis Parameters.

The Area under the Rutting Curve, Δ

To account for the HWTT rutting path-history of the tested samples, one of the parameters considered is the area under the HWTT rut depth versus the number of load passes curve. Ideally, when comparing two mixes with the same rut depth after 20,000 load passes (Rut_{max}), the mix with a lower Δ value would have the more desirable shape of the rutting curve (less convex). The area under the rut depth versus number of passes curve is calculated using the trapezoidal formula by dividing the area into n number of trapezoids as follows:

$$\Delta = \frac{N_d}{2n}\left[f(x_o) + 2f(x_1) + 2f(x_2) + ... + 2f(x_{n-1}) + f(x_n) \right]$$

3.1

where, $f(x_i)$ and $f(x_{i+1})$ are rut depth values at the left and right end of each trapezoid, respectively. However, Δ is not ideal for comparing two mixes with different failure cycles (N_d) since a mix with lower N_d would naturally have a lower Δ as compared to a mix that has higher failure cycles, even though the former is a more rut susceptible mix. To take this into account, the researchers introduced the normalized rutting area, Rut_Δ, parameter.

16

Normalized Rutting Area, Rut_Δ

The normalized rutting area is defined and computed as follows:

$$Rut_\Delta = \frac{Area\,under\,Rutting\,curve}{Number\,of\,Passes\,to\,Failure} = \frac{\Delta}{N_d} \qquad 3.2$$

The Rut_Δ takes into account the total rutting as well as the shape of the rutting curve by normalizing the area under the rutting curve (Δ). Thus, this parameter is able to compare two mixes with different N_d values. Ideally, higher Rut_Δ indicates poor rutting resistance for a mix.

Shape Factor, SF

The shape factor (SF) parameter is defined as the ratio of the area under the rutting curve for any mix, Δ, to that of a hypothetical mix having the same rut depth (Rut_{max}) with a linear rutting curve, as shown in Figure 3-3. Therefore:

$$SF = \frac{Area\,under\,'Rutting'\,curve}{Area\,under\,a\,linear\,curve} = \frac{\Delta_A}{0.5 \times N_d \times Rut_{max}} = \frac{\Delta_A}{\Delta_B} \qquad 3.3$$

where, Δ_B is the area under the hypothetical linear rutting curve as shown in Figure 3-3. From Equation 3.3 , it is noted that $SF > 1$ denotes a convex shape of the rutting curve, whereas, $SF < 1$ denotes a concave shape. Ideally, to mitigate early-life rutting, lower *SF* value or concave is preferred.

Several commonly used Texas HMA mixes were tested in the HWTT setup, and the resulting outputs were analyzed to produce these newly introduced HWTT parameters. Table 3-1 and Figure 3-4 present both traditional and newly introduced HWTT parameters for the tested mixes.

Table 3-1. Comparison of Traditional and Newly Introduced HWTT Parameters.

Mix Type	Hwy	Traditional HWTT Parameters		Introduced HWTT Parameters		
		Rut_{max} (mm)	N_d	Rutting Area (Δ)	Rut_Δ (mm)	SF
Type B	IH 35	2.84	20000	43,600	2.18	1.530
Type B	APT	12.5	15147	132,082	8.72	1.395
Type C	US 181	5.52	20000	73,800	3.69	1.336
Type C	US 83	8.22	20000	67,800	3.39	0.824
Type C	Loop 480	3.59	20000	60,200	3.01	1.679
Type C	SH 21	9.39	20000	103,000	5.15	1.098
Type C	US 259	12.5	19570	162,040	8.28	1.298
Type D	US 59	4.31	20000	47,400	2.37	1.099
Type D	US 277	12.5	16275	133,781	8.22	1.315
Type F	US 82	6.78	20000	91,400	4.57	1.348
Type F	US 271	5.45	20000	71,200	3.56	1.306
CAM	SH 121	12.49	20000	164,600	8.23	1.316
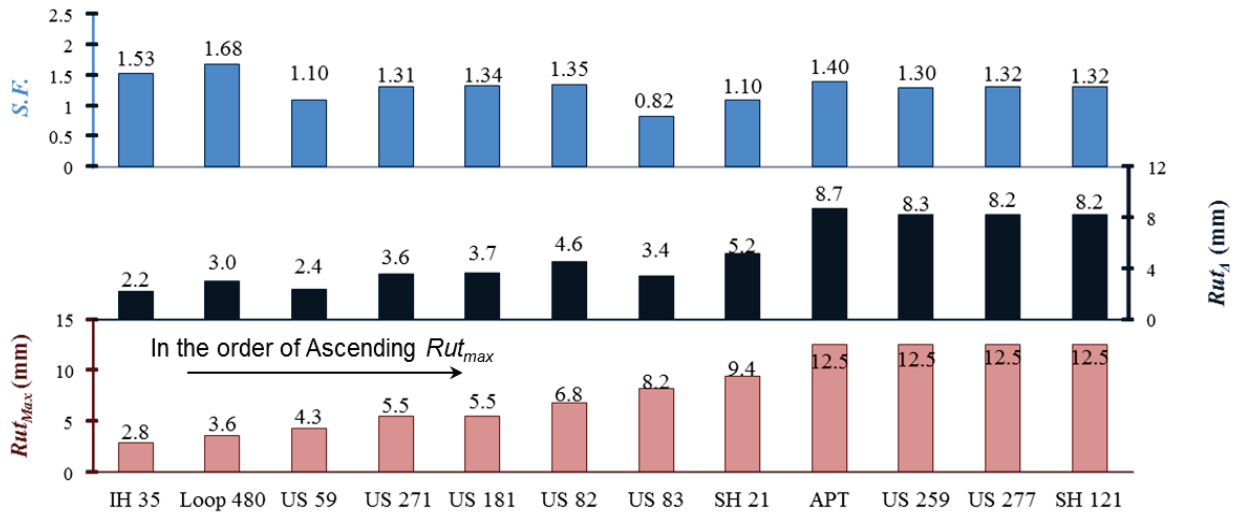
Figure 3-4. Comparison of Traditional and Newly Introduced HWTT Parameters.

Figure 3-4 arranges the tested mixes in the order of their increasing traditional HWTT rutting susceptibility (ascending Rut_{max}) after 20,000 HWTT load passes. It is generally observed that the normalized rutting area (Rut_Δ) also closely follows this ranking of the mixes. However, there are some obvious outliers. For example, the US 83 (Type C) mix ranks worse than each of US 271 (Type F), US 181 (Type C), and US 82 (Type F) mixes based on the traditional HWTT result (Rut_{max}), whereas, due to a superior shape of the rutting curve, it ranks better than each of these three mixes in terms of the Rut_Δ parameter. Also, notable from

18

Table 3-1 and Figure 3-4 is that the SF parameter does not seem to have any correlation with the traditional HWTT parameter (Rut_{max}), implying that the shape of the curve does not depend on the final rut depth of the mix. These observations are further confirmed by the correlation curves presented in Figure 3-5.
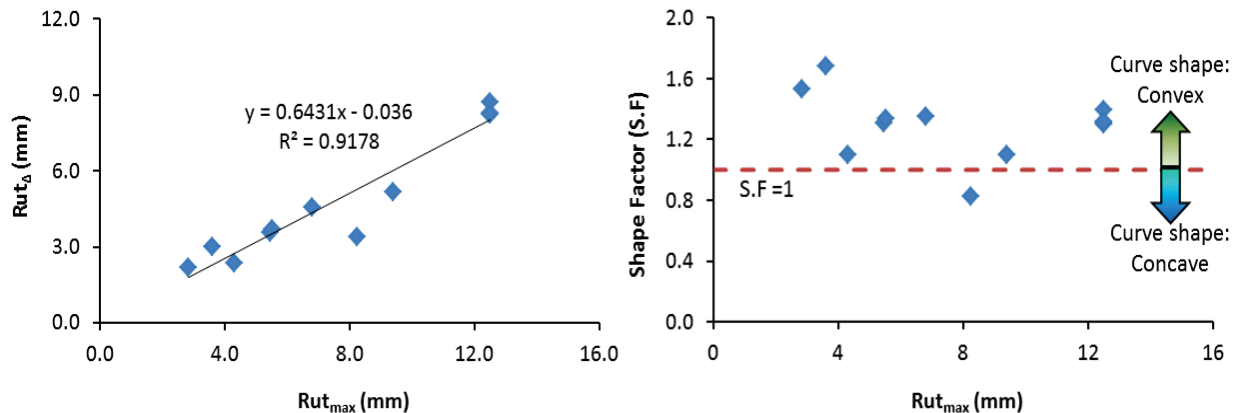
Figure 3-5. Correlation of Traditional vs. Newly Introduced HWTT Parameters.

The correlation curves are presented in Figure 3-5 between the traditional and newly introduced HWTT parameters, and both curves reconfirm the arguments drawn in the preceding paragraph. The parameter Rut_Δ has a fairly linear correlation with HWTT rut depth (Rut_{max}). However, the correlation is not 100 percent linear (91.8 percent), which suggests that the Rut_Δ parameter is somewhat able to capture the effects of the HWTT rutting path-history as well as the total rut depth. On the other hand, the *SF* shows no correlation whatsoever with the Rut_{max}, signifying that the shape of the curve does not depend on the final rut depth of the mix. In other words, the magnitude of the final rut depth of any given mix is rutting path independent. Based on this preliminary study, the following mix screening criteria are tentatively proposed for the newly introduced HWTT parameters as a safeguard against early-life mixture rutting:

- $Rut_\Delta < 8.0$.
- $SF < 1.25$.

HWTT SENSITIVITY EVALUATION

As an attempt to optimize the HWTT method in screening HMA mixes in the laboratory in terms of their field rutting performances, a comprehensive sensitivity evaluation of the critical

steps of the Tex-242-F test procedure was conducted. The researchers identified critical variables in the HWTT protocol that could be improved/modified so as to enhance the HWTT's potential in simulating field conditions and evaluating the HMA rutting performance in the lab. These variables are listed below:

- HWTT temperature.
- HWTT wheel speed.
- HWTT specimen sitting time.
- HWTT specimen compaction and air void content.

Plant-mix and raw materials (asphalt-binders and aggregates) were collected from various field projects, and extensive laboratory HWTTs were conducted by varying the parameters for each of these critical steps to analyze the sensitivity of the HWTT results. For all the sample fabrication procedures and testing, the same operators with similar skill level and the same HWTT equipment were used in the TTI lab. This was necessary to exclude the operator and/or equipment effect in the analysis. The results obtained from the studies are discussed in detail in the following subsections.

HWTT TEMPERATURE

In recent years, many pavements in Texas have experienced a higher degree of rutting failures that have largely been attributed to the escalated summer pavement temperatures, which, in many cases, exceed 122°F (50°C) for many hours each day over a period of weeks. The data in Table 3-2 indicates that the recently measured field PVMNT temperatures for some selected in-service Hwys around the State of Texas are substantially higher than the current Tex-242-F lab test temperature specification of 122 ± 2°F (50 ± 1°C).

Table 3-2. Measured Field PVMNT Temperatures on Selected Hwys in 2011–2014.

#	Hwy	District	Climatic Zone	Maximum Temperature Recorded in 2011–2014 (°F)	
				Air	**PVMNT @ 1-Inch Depth**
1	IH 35	Waco	Moderate (M)	112	131.3
2	APT site	Fort Worth	Wet-Cold (WC)	107	130.0
3	US 83	Laredo	Dry-Warm (DW)	114	140.0
4	Loop 480	Laredo	Dry-Warm	114	145.5
5	SH 21	Bryan	Wet-Warm (WW)	112	140.0
6	US 277	Wichita Falls	Dry-Cold (DC)	109	135.5
7	US 271	Paris	Wet-Cold (WC)	108	136.0
Avg.				110.9 (43.8°C)	136.9 (58.3°C)

The average maximum field PVMNT temperature shown in Table 3-2 is 136.9°F (58.3°C) while the maximum measured was 145.5°F (63.1° C). These field PVMNT temperatures are significantly higher than the 50°C test temperature that is specified in the current HWTT test procedure, Tex-242-F. Evidently, this suggests the need to review the current Texas HWTT temperature so as to accurately simulate these field PVMNT temperatures in the lab.

One of the issues of concern has been that many of the Texas mixes performed satisfactorily in the laboratory under the HWTT, but they fail by rutting/shoving in the field. Based on the Tex-242-F test procedure, the HWTT is currently run at 122 °F (50 °C); as can be noted from Table 3-2, this temperature is arguably insufficient to effectively capture the thermal conditions that the mixes experience in the field. This difference may partially explain the mixes passing tests in the laboratory but failing in the field when exposed to sustained elevated summer temperatures. Therefore, these researchers identified the HWTT temperature as one of the key test parameters to be studied in order to check the adequacy of the current test procedure (Tex-242-F). The research team tested six commonly used Texas mixes with varying temperatures, ranging from 122 to 158 °F (50 to 70°C). The resulting HWTT rutting response curves are presented in Figure 3-6.
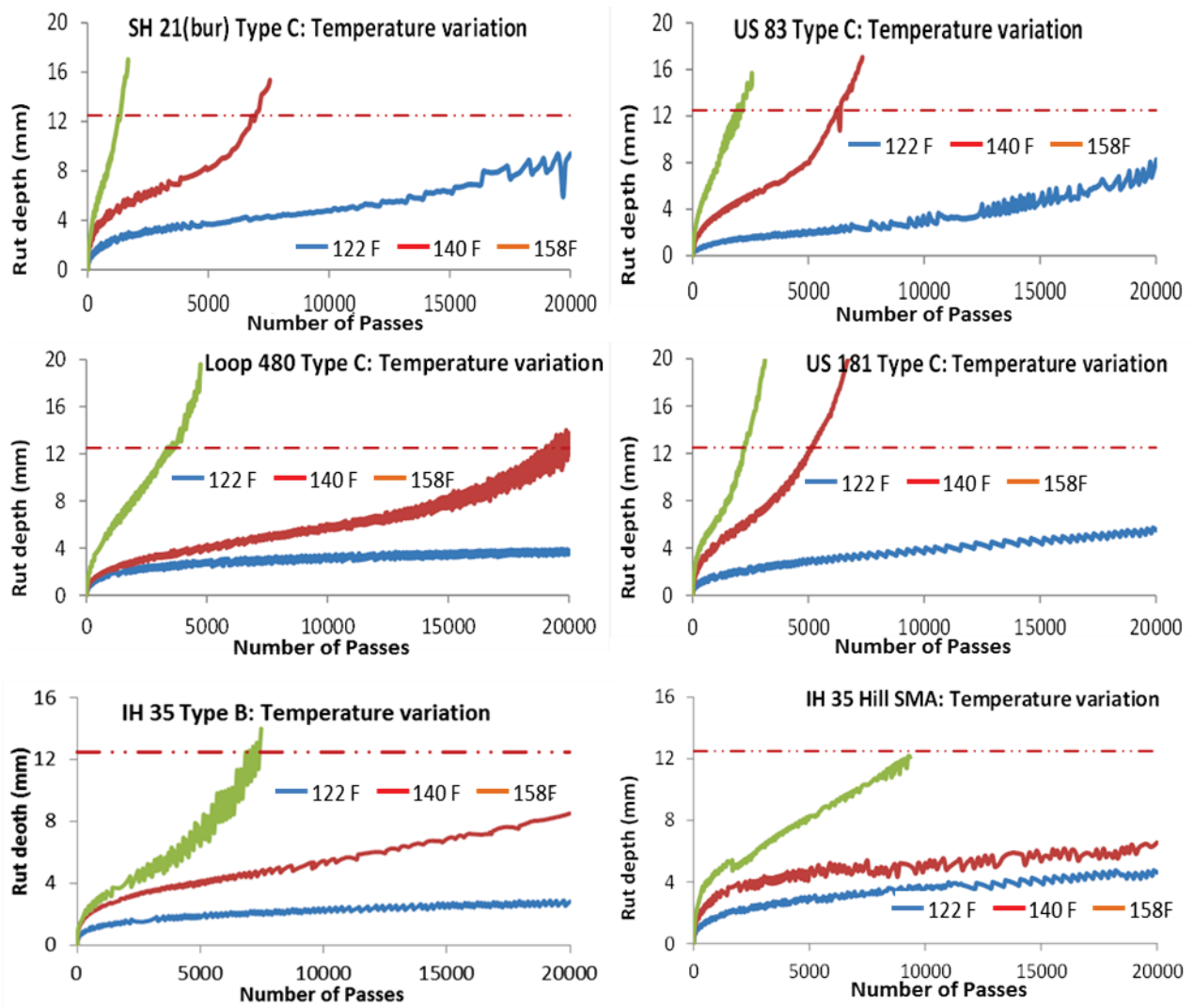
Figure 3-6. HWTT Rutting Curves for Temperature Variation.

It is evident from Figure 3-6 that the HWTT performances of the mixes are highly sensitive to test temperature. Four out of the six mixes that were tested failed ($Rut_{max} \geq 12.5$ mm) when the test temperature was increased from 122 to 140 °F, and all six mixes failed when tested at 1580°F. This behavior is, of course, theoretically expected since at higher temperature the mixes get softer and, thus, are more susceptible to rutting/shear failure. Nonetheless, these observations reinforce the concerns regarding the current practice of the HWTT temperature (122°F). Clearly, these tested mixes, which all pass the current HWTT specification, would be susceptible to field rutting failure when subjected to high PVMNT temperatures. This is of particular concern given the continued escalation of summer temperatures, which in recent years averaged about 136.9 °F (58.3 °C) for some of the selected highways (see Table 3-2).

The obtained HWTT outputs were further analyzed to compute various HMA rutting parameters. Both traditional (Rut_{max} and N_d) and the newly introduced HWTT parameters (Δ, Rut_Δ, and SF) were computed and comparatively evaluated using the formulae presented in the preceding sections. The results are presented in Table 3-3 and Figure 3-7.

Table 3-3. HWTT Parameter Summary for Temperature Variation.

Mix Description	Temperature (°F)	Rut_{max} (mm)	N_d	Rutting Area (Δ)	Rut_Δ (mm)	SF
SH 21 Type C	122	9.39	20,000	103,000	5.15	1.098
	140	12.5	6964	59,403	8.53	1.112
	158	12.5	1347	15,248	11.32	1.33
US 83 Type C	122	8.22	20,000	67,800	3.39	0.824
	140	12.5	6391	54,196	8.48	0.997
	158	12.5	2063	23,745	11.51	1.573
Loop 480 Type C	122	3.59	20,000	60,200	3.01	1.679
	140	12.32	20,000	122,600	6.13	0.996
	158	12.5	3455	45,019	13.03	1.33
US 181 Type C	122	5.52	20,000	73,800	3.69	1.336
	140	12.5	5178	61,152	11.81	1.176
	158	12.5	2199	31,028	14.11	1.418
IH 35 Type B	122	2.90	20,000	43,386	2.17	1.496
	140	8.53	20,000	108,180	5.41	1.268
	158	12.5	6992	40,701	5.82	0.931
IH 35 SMA	122	4.61	20,000	68,800	3.44	1.491
	140	6.56	20,000	100,200	5.01	1.529
	158	12.5	9849	161,819	16.43	1.926
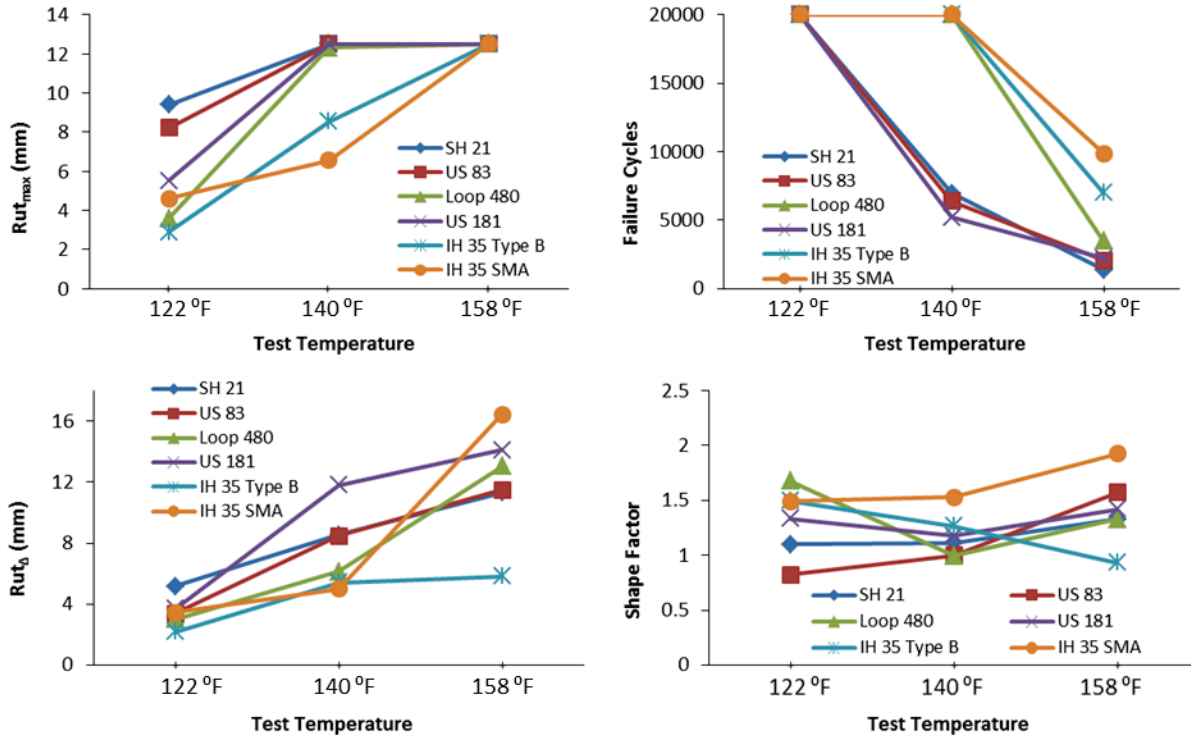
Figure 3-7. Effect of Temperature Variation on HWTT Parameters.

The findings in Table 3-3 and Figure 3-7 reinforce the discussion of the preceding sections regarding the high level of sensitivity the HMA rutting parameters under HMA testing have to test temperature. Rutting performances of all six mixes worsened considerably with increasing test temperature for both traditional and newly introduced HWTT parameters.

Based on these findings and considering the current high field temperature trends as exemplified in Table 3-2, the researchers recommend that higher or multiple HWTT temperature (e.g., 122, 131, 140 °F [50, 55, 60 °C]) should be considered for mixes to be placed in high temperature areas. Perhaps even more critical, testing via the HWTT at elevated and/or multiple temperatures should be considered for surface and near surface HMA mixes used in critical Hwy locations such as intersections, urban stop-go sections, high shear-stress locations, etc., or where low PG asphalt-binder grades are used.

HWTT WHEEL SPEED

One of the key issues concerning the HWTT protocol, as identified by the research team, is its inability to capture the effects of traffic speed variations due to a constant specified wheel speed (50 ± 2 passes/minute). Indeed, rutting is especially critical at intersections and "urban

stop-go environments" with slow-moving, accelerating, and/or decelerating traffic. Therefore, in this study, four HMA mixes that are commonly used in Texas were tested with the HWTT wheel speed varied between 25 to 52 passes/minute. The obtained HWTT results are presented in Table 3-4 and Figure 3-8.

Table 3-4. HWTT Parameter Summary for Wheel Speed Variation.

Mix Description	Wheel Speed (passes/min)	Rut_{max} (mm)	N_d	Rutting Area (Δ)	Rut_Δ (mm)	SF
US 277 Type D (TTI Lab)	36	12.5	15,900	90,153	5.67	0.907
	47	11.75	20,000	101,000	5.05	0.859
	52	7.15	20,000	68,600	3.43	0.959
US 277 Type D (TxDOT Lab)	36	8.23	20,000	79,200	3.96	0.961
	47	4.50	20,000	55,400	2.77	1.099
	52	3.99	20,000	49,400	2.47	1.389
US 271 Type F	25	3.7	20,000	57,200	2.86	1.549
	35	2.31	20,000	38,400	1.92	1.662
	42	2.58	20,000	40,600	2.03	1.575
	47	2.58	20,000	40,200	2.01	1.560
	52	3.45	20,000	45,000	2.25	1.306
FM 2100 Type D	35	12.50	10,850	78,120	7.20	1.151
	42	12.50	19,000	108,870	5.73	0.917
	47	8.29	20,000	98,000	4.90	1.183
	52	4.23	20,000	57,000	2.85	1.35
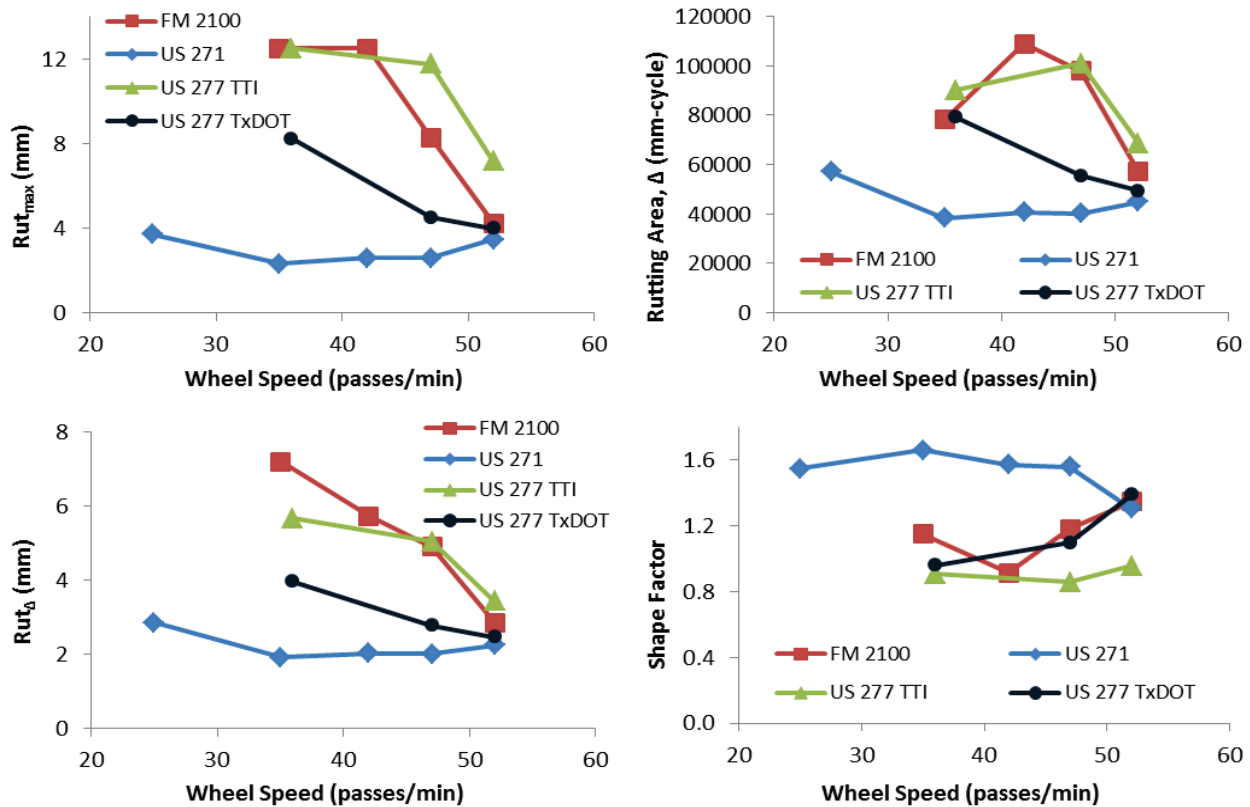
Figure 3-8. Effect of Wheel Speed Variation on HWTT Parameters.

From the results presented in Table 3-4 and Figure 3-8, it is evident that the rutting performances of mixes worsen at lower wheel speeds. Both Rut_{max} and Rut_Δ exhibit an increasing trend with decreasing wheel speed for three out of the four mixes tested; only one of the mixes (US 271 Type F) did not show any considerable sensitivity. On the other hand, the rutting area and SF parameters did not show any definitive trend.

Based on these observations, it is argued that the HWTT should be tested at lower speeds than the currently specified 50 ± 2 passes /minute. For mixes to be used in slow vehicle-speed areas such as intersections, urban city roads, etc., consideration for testing at lower or multiple HWTT wheel speeds should be undertaken, i.e., from 50 down to as low as 35 passes/minute. However, at lower HWTT wheel speeds, some HMA mixes may take more time to reach the current 20,000 pass threshold, thus increasing the test time and operating cost. Any potential change to the HWTT wheel speed should take this factor into consideration.

HWTT SPECIMEN SITTING TIME

Due to simple sample preparation methods for the HWTT, test specimens can be practically ready for testing within one day of fabrication. However, the current Tex-242-F test procedure does not specify the allowable time frame between sample fabrication and testing, i.e., the specimen sitting time. Several studies have shown that specimen sitting time has considerable effect on HMA laboratory test performance due to the oxidizing and short-term aging effects that have a tendency to stiffen up the HMA (Walubita et al., 2012, Zeinali, 2014). Therefore, with a view of studying the effect of specimen sitting time on the HWTT rutting response parameters, two HMA mixes were tested in the HWTT setup with varying duration of specimen sitting times. The obtained rutting curves, from 1-day up to 14-day specimen sitting time, are presented in Figure 3-9.
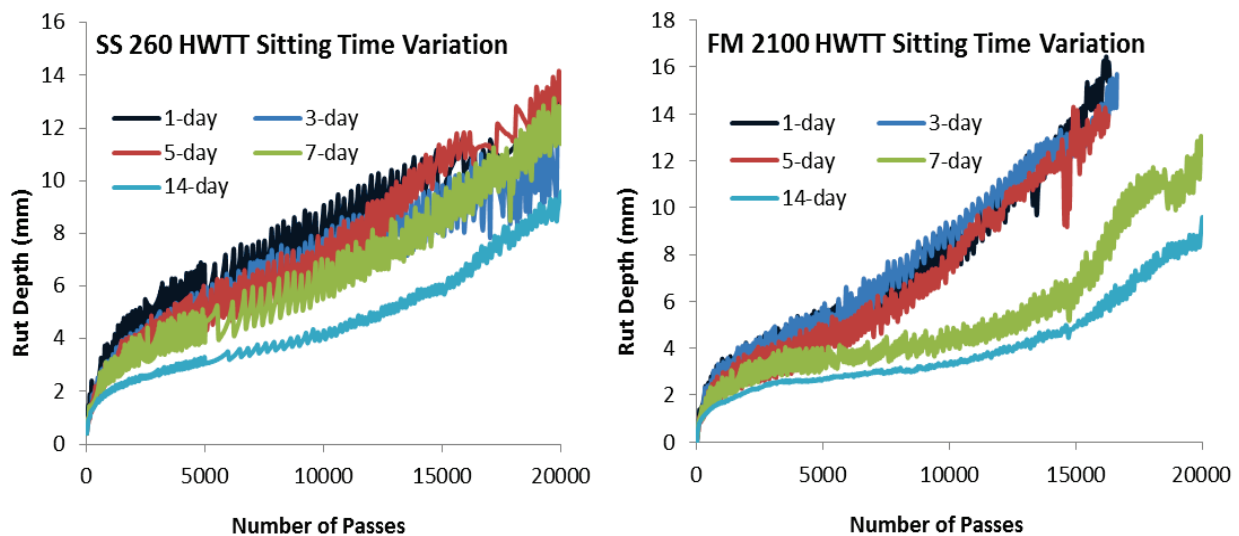
Figure 3-9. HWTT Rutting Curves for Varying Specimen Sitting Time.

Figure 3-9 indicates that the sample sitting time, indeed, has some effects on the HWTT rutting responses of the mixes. Particularly, the rutting performance of the FM 2100 Type D mix considerably improves when tested after 7 and 14 days of sample fabrication date. The HWTT curves were further analyzed to obtain the HWTT rutting parameters presented in Table 3-5 and Figure 3-10.

Table 3-5. HWTT Parameter Summary for Sample Sitting Time Variation.

Mix Description	Sitting Time (days)	Rut_{max} (mm)	N_d	Rutting Area (Δ)	Rut_Δ (mm)	SF
SS 260 Type C	1	12.50	19,473	154,459	7.932	1.269
	3	12.12	20,000	140,032	7.00	1.155
	5	12.50	18,076	127,901	7.076	1.132
	7	12.50	19,048	121,255	6.366	1.018
	14	9.59	20,000	93,859	4.69	0.978
FM 2100 Type D	1	12.50	13,965	90,253	6.46	1.034
	3	12.50	13,429	88,300	6.58	1.052
	5	12.50	14,420	89,020	6.17	0.988
	7	12.50	19,793	106,688	5.39	0.862
	14	9.59	20,000	81,051	4.05	0.845
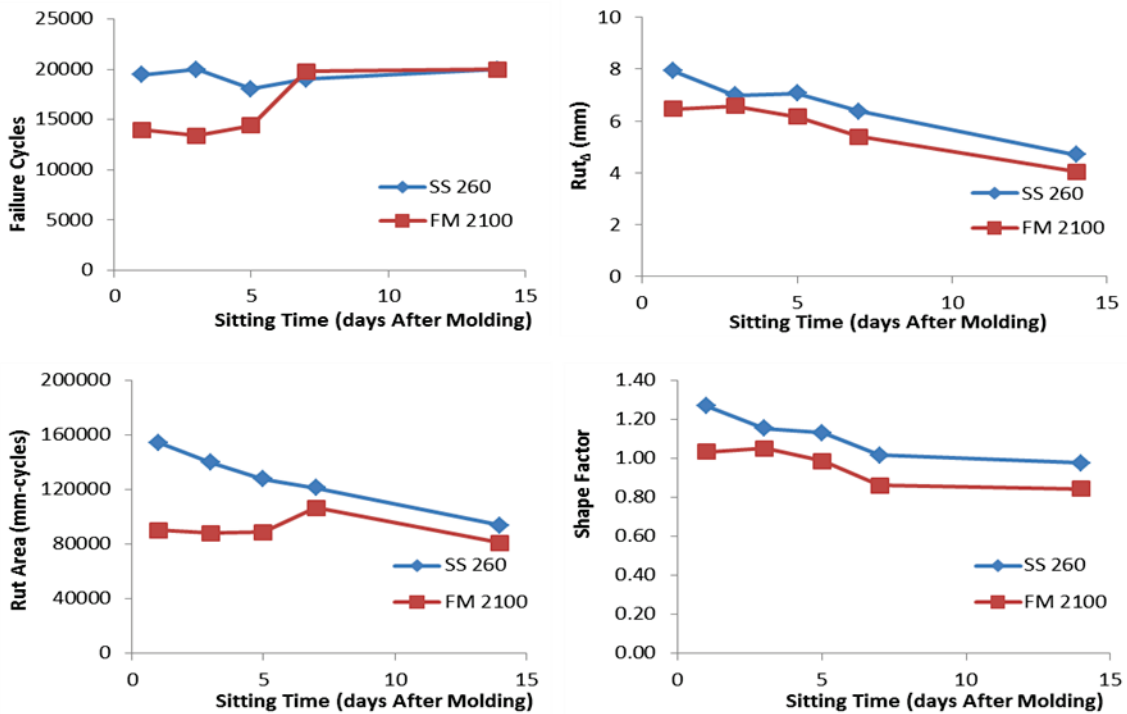
Figure 3-10. Effect of Sitting Time Variation on HWTT Parameters.

Figure 3-10 clearly shows that the rutting performances of the mixes are evidently improving with increased sitting time. Both mixes fail the HWTT specification ($Rut_{max} \geq$ 12.5 mm) if tested within three days of sample fabrication. However, if the sample sitting time exceeds five days, both mixes pass the HWTT. The shape of the rutting curves also improves (turning from convex to the more desirable concave shapes) as the sample is left untested for

longer sitting-time durations; a significant change occurs beyond five days in both Figure 3-9 and Figure 3-10.

For one-, three-, and five-day specimen sitting time, the rutting response curves are almost overlapping in Figure 3-9. In Figure 3-10, a significant change in both the shape and slope of the graphs appears to occur after five days of specimen sitting time. Thus, five days appears to be the maximum sitting time within which to test HWTT specimens.

The implications of these findings are that, in the absence of a specified sample sitting time, samples are often tested at random times and not soon after fabrication, thus increasing the chance of misleading laboratory rutting performance evaluations. For example, a mix could misleadingly pass the HWTT simply because the specimens were tested after a longer sitting period, and then fail prematurely in the field. This aspect is synonymous to what is currently being observed: mixes are passing the HWTT in the lab but are failing prematurely in the field. Specimen sitting time and possible HMA stiffening due to oxidative aging could be one cause. Thus, to ensure consistency, these researchers recommend testing all HWTT specimens within five days of sample molding/fabrication.

HWTT SPECIMEN AIR VOID CONTENT

Currently the HWTT samples are prepared in the laboratory at a target density of 93 ± 1 percent (i.e., 7 ± 1 percent AV). However, most mixes in the field are compacted to a target density range of 96 to 98 percent (4 to 2 percent AV). Therefore, to study the effects of sample AV on the HWTT results, the researchers tested three mixes with varying sample AV. The results are presented in Table 3-6 and Figure 3-11.

Table 3-6. HWTT Parameter Summary for Sample AV Variation.

Mix Description	AV (%)	Rut_{max} (mm)	N_d	Rutting Area (Δ)	Rut_Δ (mm)	SF
	2	1.57	20,000	30,600	1.53	1.945
US 59 Type D	4	2.29	20,000	38,800	1.94	1.696
	7	2.76	20,000	58,600	2.93	2.117
	4	4.38	20,000	49,200	2.46	1.126
US 83 Type C	7	8.22	20,000	67,800	3.39	0.824
	9	10.31	20,000	117,400	5.87	1.14
	4	1.44	20,000	24,600	1.23	1.7
IH 35 Type B	7	1.65	20,000	27,000	1.35	1.639
	9	2.84	20,000	43,600	2.18	1.53
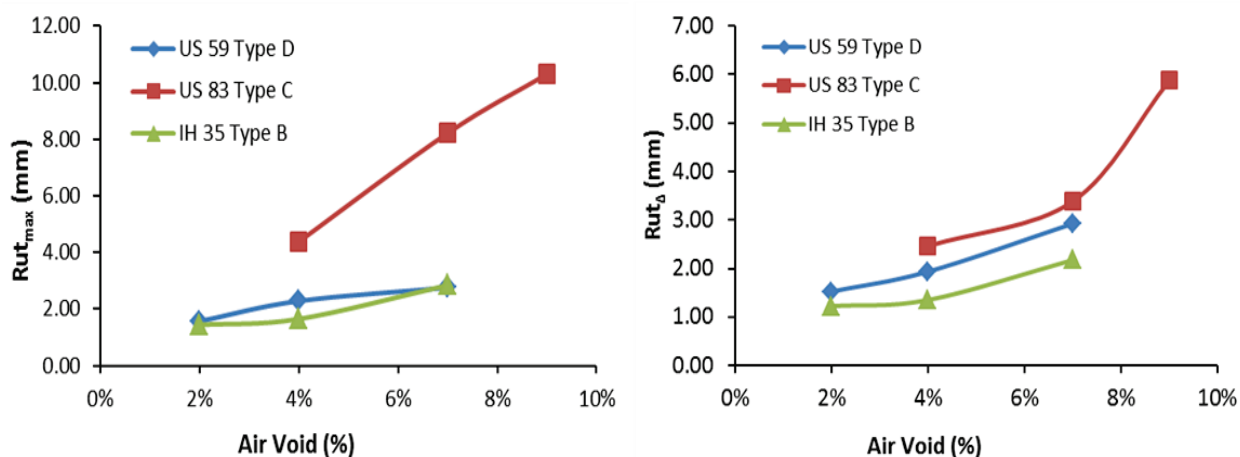
Figure 3-11. Effect of Sample AV Variation on HWTT Parameters.

From the results presented in Figure 3-11 and Table 3-6, it is evident that rutting is more critical at higher sample AV and is marked by higher Rut_{max} and Rut_{Δ} values with increasing sample AV. Since the mixes in the field are usually compacted to lower AV, the current HWTT protocol is conservative in terms of test sample air voids. Therefore, no modification to the current HWTT sample AV specification is suggested.

SUMMARY

In this chapter, the HWTT protocol was thoroughly evaluated with the onus of proposing modifications to the current Tex-242-F test procedure such that it is more comprehensive in capturing the field rutting performances of commonly used Texas HMA mixes. The HWTT data analysis procedure was also reviewed and modified in an attempt to generate HWTT parameters that better reflect mixture field performance. Key findings from the data presented in this chapter are as follows:

- Current HWTT protocol specifies rutting performance of any mix at the end of the test only without considering the rutting path-history. Thus, the current HWTT protocol fails to explain mixes having similar laboratory rutting performances but widely varied field rutting, especially in terms of early-life rutting failures. To address this issue and to capture the HWTT rutting path-history, three new HWTT parameters were introduced, namely the rutting area (Δ), the normalized rutting area (Rut_{Δ}), and the shape factor (SF).

30

Among these, the Rut$_\Delta$ and the SF parameters showed promising potential to capture the HWTT rutting response and path-history.

- Analysis of the HWTT data of several commonly used Texas mixes conceptually confirmed the superiority of the Rut$_\Delta$ and the SF parameters in capturing the effects of the HWTT rutting path-history as well as the total rut depth. Therefore, the researchers recommend that these two parameters should be considered in the HWTT protocol and Tex-242-F test procedure, with the following tentative HMA mix screening criteria:

  1) $Rut_\Delta < 8.0$.

  2) $SF < 1.25$.

- HWTT rutting increases significantly with temperature with most mixes failing at 70°C. Therefore, considering the recent increase in rutting/shoving failures under sustained high temperature/high traffic stress environments, evaluating HWTT results under higher or multiple test temperatures should be considered for mixes to be placed in high shear stress environments.

- Rutting performance of mixes worsens at lower wheel speeds. This observation to some extent explains the higher degree of rutting failures observed at the intersections with stop-and-go traffic conditions. Based on this, the researchers suggest that the HWTT should in some circumstances be tested at lower speeds (as low as 35 passes/minute) to supplement the standard 50 ± 2 passes/minute, particularly for mixes to be placed in slow vehicle-speed areas such as intersections or urban stop-go zones. However, at lower HWTT wheel speeds, some HMA mixes may take more time to reach the currently specified 20,000 passes threshold, thus increasing the test time and operating cost.

- Rutting-resistance performance of HMA improves with increasing sample sitting time, i.e., the time between sample fabrication and testing due to short-term aging of asphalt. Therefore, allowing long and inconsistent sitting times for HWTT samples can lead to misleading rutting performance of mixes, thus increasing the risk of premature early-life rutting failures in the field. To ensure consistency, and based on the results of this study, the researchers recommend testing all HWTT specimens within five days of sample molding/fabrication.

- The current HWTT protocol is conservative in terms of test sample air void content, thus no modifications are suggested in this aspect.

CHAPTER 4   THE SPST METHOD – CONCEPTUAL DEVELOPMENT

One of the primary goals of this study was to develop a supplementary and/or surrogate HMA rutting shear test to complement the existing tests, such as the HWTT, RLPD, DM test, etc. Current permanent deformation and rutting tests such as the HWTT have a proven history of successfully identifying and screening HMA mixes that are prone to rutting and/or susceptible to moisture damage (stripping). However, one of the key limitations of the existing HMA rutting/PD tests identified in this study (Walubita et al., 2013) has been their inability to directly capture the HMA shear properties, e.g., shear strength, shear strain, shear modulus. Indeed, one of the contributing mechanisms of permanent deformation in HMA is the lateral movement, i.e., the shear failure of the HMA under traffic; see Figure 4-1 (Brown et al., 2001).
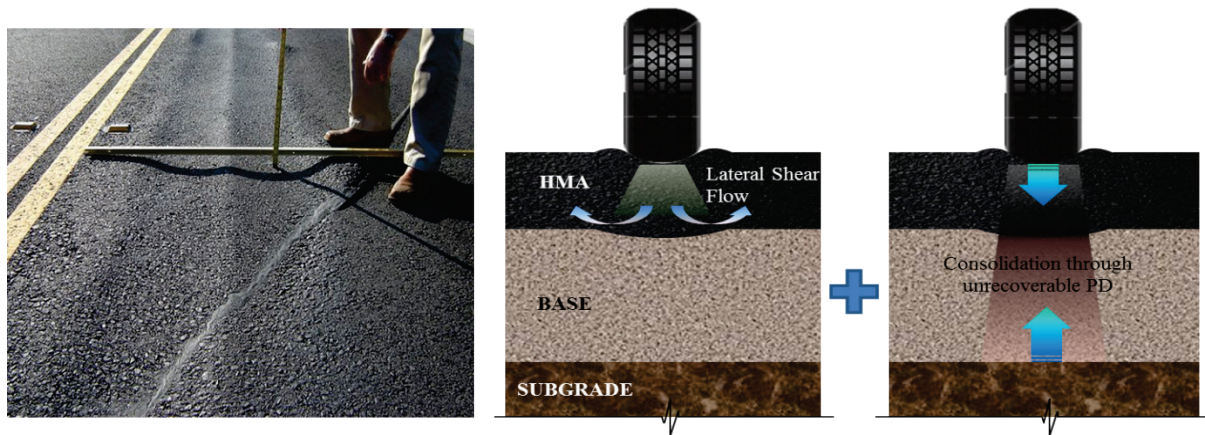
Figure 4-1. Mechanisms of Rutting in HMA Pavements.

While the HWTT and the other routine rutting/PD tests are able to capture the consolidation of the HMA through accumulation of small amounts of unrecoverable strain as a result of repeated loads applied to the pavement, they are not inherently designed to directly measure the HMA shear properties. To address this issue, the researchers explored the simple punching shear test (SPST) as a supplementary and/or surrogate HMA rutting shear test to complement the existing rutting/PD tests. This chapter discusses the SPST setup, including selection of the loading parameters, development of the data analysis models, and some preliminary test results.

TEST SETUP AND SELECTION OF INPUT PARAMETERS

The SPST was developed as a simple performance test to characterize HMA shear properties. In the SPST setup, a cylindrical HMA specimen is compressed vertically via a steel punch placed concentrically on the top of an opening at the base (Figure 4-2). The specimen fails along the diametrical plane due to the shear strain generated in the tangential direction.

The SPST protocol was developed by selecting the test input parameters through a series of preliminary tests. The test input parameters were carefully selected so as to ensure that the test can be routinely conducted in commonly available laboratory testing equipment such as the universal testing machine (UTM), indirect tension (IDT) setup, etc., and that the test captures meaningful interpretable data that are comparable with other routine HMA tests. Figure 4-2 and Table 4-1 present the SPST setup and the test parameters, respectively, followed by brief discussions of the factors considered while selecting some of the key input parameters, e.g., sample confinement, diameter of the loading head, loading rate, and test temperature.
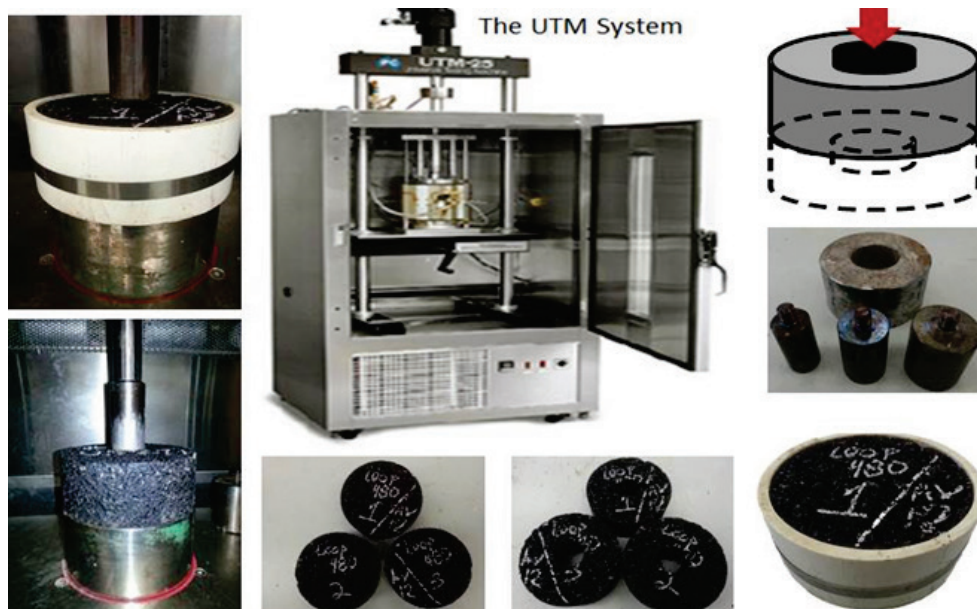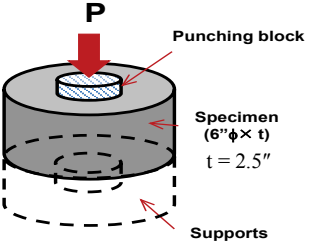
Figure 4-2. The SPST Setup.

Table 4-1. **The SPST Protocol.**

#	Item	Description
1	Schematic	
2	Test objective	Characterization of HMA shear resistance properties
3	Specimen dimension	2.5" (63.5 mm) thick × 6.0" (152.4 mm) φ
4	Loading mode	Monotonic axial compressive loading. Displacement controlled (axial continuously increasing displacement)
5	Sitting load	8 lbs (0.036 kN) or sitting stress of 0.29 psi (2 kPa)
6	Loading rate (mm/s)	0.2 mm/s (0.50 inch/min)
7	Specimen confinement	Yes
8	Loading head diameter	a) 1.5" (38.1 mm) φ
9	Test temperatures	50 ± 2°C (122°F)
10	Data capturing frequency	Every 0.10 second (except temperature; at least every 5 seconds)
11	Test termination	2.49" (63.2 mm) vertical RAM movement
12	Total test time	≤ 10 minutes
13	Measured parameters	Temperature, time, load, & shear deformations (actuator [RAM] – No LVDTs)
14	Number of specimen replicates per test condition	≥3
15	Target specimen air voids	7 ± 1% for all HMA mixes, except PFC mixes at 20 ± 2%.
16	Specimen temperature conditioning time	≤ 3 hrs (it is recommended to monitor the temperature from a thermocouple wire inserted insde a dummy specimen that is also placed in the same temperature chamber as the test specimens)

Test Temperature

The test temperature was selected through a set of trial testing at three different temperatures, namely 40, 50, and 60°C to simulate the high Texas pavement temperatures during the summer. The results are presented in Figure 4-3.
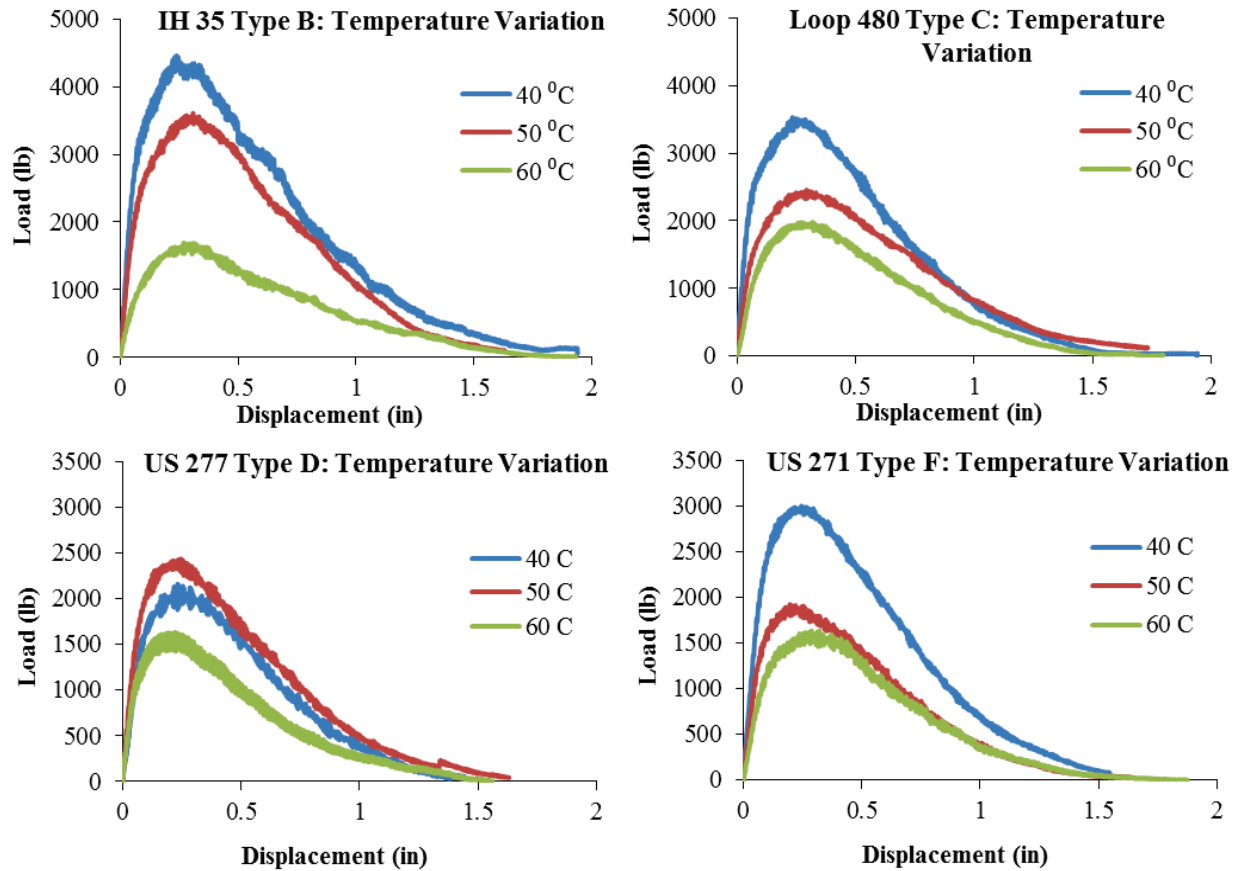
Figure 4-3. SPST Temperature Selection.

These results show that for the four mixes tested, the SPST is able to capture the effects of high test temperatures. As theoretically expected, the mixes get softer and less shear resistant at higher temperatures, and this behavior is successfully captured by the SPST. Thus, according to these trial tests, the SPST can be suitably run at high test temperatures to simulate critical field conditions. Thus, the research team selected 50°C as the preliminary SPST temperature to facilitate easy comparison with the other rutting/PD tests, e.g., HWTT (at 50°C), RLPD (at 40 and 50°C), FN (at 50°C), and DM (i.e., 54°C) (TxDOT, 2009; AASHTO, 2005; Walubita et al., 2011).

However, for mixes to be placed in high temperature areas, high shear stress locations, and "urban stop-go environments" (near intersections), samples can be tested at multiple temperatures, i.e., 50°C, 55°C, 60°C for better evaluation of the mixes' shear resistance. In the recent summers, field PVMNT maximum temperatures in Texas have, in fact, averaged around

58.3°C (Table 3-2) and, therefore, justify the need to test at temperatures closer to 60°C in these circumstances.

Sample Dimension and Loading Rate

For practicality, simplicity of sample fabrication, and ease of comparison, Hamburg type HMA specimens were adapted for the SPST, i.e., 2.5-inch thick by 6.0-inch diameter (63.5 mm × 152.4 mm ϕ). The SPST is conducted in a displacement controlled mode; therefore, the output results show sensitivity to the loading rate (applied displacement rate) as seen in Figure 4-4.
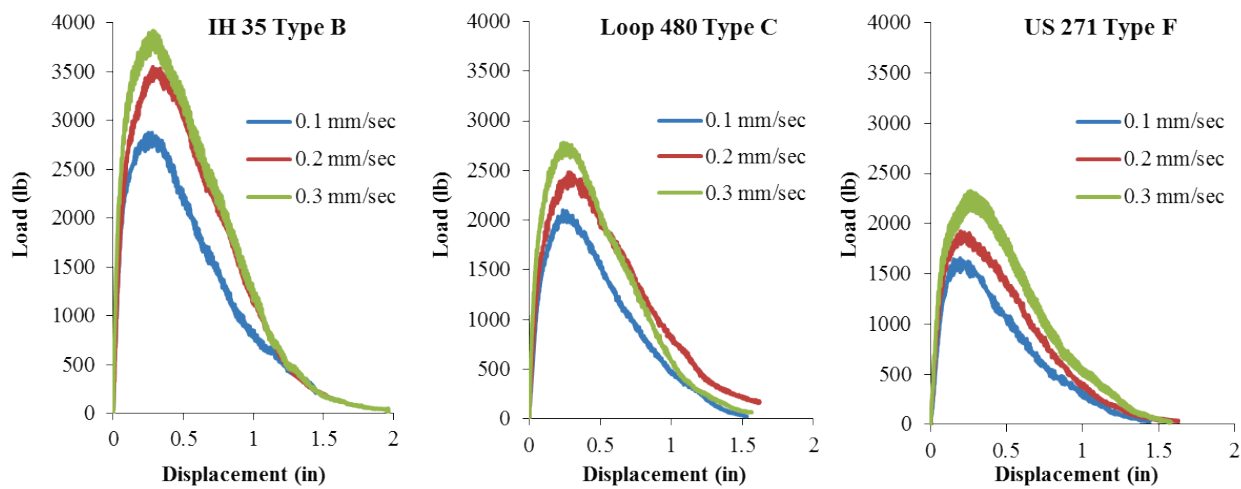
Figure 4-4. SPST Loading Rate Selection.

The 0.2 mm/sec loading rate yielded the best results in terms of consistency of the load-displacement response curve; thus, it was selected for use throughout this study. For the 0.3 mm/sec loading rate, the resulting peak load was comparatively higher for some mixes, thus posing a risk of maxing out the UTM load cell when testing stiff mixes. On the other hand, the result variability was relatively higher for the samples tested at 0.1 mm/sec loading rate.

Sample Confinement

SPST specimen testing protocol was evaluated in both unconfined and confined loading modes. A PVC (polyvinyl chloride) enclosure with 6-inch inner diameter (the same as the diameter of the sample) was used to confine the samples. The PVC enclosure was attached to the sample tightly with the help of a metal clamp, tightened at 25 inch-lb of torque. The confining pressure was theoretically calculated to be in the order of 20 psi. As evident in Figure 4-5, the

unconfined loading configuration resulted in rupturing of the specimens prematurely without capturing the representative HMA shear behavior or yielding any meaningful results. Figure 4-6 provides the SPST load-displacement (L-D) response for both sets of samples.
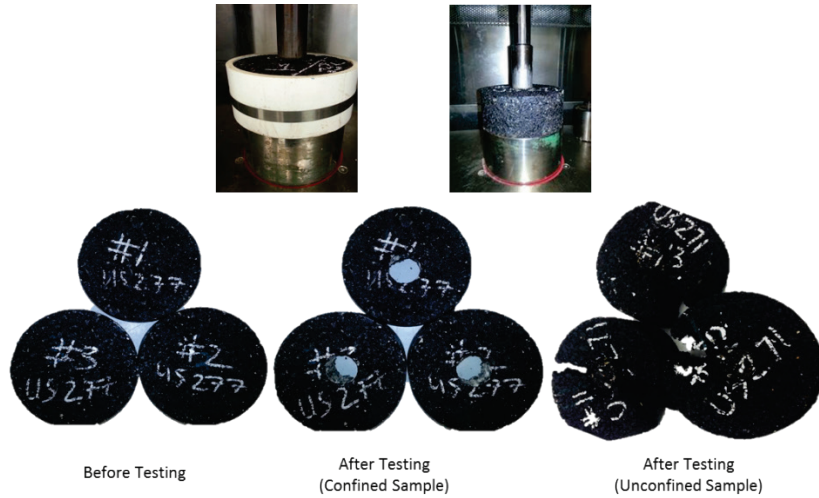
Figure 4-5. SPST Samples before and after Testing: Confined and Unconfined Samples.
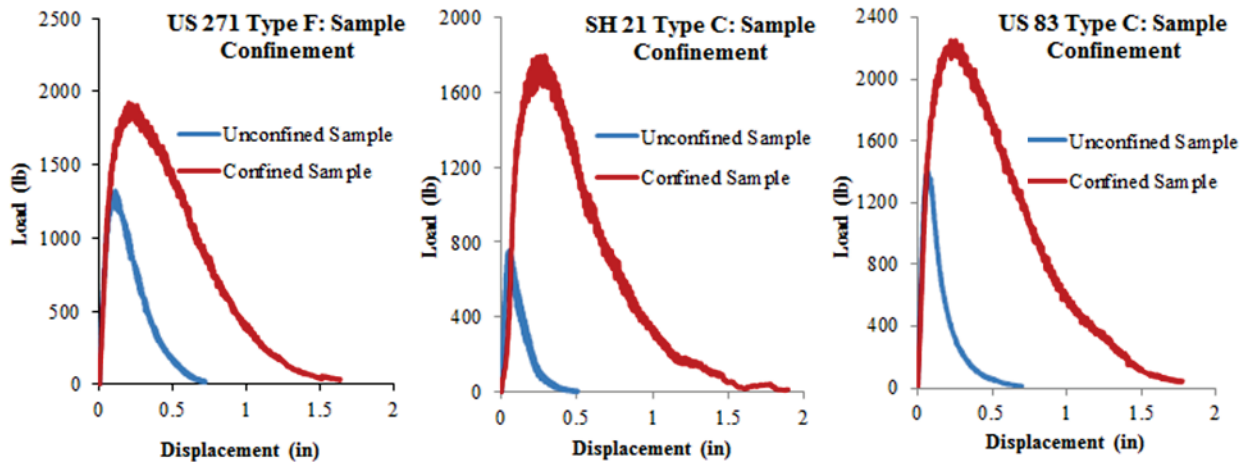
Figure 4-6. SPST Load-Displacement Response: Confined vs. Unconfined Samples.

In the absence of any lateral confinement, the specimens were susceptible to radial crack propagation; thus, the failure mode was fracture rather than shear. As a result, the unconfined specimens failed prematurely at about 30 to 50 percent lower load than the confined specimens. Thus, all subsequent testing by SPST in the study was conducted in a confined mode.

Loading Head Diameter

Three loading (punching) heads of diameters 1.5, 2.0, and 2.5 inches were investigated, and the results are shown in Figure 4-7.
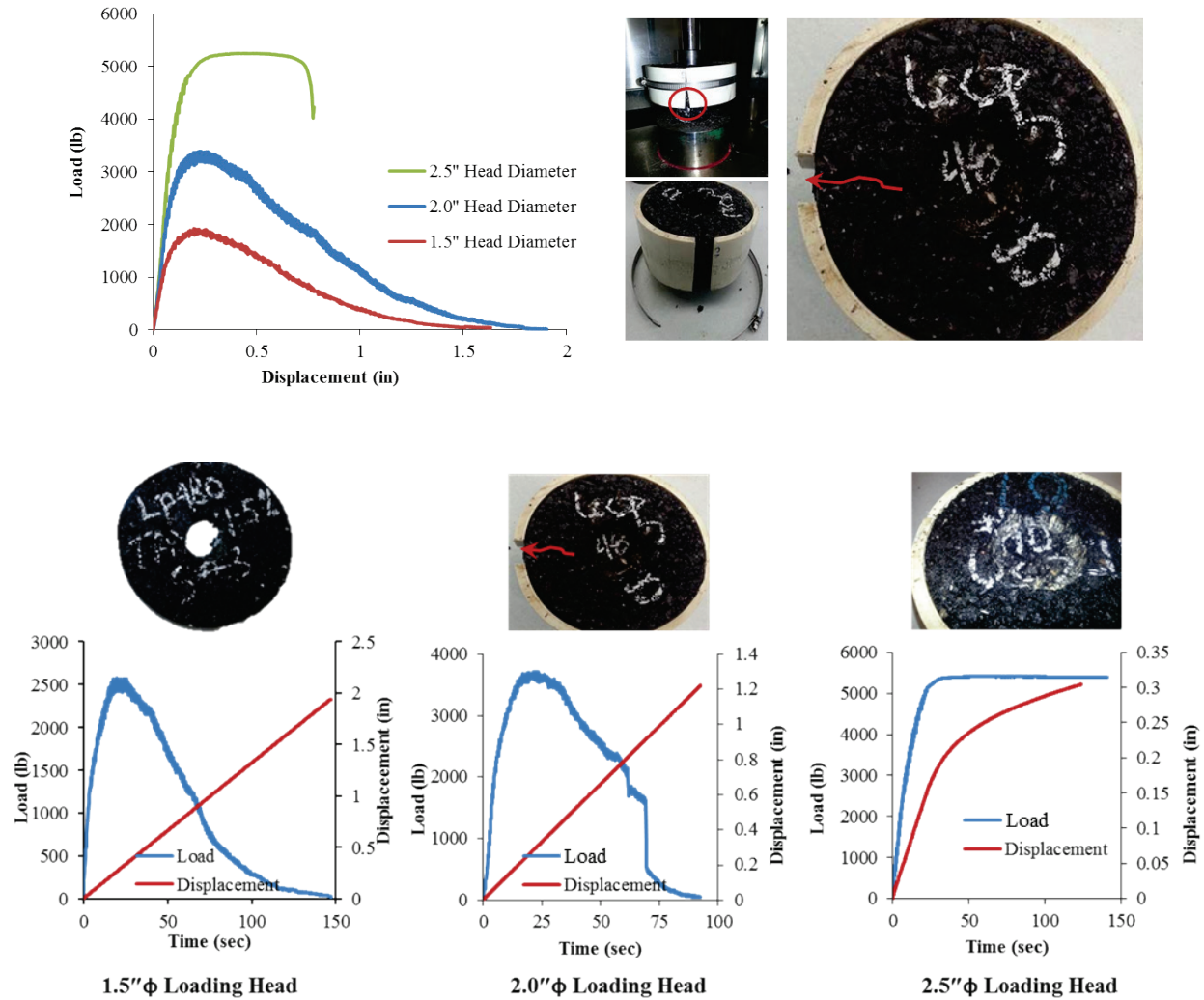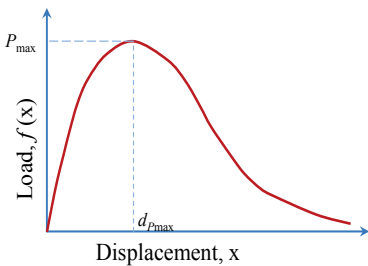
Figure 4-7. SPST Loading Head Selection.

In the case of the 2.0-inch diameter head, the induced high loading due to high shear resistance of the head's surface area caused the confinement enclosure to rupture prior to the specimen reaching its failure point. Thus, the results could not capture the true shear response of the HMA or any meaningful data. With the 2.5-inch diameter head, the UTM load cell capacity was exhausted due to high shear resistance induced by the large surface area of the head (Figure 4-7). So, the 1.5-inch loading head was selected for use throughout the study.

SPST OUTPUT DATA AND DATA ANALYSIS MODELS

The primary output result obtained from an SPST run is the shear load versus displacement curve that can be further analyzed to generate HMA shear properties. To facilitate this, data analysis models were derived based on the fundamental principles of mechanics and HMA visco-elastic behavior when subjected to monotonic loading. The derived parameters and their associated analysis models are presented in Table 4-2.

Table 4-2. SPST Data Analysis Models.

#	Item	Analytical Model
1	Output data	
2	Shear peak failure load (lb or kN)	$P_{\max}$
3	Shear failure deformation @ peak load (inch or mm)	$Deformation\ @\ P_{\max} = d_{P_{\max}}$
4	HMA shear strength (psi or kPa)	$\tau_s = \dfrac{P_{\max}}{A} = \dfrac{P_{\max}}{\pi D t}$
5	Shear failure strain @ peak load (in/in or mm/mm)	$\gamma_s = \dfrac{d_{P_{max}}}{t}$
6	HMA shear modulus (psi or kPa)	$G_s = \dfrac{\tau_s}{\gamma_s} = \dfrac{P_{\max}}{\pi D \left(d_{P_{\max}} \right)}$
7	Shear strain energy (lb-in/in^2 or J/m^2)	$SSE = \dfrac{1}{A} \int\limits_{o}^{\infty} f(x)\,dx = \dfrac{1}{\pi D t} \int\limits_{o}^{\infty} f(x)\,dx$
8	SSE Index	$10^3 \times SSE \dfrac{\gamma_s}{t \tau_s}$
9	Description of equation parameters:	$\int f(x)\,dx$ = Area under the shear stress-strain response curve D = Diameter of the punching (loading) head (inches) t = Thickness of the sample (inches)

Along with the routine HMA shear properties, i.e., the shear strength (τ_s), shear strain (γ_s), and shear modulus (G_s), this study introduced and explored two novel HMA shear parameters, namely the shear strain energy (SSE) and the SSE Index. Measured in J/m^2, the SSE

is defined as the total work done to shear the HMA by a unit area. The total work done is measured as the area under the load-displacement (L-D) curve as presented in Table 4-2. Whereas, the SSE Index is a mathematical parameter defined as a parametric ratio of the SSE to the HMA shear strength (τ_s) and shear strain (γ_s) per unit length of the sheared plane (specimen thickness, t, in the case of the SPST) under punching-shear loading.

In general, the physical interpretation of the SSE parameter is based on the assumption that a good shear resistant mix will absorb a higher amount of shear strain energy denoted by a larger area under the L-D curve.

LABORATORY TEST RESULTS AND ANALYSIS

Several HMA mixes were tested following the SPST procedures described above. The mix descriptions are presented in Chapter 2. Figure 4-8 presents the obtained L-D response curves for these mixes. The output results were analyzed to generate HMA shear properties following the aforementioned data analysis models (Table 4-2), and they are presented in Table 4-3. The results represent the averaged statistics of a minimum of three replicate specimens per HMA mix per test condition with a target COV threshold of 30 percent.
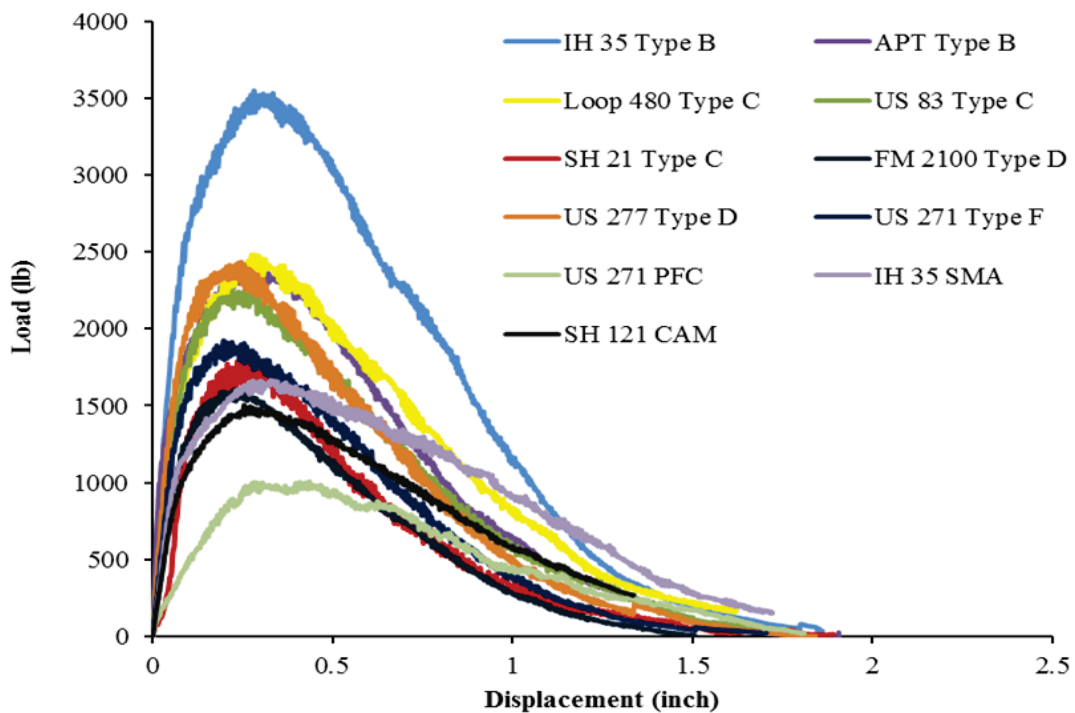
Figure 4-8. SPST Load-Displacement Response Summaries.

The L-D response curves, presented in Figure 4-8 are interpreted as follows: mixes with higher peak shear failure load are indicative of higher shear resistance. Also, a steeper L-D curve (higher shear modulus) will indicate less shear strain under similar loading, and thus will theoretically infer less rutting in the field under traffic loading.

The very first observation from the SPST output curves presented in Figure 4-8 is that the test method is fairly successful in differentiating various mixes based on their shear resistance potential. Indeed, for the mixtures evaluated, the ratio of the peak shear loads at the two extremities of shear resistance potential (IH 35 Type B and US 271 PFC, respectively) is on the order of 3.5. Similarly, the coarse-graded Type B and C mixes, known historically for their good field rut resistance performances are located at the upper echelon of the L-D response curves, whereas, traditionally less rut-resistant mixes such as the CAM have relatively low peak failure load and less steepness in the response curve.

Table 4-3. SPST Results.

Mix Type	Highway	τ_s (psi)	γ_s (in/in)	G_s (ksi)	SSE (kJ/m^2)	SSE Index	AV (%)	Comment*
Type B	IH 35	456	0.120	3.82	62.6	37.43	7.48%	
		(7.0%) **	(5.9%)	(0.7%)	(1.2%)	(1.9%)		
	APT	310	0.108	2.95	40.1	31.94	6.86%	Very good
		(5.6%)	(21.4%)	(26.9%)	(6.2%)	(20.8%)		
SMA	IH 35	222	0.139	1.66	37.2	53.006	23.2%	
		(6.7%)	(26.3%)	(24.6%)	(8.1%)	(22.2%)		
Type C	US 83	292	0.091	3.27	34.7	24.87	7.5%	
		(9.1%)	(13.7%)	(21.2%)	(5.2%)	(19.4%)		
	Loop 480	321	0.108	2.97	42.9	32.96	7.35%	
		(1.8%)	(1.9%)	(3.5%)	(7.4%)	(7.5%)		
	SH 21	228	0.114	2.00	18.6	21.27	7.24%	
		(4.5%)	(9.2%)	(12.4%)	(5.7%)	(9.6%)		Good
Type D	US 277	319	0.087	3.67	36.4	22.66	6.95%	
		(1.1%)	(9.8%)	(8.5%)	(4.4%)	(13.5%)		
	FM 2100	206	0.087	2.37	23.1	22.396	6.81%	
		(13.3%)	(11.6%)	(10.7%)	(12.7%)	(11.2%)		
Type F	US 271	248	0.089	2.82	28.8	23.55	7.28%	
		(9.8%)	(19.1%)	(11.0%)	(4.1%)	(14.1%)		
CAM	SH 121	178	0.085	2.11	19.4	21.440	6.9%	
		(4.9%)	(14.7%)	(19.4%)	(6.6%)	(15.1%)		Poor
PFC	US 271	127	0.157	0.87	18.6	52.157	29.8%	
		(12.6%)	(26.1%)	(41.2%)	(18.3%)	(21.2%)		

* The ratings of the mixes in the last column are based on their historical rutting performance in the field and the lab (HWTT).
** Values in the parentheses denote coefficient of variation (COV) of the replicates tested.

The SPST results showed potential to characterize and differentiate the HMA shear resistance properties. As theoretically expected, the coarse-graded Type B mix exhibited the highest shear resistance potential based on its higher shear strength (456 psi) compared to the other mixes evaluated (Table 4-3). The SSE results also reaffirmed that a higher amount of energy (62.6 kJ/m^2) was expended to impart shear failure to this mix as compared to the less shear resistant mixes such as US 271 PFC (18.6 kJ/m^2).

Compared to the other mixes listed in Table 4-3 such as Type C (Loop 480), the SMA mix, which is traditionally known to exhibit good rutting resistance properties, did not perform as theoretically expected. However, the unexpected performance of this particular SMA mix (i.e., τ_s = 222 psi versus for 321 psi for Type C Loop 480 for instance) is possibly attributed to its high sample AVs that were erroneously molded at 23.2 percent. It is most likely from Table 4-3 and Figure 4-8 that its SPST performance would probably have been in the top rank if the SMA samples were evaluated at 7 ± 1 percent AV. Unlike PFC mixes, which are placed at around 80 percent AV, SMA mixes are typically placed at target densities around 96 percent and 97 percent in the field with laboratory performance testing conducted at 7 ± 1 percent AV. Thus, there is need to evaluate more SMA mixes in the SPST at 7 ± 1 percent AV.

From Table 4-3, it is also evident that the SPST produces fairly repeatable test results marked by the COV values that are well within the 30 percent benchmark. With the exception of the porous-graded PFC mix, the COV values for shear strength and SSE parameters are, in fact, less than 15 percent.

SCREENING OF HMA MIXES: DISCRIMINATORY RATIO AND STATISTICAL ANALYSIS

One important aspect to consider for the newly introduced SPST shear test is its ability to serve as an HMA mix screener, which is a very crucial aspect of the HMA mix-design process. The results presented in Table 4-3 and Figure 4-8 already provide an assessment of the evaluated shear parameters' ability to differentiate the shear resistance potential of the mixes. To further investigate the ability of the shear parameters to screen mixes, two approaches were used: 1) the discriminatory ratio (DR) concept and 2) Tukey's honestly significant difference (HSD) statistical analysis.

The DR is an arithmetic ratio of two corresponding parametric values (e.g., τ_s, γ_s, G_s, SSE, and SSE Index) comparing a good shear resistant mix with a relatively poor shear resistant or reference mix. The larger the DR in magnitude, the greater the difference between the mixes and the more effective the shear parameter is in discriminating mixes. To compare the DR-based mix screening ability of the shear parameters, three mixes were intuitively chosen, namely the IH 35 Type B designated as "very good" (VG) mix, the Loop 480 Type C as a "good" (G) mix, and the SH 121 CAM as a "poor" (P) mix. The resulting DR values are presented in Table 4-4.

Table 4-4. Screening of HMA Mixes Based on Discriminatory Ratios.

Mix Type	τ_s	γ_s	G_s	SSE	SSE Index	Comment
Type B/CAM	2.562	1.412	1.810	3.227	1.746	VG/P
Type B/Type C	1.421	1.111	1.286	1.459	1.136	VG/G
Type C/CAM	1.803	1.271	1.408	2.211	1.537	G/P

Using the DR concept in Table 4-4, it is evident that the SPST has potential to differentiate, discriminate, and screen mixes. Based on the higher DR values in magnitude, it can also be concluded that the "shear strength" and "SSE" are the best parameters for discriminating and screening mixes. For instance, the shear strength parameter indicates that the Type B mix is about 2.6 times better than the CAM mix and over three times better in terms of the SSE parameter. The other shear parameters, such as G_s, show that the Type B mix is at maximum 81 percent better than the CAM mix; with the least difference indicataed for the γ_s parameter at 41.2 percent.

Analysis of variance (ANOVA) and Tukey's HSD multiple comparison procedure at a 95 percent confidence level were also used to statistically investigate the potential of the test parameters' ability to differentiate the rutting resistance potential of the HMA mixes (Tukey, 1953). The obtained results are listed in Table 4-5.

Table 4-5. Screening of HMA Mixes Based on ANOVA and Tukey's HSD Analysis.

Mix Type	Highway	τ_s	γ_s	G_s	SSE	SSE Index
Type B	IH 35	A	B	A	A	B
Type B	APT	B	B	A	B	B
Type C	US 83	B	B	A	B	B
Type C	Loop 480	B	B	A	B	B
Type C	SH 21	C	B	B	C	B
Type D	FM 2100	C	B	A	C	B
Type D	US 277	B	B	A	B	B
Type F	US 271	C	B	A	C	B
CAM	SH 121	D	B	A	C	B
SMA	IH 35	C	A	B	B	A
PFC	US 271	D	A	B	C	A

The interpretation of ANOVA results in Table 4-5 is as follows: for each parameter, the mixes are categorized in up to four different "alphabetical groups" (A, B, C, and D). Mixes in the same group have parametric values that are statistically not (significantly) different and vice versa. Numerical values of parameters in groups are arranged in the following order of superiority A > B > C > D. For example, consider the shear strength parameter. The SH 121 CAM and the US 271 PFC mixes are listed in the same statistical group (D), meaning that the shear strength of these two mixes are statistically not significantly different. However, the shear strength values of these two mixes are less than each of the four mixes in statistical group C (SH 21 Type C, FM 2100 Type D, US 271 Type F, and IH 35 SMA) and the difference is statistically significant.

From the statistical analysis presented in Table 4-4, it was evident that the SPST shear strength is the most suitable parameter for HMA mix screening and differentiation, categorizing the 11 mixes into four statistically distinct groups. The SSE is able to categorize the mixes into three statistically distinct groups, whereas, for the remaining three parameters, there were only two statistically distinct groups. However, the relatively low variability of the shear strength and

SSE (denoted by low COV values in Table 4-3) contribute to their better differentiation/screening performance in any statistical comparison.

A ranking of the mixes based on the SPST parameters are presented in Table 4-6.

Table 4-6. Ranking of the HMA Mixes Based on the SPST Parameters.

Mix Type	Highway	τ_s	γ_s	G_s	SSE	SSE Index	Avg all	Avg (τ_s, G_s, SSE)
Type B	IH 35	1	3	1	1	3	1.8	1.0
Type C	Loop 480	2	5	4	2	4	3.4	2.7
Type D	US 277	3	9	2	5	8	5.4	3.3
Type B	APT	4	6	5	3	5	4.6	4.0
Type C	US 83	5	7	3	6	6	5.4	4.7
Type F	US 271	6	8	6	7	7	6.8	6.3
Type C	SH 21	7	4	9	10	11	8.2	8.7
SMA	IH 35	8	2	10	4	1	5.0	7.3
Type D	FM 2100	9	10	7	8	9	8.6	8.0
CAM	SH 121	10	11	8	9	10	9.6	9.0
PFC	US 271	11	1	11	11	2	7.2	11.0

The mixes were initially arranged (ranked) on a descending order of shear strength, then numerical ranking of each mix was assigned in terms of each respective SPST parameter. From the table, it is immediately observed that the coarse graded IH 35 Type B mix tops the ranking on almost all the SPST parameters, the two exceptions being the shear strain and the SSE Index. On the other hand, the dense graded mixes SH 121 CAM and FM 2100 Type D consistently ranked poorly on all the shear parameters. In general, for the shear strength, modulus, and SSE, the ranking of the mixes follows somewhat similar patterns.

Also interesting is the overall ranking trend of the PFC mix. The PFC ranks very highly when arranged based on shear strain and SSE Index. However, it ranks as the poorest mix in terms of the other three SPST parameters. Traditionally, the PFC, though a poor shear resistant mix, performs fairly well in the field due to the interlocking of the aggregates. However, this behavior is not effectively captured by the SPST results, an aspect that may limit the SPST application to open-graded mixes.

Similarly, the SMA, though not an open-graded mix, in general has aggregate structure that contributes to good shear-resistant performance in the field. However, this behavior is also not reflected in the SPST performance of the particular SMA mix that was evaluated in this study, partly due to the high erroneous sample AV (see Table 4-3). Nonetheless, only one of each of these mix types was evaluated in this initial SPST developmental study. Therefore, testing of more PFC (AV at N_{design}) and SMA (at 7 ± 1 percent AV) mixes in future SPST implementation or follow-up studies is strongly recommended.

The last two columns of Table 4-6 present the average ranking of the mixes. Values in the "Avg all" column are calculated by averaging all five numerical rankings of each mix and are expected to give an overall ranking of the mixes from the SPST. However, as discussed above, the ranking produced by the shear strain and the SSE Index parameters shows some inconsistency. Therefore, a second set of average ranking is produced in the last column (Avg of τ_s, G_s, SSE) by excluding these two parameters. The average ranking of mixes, thus produced, is very consistent with the ranking of mixes by the SPST shear stress.

SUMMARY

This chapter introduced the SPST as a simple HMA shear test method. The test method development was described, including the test parameter selection and development of the data analysis models. The overall findings from this study, based on the laboratory tests performed on mixes commonly used in Texas, suggest that the test has promising potential as an HMA routine shear test. The proposed SPST parameters with samples in confined conditions are bullet-listed below:

- HMA specimen dimensions: 2.5-inch thick by 6.0-inch diameter
- HMA sample sitting time: Test lab-molded samples within 5 days of molding
- Monotonic compressive-loading rate: 0.2 mm/sec
- Punching loading head: 1.5 inches
- Test temperature: 50°C (test at 50, 55, and 60°C for mixes to be used in high temperature locations, high shear stress areas, urban stop-go sections, intersections, etc.).
- Sample restraint: Laterally confined

- Output and measurable data: Peak shear failure load, shear failure displacement at peak load, HMA shear strength (τ_s), shear strain (γ_s), HMA shear modulus (G_s), shear strain energy (SSE), and SSE Index.

- HMA mix screening parameters: Shear strength and SSE. These two parameters also exhibited superior repeatability with variability and COV values less than 30 percent.

- Confining torque 25 in-lb

CHAPTER 5   SPST SENSITIVITY EVALUATION

This chapter discusses the sensitivity evaluation of the newly developed HMA shear test, namely the SPST. For the SPST to be considered as a routine supplementary test for evaluating HMA rutting/shear properties in the laboratory, it is vital that the test's sensitivity to HMA mix-design parameters and the test input parameters are properly studied. The research team studied the SPST sensitivity to the following variables:

- SPST loading rate.
- SPST temperature.
- Asphalt-binder type.
- Asphalt-binder content.

Plant-mix and raw materials (asphalt-binders and aggregates) were collected from various field projects, and extensive laboratory tests were conducted by varying the parameters for each of these critical steps to analyze the sensitivity of the SPST results. The mix design descriptions are presented in Chapter 2 of this report. For all the sample fabrication procedures and testing, the same operators with similar skill level and the same test equipment were used in the TTI lab. This was necessary to exclude the operator and/or equipment effect in the analysis. The results obtained from the studies are discussed in detail in the following subsections.

SPST LOADING RATE

The SPST is run in a monotonic-loading displacement controlled mode. Therefore, the loading rate (applied displacement rate) should have a considerable effect on the output results. To study this effect, four mixes were tested with the SPST loading rate varied between 0.1 mm/sec and 0.3 mm/sec. The obtained L-D response curves from this study are presented in Figure 5-1.
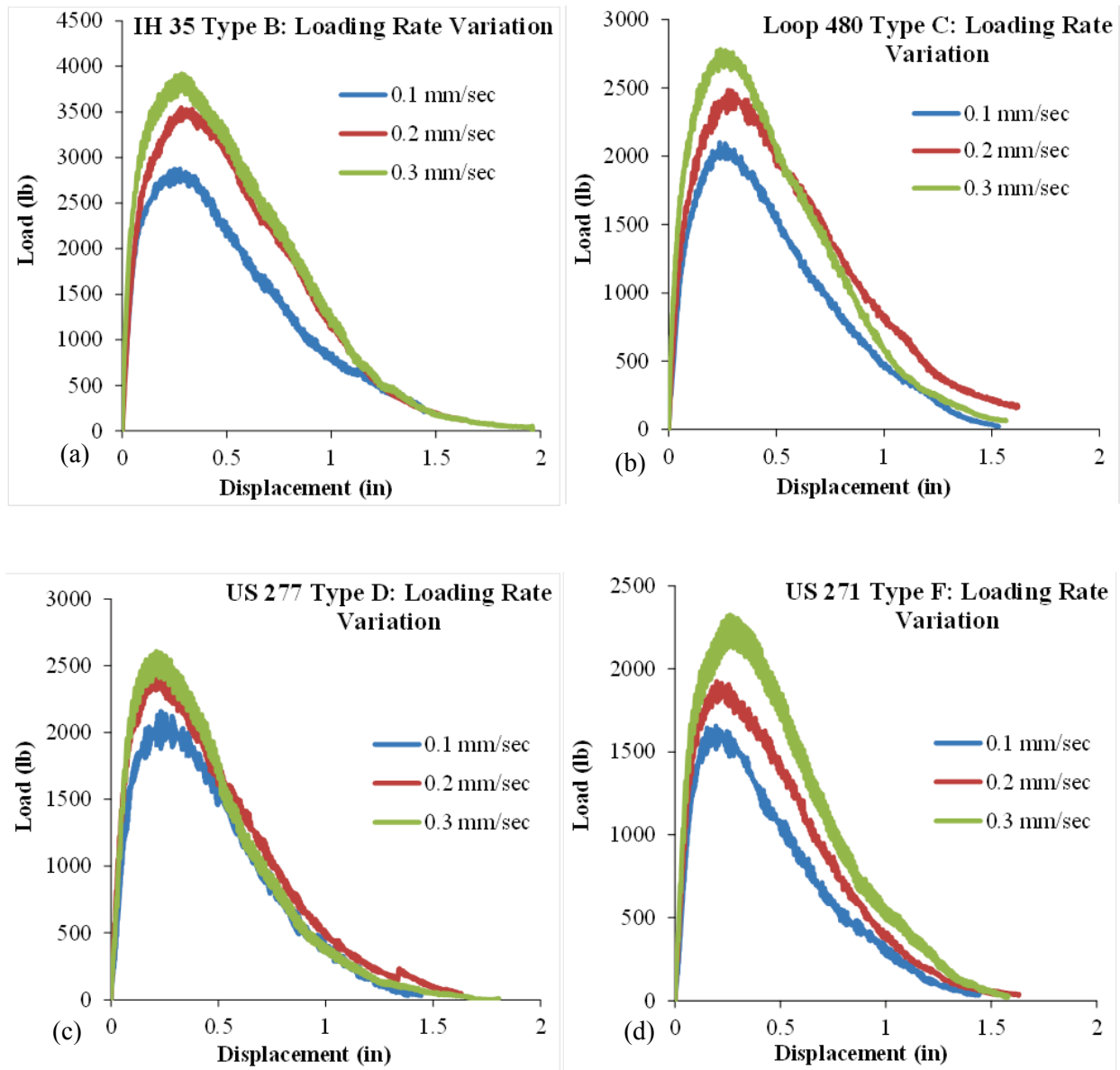
Figure 5-1. Comparison of SPST Results in Terms of Loading Rate: (a) IH 35 Type B, (b) Loop 480 Type C, (c) US 277 Type D, and (d) US 271 Type F.

For the four mixes that were evaluated for this study, Figure 5-1 shows good sensitivity of the SPST L-D output with loading rate variation. The SPST L-D data were further analyzed to comparatively study the HMA shear properties of the mixes. The computed SPST-HMA shear parameters are presented in Table 5-1 and Figure 5-2.

Table 5-1. Results Summary: SPST Loading Rate Variation.

Mix Description	Loading Rate (mm/sec)	Shear Strength (psi)	Shear Strain (in/in)	Shear Mod. (ksi)	SSE (kJ/m^2)	SSE Index
IH 35 Type B	0.10	368	0.112	3.30	48.5	33.697
		0.6%	*8.8%*	*9.3%*	*0.7%*	*8.6%*
	0.20	456	0.120	3.82	62.6	37.429
		7.0%	*5.9%*	*0.7%*	*1.2%*	*1.9%*
	0.30	497	0.114	4.37	65.8	34.357
		0.6%	*0.6%*	*0.4%*	*3.4%*	*3.0%*
Loop 480 Type C	0.10	269	0.097	2.77	31.7	26.170
		2.1%	*6.8%*	*7.5%*	*5.0%*	*2.9%*
	0.20	321	0.108	2.97	42.9	32.958
		1.8%	*1.9%*	*3.5%*	*7.4%*	*7.5%*
	0.30	361	0.110	3.30	42.7	29.763
		8.1%	*7.1%*	*15.2%*	*6.1%*	*9.1%*
US 277 Type D	0.10	277	0.097	2.86	30.3	24.157
		3.30%	*5.80%*	*2.40%*	*3.10%*	*0.60%*
	0.20	319	0.087	3.67	36.4	22.659
		1.10%	*9.80%*	*8.50%*	*4.40%*	*13.50%*
	0.30	325	0.086	3.79	36.5	22.058
		2.90%	*1.60%*	*4.90%*	*4.70%*	*9.60%*
US 271 Type F	0.10	213	0.07	3.09	27.8	20.546
		0.10%	*18.20%*	*18.60%*	*19.20%*	*0.60%*
	0.20	248	0.089	2.82	28.8	23.545
		9.80%	*19.10%*	*11.00%*	*4.10%*	*14.10%*
	0.30	296	0.094	3.19	35.9	26.059
		0.30%	*16.50%*	*15.90%*	*0.50%*	*15.30%*

* Coefficient of Variation (COV) in Italic
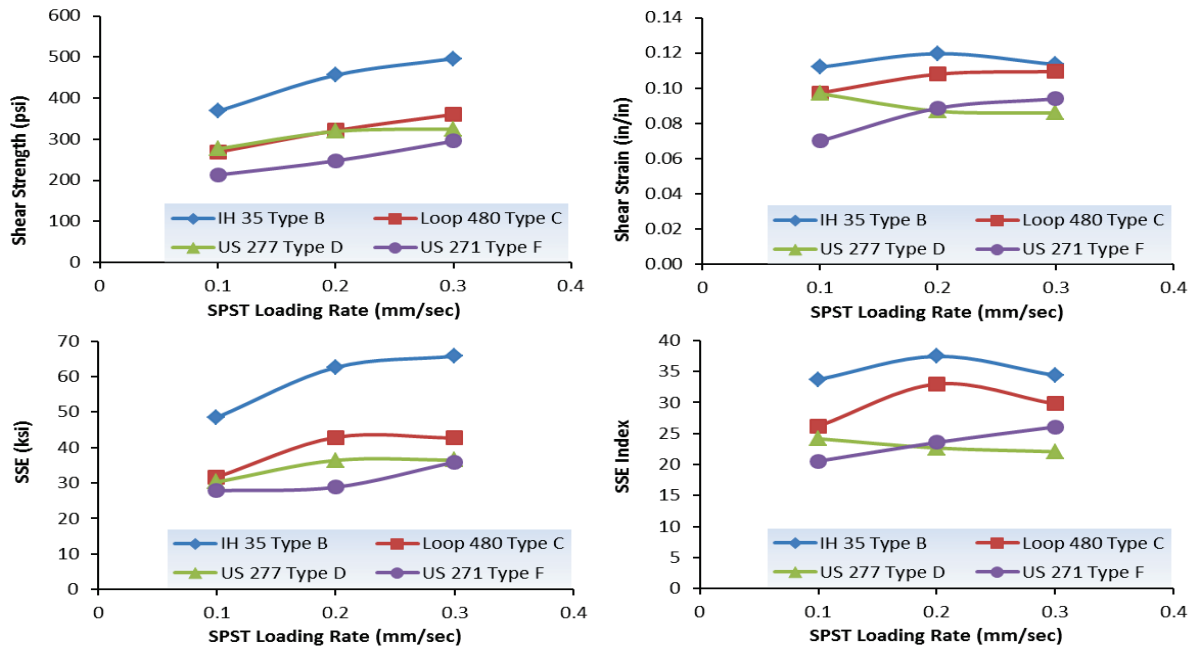
Figure 5-2. SPST Sensitivity to Loading Rate Variation.

From the results in Table 5-1 and Figure 5-2, it is evident that the obtained SPST results show good sensitivity to SPST loading rate variation. Especially, the shear strength and shear strain energy parameters show a definitive increasing trend with increasing loading rate for all four mixes. This behavior is, indeed, theoretically expected. At a higher loading rate, the mix is given less recovery time; hence, there is a greater resistance to shear failure, which consequently results in greater shear strength building up. This may, partially, explain some HMA shear failure behaviors observed in the field, where greater rutting rates have been recorded at intersections with slow-moving vehicles. Notably, no definitive trend is observed for the SSE and SSE Index parameters with varying loading rate.

The sensitivity of the SPST results to loading rate variation is statistically analyzed using ANOVA and Tukey's HSD comparison at a 95 percent reliability level, and the results are shown in Table 5-2.

Table 5-2. Sensitivity to Loading Rate: ANOVA and Tukey's HSD Statistical Analysis.

Mix Description	Loading Rate (mm/sec)	Shear Strength (psi)	Shear Strain (in/in)	Shear Mod. (ksi)	SSE (kJ/m^2)	SSE Index
IH 35 Type B	0.1	C	A	C	B	A
	0.2	B	A	B	A	A
	0.3	A	A	A	A	A
Loop 480 Type C	0.1	C	A	A	B	B
	0.2	B	A	A	A	A
	0.3	A	A	A	A	A
US 277 Type D	0.1	C	A	B	A	A
	0.2	B	A	A	A	A
	0.3	A	A	A	A	A
US 271 Type F	0.1	C	A	A	B	A
	0.2	B	A	A	B	A
	0.3	A	A	A	A	A

The interpretation of ANOVA results in Table 5-2 is as follows: for each parameter, the mixes are categorized in different "alphabetical groups" (A, B, and C). Mixes in the same group have parametric values that are statistically not (significantly) different and vice versa. Numerical values of parameters in groups are arranged in the following statistical order of superiority: A > B > C.

Table 5-2 gives statistical validity to the observations made from Table 5-1 and Figure 5-1 and Figure 5-2 regarding the sensitivity of the SPST to loading rate. Especially, the shear strength parameter clearly captures the SPST sensitivity to varying loading rate, whereas the sensitivity of the shear modulus and the SSE parameters are also fairly good. However, the relatively low variability of the shear strength (denoted by low COV values in Table 5-1) contributes to their better differentiation/screening performance in any statistical comparison.

SPST TEMPERATURE

Higher field rutting and shear failure rates caused by high pavement temperatures in Texas have been an issue of concern in recent years. Studying the effect of temperature on HMA shear properties is particularly important to properly address this issue. Therefore, the research team thoroughly studied the temperature sensitivity of the newly developed SPST. Four mixes

were tested in the SPST setup with the test temperature varied between 40 and 60°C. The generated SPST L-D response curves are illustrated in Figure 5-3.
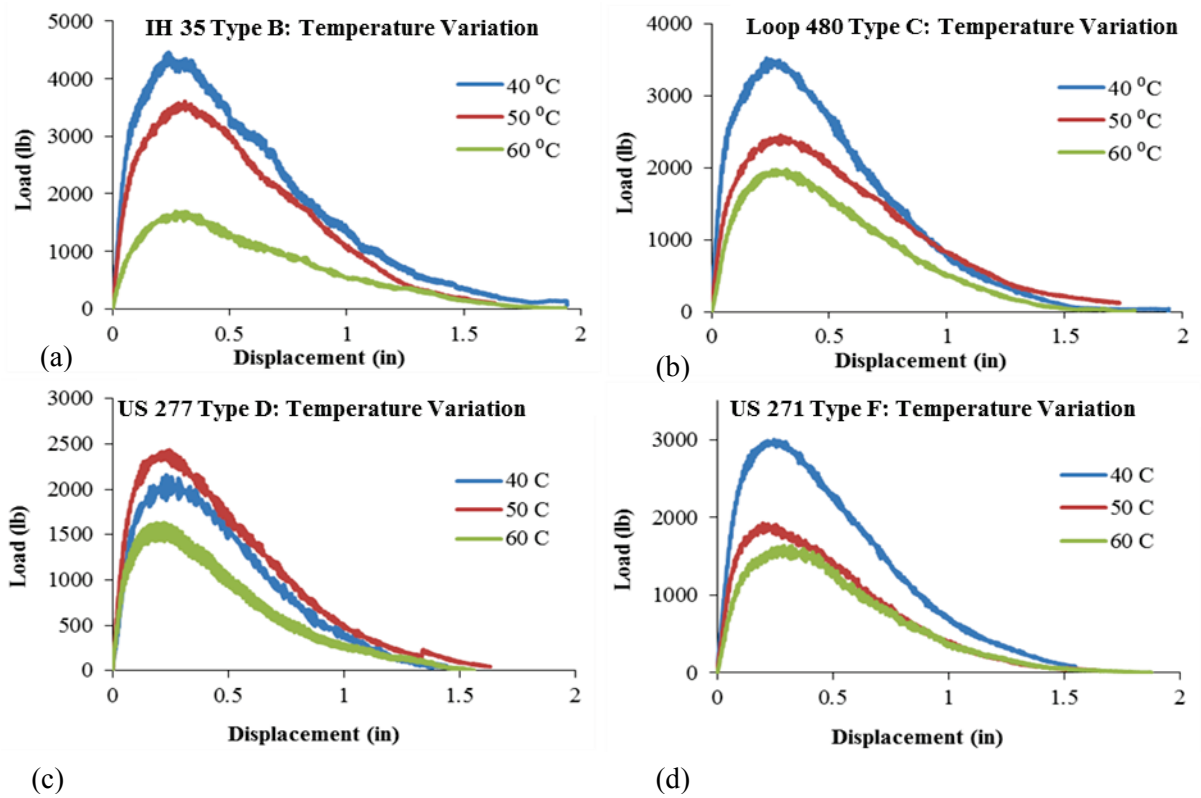
Figure 5-3. SPST Output Sensitivity to Temperature Variation: (a) IH 35 Type B, (b) Loop 480 Type C, (c) US 277 Type D, and (d) US 271 Type F.

For the four mixes that were evaluated for this study, Figure 5-3 shows good sensitivity of the SPST L-D output with temperature variation. As shown in Table 5-3 and Figure 5-4, the SPST L-D data were further analyzed to comparatively study the HMA shear properties of the mixes.

Table 5-3. Results Summary: SPST Temperature Variation.

Mix Description	Temperature (°C)	Shear Strength (psi)	Shear Strain (in/in)	Shear Mod. (ksi)	SSE (kJ/m^2)	SSE Index
IH 35 Type B	40	579	0.106	5.48	63.3	31.739
		3.6%	*8.4%*	*7.0%*	*5.7%*	*5.2%*
	50	456	0.108	3.82	62.6	31.940
		5.6%	*21.4%*	*26.9%*	*6.2%*	*20.8%*
	60	217	0.108	1.87	29.1	45.437
		6.7%	*8.0%*	*14.7%*	*0.7%*	*14.0%*
Loop 480 Type C	40	458	0.110	4.18	55.1	30.176
		2.4%	*7.4%*	*9.8%*	*5.8%*	*7.5%*
	50	321	0.108	2.97	42.9	31.940
		5.6%	*21.4%*	*26.9%*	*6.2%*	*20.8%*
	60	255	0.108	2.34	32.2	45.437
		6.7%	*8.0%*	*14.7%*	*0.7%*	*14.0%*
US 277 Type D	40	358	0.086	4.17	40.1	22.058
		3.0%	*1.6%*	*4.9%*	*4.7%*	*9.6%*
	50	319	0.087	3.67	36.4	22.659
		1.1%	*9.8%*	*8.5%*	*4.4%*	*13.5%*
	60	220	0.089	2.47	22.8	21.129
		7.5%	*0.0%*	*7.2%*	*5.3%*	*2.0%*
US 271 Type F	40	391	0.093	4.25	47.5	26.031
		2.30%	*14.1%*	*11.8%*	*12.4%*	*25.3%*
	50	248	0.089	2.82	28.8	23.545
		9.8%	*19.1%*	*11.0%*	*4.1%*	*14.1%*
	60	212	0.126	1.71	25.2	34.341
		14.2%	*25.8%*	*12.1%*	*16.5%*	*28.3%*

* Coefficient of Variation (COV) in Italic
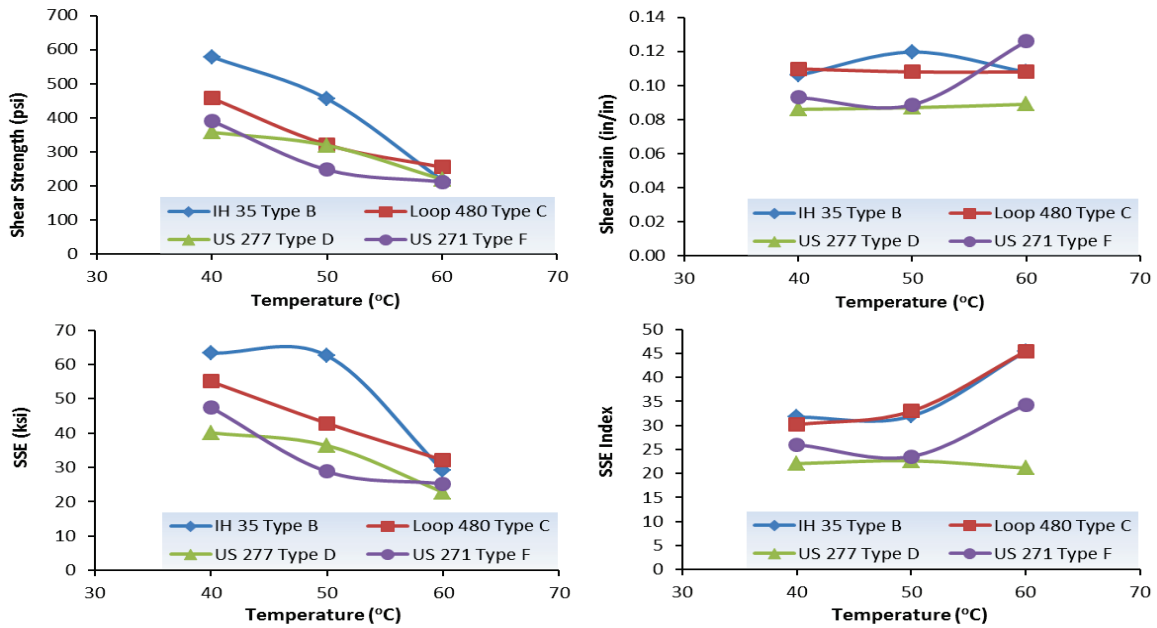
Figure 5-4. SPST Sensitivity to Temperature Variation.

From the results in Table 5-3 and Figure 5-4, it is evident that the SPST results show good sensitivity to test temperature variation. In particular, the shear strength and shear strain energy parameters show a definitive decreasing trend with increasing temperature for all four mixes. This behavior is, indeed, theoretically expected. At higher temperatures, the mixes get softer; as a result, both shear strength and the strain energy required to cause shear failure are reduced. Similar to the study of loading rate variation, the shear strain and SSE Index sensitivity to temperature variation, as seen in Figure 5-4, shows no definitive trend.

The sensitivity of the SPST results to temperature variation was also statistically analyzed using ANOVA and Tukey's HSD comparison at a 95 percent reliability level. The results of these statistical analyses are presented in Table 5-4.

Table 5-4. SPST Temperature Sensitivity: ANOVA and Tukey's HSD Statistical Analysis.

Mix Description	Temperature (°C)	Shear Strength (psi)	Shear Strain (in/in)	Shear Mod. (ksi)	SSE (kJ/m^2)	SSE Index
IH 35 Type B	40	A	A	A	A	B
	50	B	A	B	A	A
	60	C	A	C	B	A
Loop 480 Type C	40	A	A	A	A	A
	50	B	A	B	B	A
	60	C	A	B	C	A
US 277 Type D	40	A	A	A	A	A
	50	B	A	B	A	A
	60	C	A	C	B	A
US 271 Type F	40	A	A	A	A	A
	50	B	A	B	B	A
	60	B	A	C	B	A

The interpretation of ANOVA results in Table 5-4 follows the same conceptual explanations discussed in the preceding subsection. Table 5-4 gives statistical validity to the observations made from Table 5-3, Figure 5-3, and Figure 5-4 regarding the sensitivity of the SPST to test temperature. In particular, the shear strength and the shear modulus parameter clearly capture the SPST sensitivity to varying temperature, whereas, the sensitivity of the SSE parameter is also fairly good. However, the relatively low variability of the shear strength (denoted by low COV values in Table 5-3) contributes to their better differentiation/screening performance in any statistical comparison.

ASPHALT-BINDER TYPE

In order to assess the sensitivity of the SPST to HMA mix-design variables, the test was run on three mixes with varying asphalt-binder type (PG grade). Three mixes were molded in the laboratory by mixing raw materials, namely a Type D mix from Atlanta District, a Type D mix from Chico, and a Type C mix from Laredo District. The optimum asphalt content for the mixes for each asphalt-binder type was determined using the Texas Gyratory Compactor methods (TxDOT, 2009). The resulting SPST L-D response curves are shown in Figure 5-5.
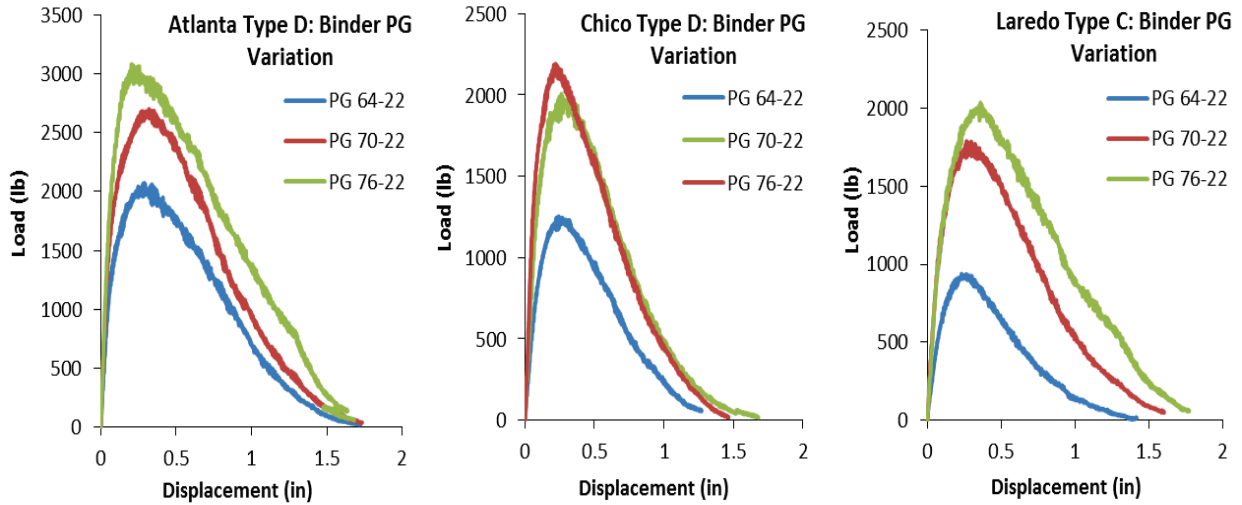
Figure 5-5. SPST L-D Output: Sensitivity to Asphalt-Binder PG Variation.

For the three mixes that were evaluated, Figure 5-5 shows good sensitivity of the SPST L-D output to the variation in asphalt-binder PG grade/type. In general, higher PG asphalt-binders are theoretically less susceptible to rutting/shear failures, and the findings from Figure 5-5 are consistent with this behavior. As presented in Table 5-5 and Figure 5-6, the SPST L-D data were further analyzed to comparatively study the shear properties of the mixes.

Table 5-5. Results Summary: SPST Binder Type Variation.

Mix Description	Binder Type	Shear Strength (psi)	Shear Strain (in/in)	Shear Mod. (ksi)	SSE (kJ/m^2)	SSE Index
Atlanta Type D	PG 64-22	269	0.115	2.37	37.0	36.242
		7.1%	*10.3%*	*17.3%*	*5.9%*	*15.7%*
	PG 70-22	350	0.117	2.99	49.2	37.484
		13.8%	*7.8%*	*10.3%*	*18.9%*	*13.2%*
	PG 76-22	426	0.124	3.57	58.3	39.069
		11.9%	*20.6%*	*29.9%*	*8.2%*	*24.1%*
Chico Type D	PG 64-22	161	0.102	1.57	18.2	26.137
		17.8%	*8.3%*	*15.0%*	*23.2%*	*8.5%*
	PG 70-22	257	0.115	2.25	31.4	31.866
		3.9%	*7.3%*	*4.1%*	*5.5%*	*4.9%*
	PG 76-22	286	0.098	2.93	32.6	25.847
		4.4%	*9.4%*	*12.0%*	*9.0%*	*20.1%*
Laredo Type C	PG 64-22	120	0.1	1.2	12.7	24.286
		1.6%	*4.2%*	*2.5%*	*4.5%*	*1.9%*
	PG 70-22	232	0.115	2.13	30.4	34.452
		11.6%	*25.8%*	*28.7%*	*15.7%*	*29.6%*
	PG 76-22	265	0.129	2.08	39.1	43.890
		2.8%	*15.3%*	*13.1%*	*12.2%*	*23.8%*

* Coefficient of Variation (COV) in Italic
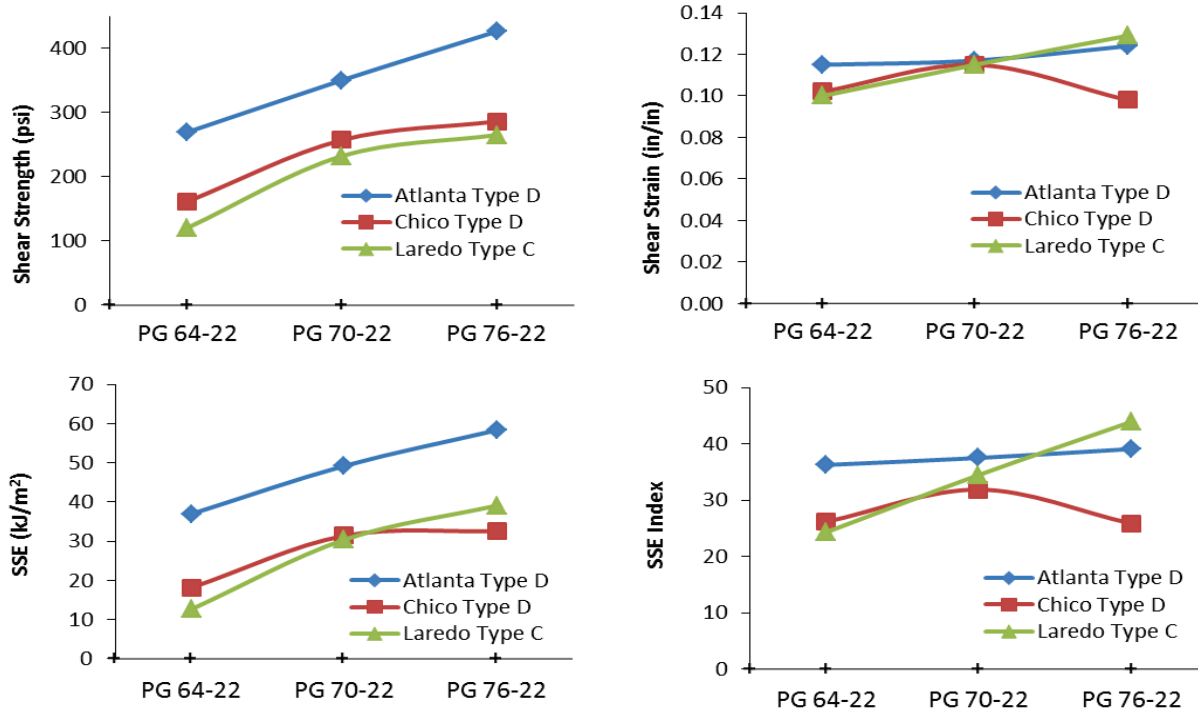
Figure 5-6. SPST Sensitivity to Asphalt-Binder Type (PG) Variation.

The sensitivity of the SPST results to variation in the asphalt-binder PG grade/type was statistically analyzed using ANOVA and Tukey's HSD at a 95 percent reliability level. The statistical results are presented in Table 5-6.

Table 5-6. SPST Sensitivity to Binder Type: ANOVA and Tukey's HSD Statistical Analysis.

Mix Description	Binder Type	Shear Strength (psi)	Shear Strain (in/in)	Shear Mod. (ksi)	SSE (kJ/m^2)	SSE Index
Atlanta Type D	PG 64-22	C	A	A	A	A
	PG 70-22	B	A	A	B	A
	PG 76-22	A	A	A	C	A
Chico Type D	PG 64-22	B	A	C	B	A
	PG 70-22	A	A	B	A	A
	PG 76-22	A	A	A	A	A
Laredo Type C	PG 64-22	C	A	A	B	A
	PG 70-22	B	A	A	A	A
	PG 76-22	A	A	A	A	A

The interpretation of ANOVA results in Table 5-4 follows the same conceptual explanations discussed in the preceding subsection. Table 5-6 gives statistical credence to the observations made from Table 5-5, Figure 5-5 and Figure 5-6. Similar to the previous observations, the shear strength and the SSE parameters exhibit superiority in capturing the SPST sensitivity to varying asphalt-binder PG grade/type, whereas the sensitivity of the shear modulus is also fairly good. However, the relatively low variability of the shear strength (denoted by low COV values in Table 5-5) contributes to their better differentiation/screening performance in any statistical comparison.

ASPHALT-BINDER CONTENT

In order to further assess the sensitivity of the SPST to HMA mix-design variables, the test was run on three mixes with varying asphalt binder content (AC). Three Type D mixes, namely from Atlanta, Chico, and Amarillo, were mixed from raw aggregates in the laboratory with the AC varied from 0.5 percent below to 0.5 percent above the OAC; all the mixes utilized PG 64-22. The corresponding SPST L-D response curves are presented in Figure 5-7.
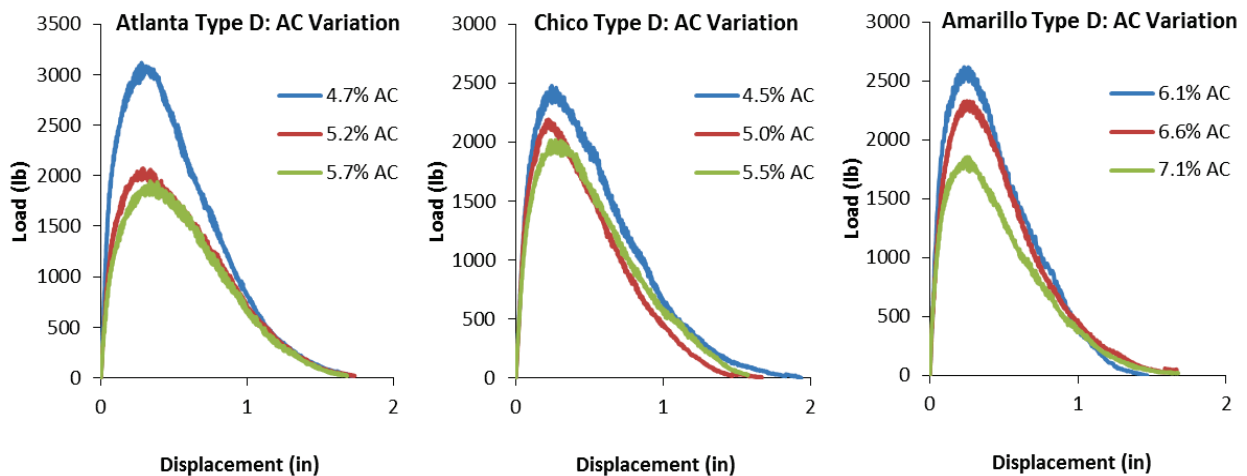
Figure 5-7. SPST L-D Output: Sensitivity to Asphalt-Binder Content Variation.

For the three mixes that were evaluated for this study, Figure 5-7 shows good sensitivity of the SPST L-D output with AC variation. The SPST L-D data were further analyzed to comparatively study the HMA shear properties of the mixes; see Table 5-7 and Figure 5-8 below. As indicated in Appendix A, the Amarillo Type D mix contains RAP and RAS with about 27.1 percent recycled asphalt-binder. Therefore, only about 4.8 percent of the 6.6 percent OAC is

virgin asphalt-binder, i.e., 27.1 percent of the AC is recycled asphalt-binder. Thus, if only considering the virgin asphalt-binder, the three AC levels in Figure 5-7 and Table 5-7 for the Amarillo Type D mix are approximately in the order 4.3, 4.8, and 5.3 percent, respectively.

Table 5-7. SPST Results Summary: AC Variation.

Mix Description	AC	Shear Strength (psi)	Shear Strain (in/in)	Shear Mod. (ksi)	SSE (kJ/m^2)	SSE Index
Atlanta Type D	4.7%	401	0.117	3.43	50.9	33.976
		8.2%	8.1%	8.3%	10.4%	10.6%
	5.2%	269	0.115	2.37	37.0	36.242
		3.9%	4.3%	0.0%	8.1%	8.9%
	5.7%	250	0.140	1.79	34.5	43.923
		11.3%	7.0%	14.0%	17.2%	4.0%
Chico Type D	4.5%	318	0.101	3.14	38.9	28.345
		1.5%	6.3%	7.4%	7.0%	7.4%
	5.0%	286	0.098	2.93	32.6	25.847
		4.1%	12.9%	16.9%	11.8%	28.3%
	5.5%	259	0.111	2.36	31.5	30.829
		5.2%	12.9%	8.5%	12.4%	20.8%
Amarillo Type D	6.1%	347	0.098	3.56	41.8	26.796
		3.9%	5.5%	8.3%	11.9%	5.0%
	6.6%	304	0.102	2.99	36.4	27.826
		7.2%	15.3%	8.0%	3.6%	11.3%
	7.1%	233	0.102	2.30	27.4	27.363
		3.2%	6.4%	9.6%	2.2%	7.8%

* Coefficient of Variation (COV) in Italic
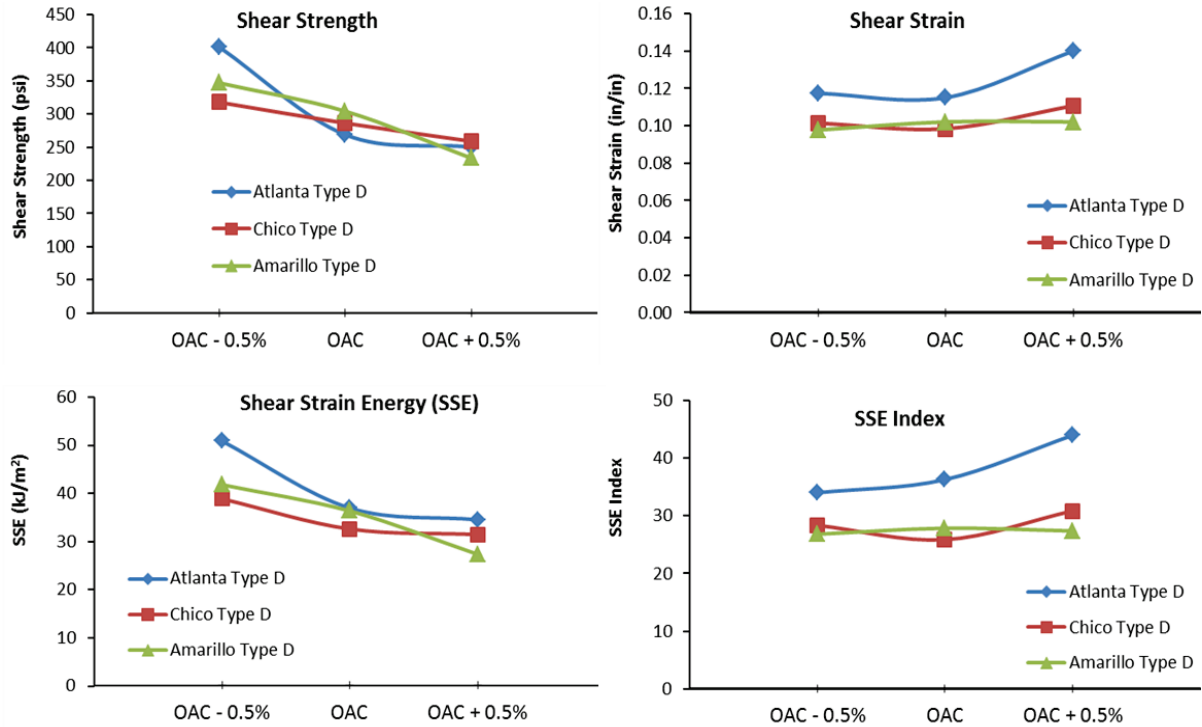
Figure 5-8. SPST Sensitivity to AC Variation.

From the presented SPST results, it is evident that the SPST has good sensitivity to AC variation. Similar to the preceding observations, the shear strength and SSE parameters show a definitive decreasing trend with increasing AC for all three mixes. In general, drier mixes with lower AC are less susceptible to rutting and shear failures in the field as compared to mixes with higher AC. The observations from Table 5-7 and Figure 5-8 are consistent with this behavior. However, the shear strain and the SSE Index parameters show no definitive trend of sensitivity with varying AC.

Similar to the preceding subsections, the sensitivity of the SPST results to AC variation was statistically analyzed using ANOVA and Tukey's HSD comparison at a 95 percent reliability level. The results of these statistical analyses are presented in Table 5-8.

Table 5-8. SPST Sensitivity to AC Variation: ANOVA and Tukey's HSD Statistical Analysis.

Mix Description	AC	Shear Strength (psi)	Shear Strain (in/in)	Shear Mod. (ksi)	SSE (kJ/m^2)	SSE Index
Atlanta Type D	4.7%	A	A	A	A	A
	5.2%	B	A	B	B	A
	5.7%	B	A	B	B	A
Chico Type D	4.5%	A	A	A	A	A
	5.0%	B	A	A	A	A
	5.5%	C	A	B	B	A
Amarillo Type D	6.1%	A	A	A	A	A
	6.6%	B	A	A	A	A
	7.1%	C	A	B	B	A

The interpretation of ANOVA results in Table 5-4 follows the same conceptual explanations discussed in the preceding subsections. Table 5-8 gives statistical credibility to the observations made in Table 5-7 and Figure 5-7 and Figure 5-8 regarding the sensitivity of the SPST to AC variation. As with the asphalt-binder PG grade, the shear strength parameter also exhibited superiority in effectively capturing the SPST sensitivity to varying AC levels. The sensitivity of the SSE and the shear modulus parameters are also fairly good. However, the relatively low variability associated with the shear strength (denoted by low COV values in Table 5-7) contribute to their better differentiation/screening performance in any statistical comparison.

SPST REPEATABILITY AND STATISTICAL VARIABILITY IN THE TEST DATA

Like most monotonic loading tests, overall, the SPST was found to be a very repeatable test. The test data and almost all the HMA parameters evaluated in this chapter exhibited acceptable consistency with low variability and COV values within the 30 percent benchmark. Parameter-wise, the shear strength exhibited superiority in terms of consistency and low variability. Although within the 30 percent threshold, the shear strain, shear modulus, and SSE Index generally appeared to be more variable. As theoretically expected of HMA due to its visco-elastic nature, variability generally tended to increase with increasing temperature.

SUMMARY

This chapter presented and discussed the sensitivity of the SPST results to test input parameters (e.g., loading rate and temperature) and HMA mix variables (e.g., asphalt-binder type and content). The overall findings from this chapter, based on the laboratory tests performed using mixes commonly used in Texas, can be summarized as follows:

- The SPST was found to be reasonably sensitive to test input parameters (e.g., loading rate and temperature) and HMA mix variables (e.g., asphalt-binder type and content).

- Among the five HMA shear parameters calculated from the SPST, the shear strength was found to be the most sensitive to the test input variables, followed by the shear strain energy and shear modulus.

- For the mixes evaluated, the shear strain and the SSE Index parameters did not show any definitive trend with changing test input parameters and HMA mix-design variables.

- Based on the observed SPST results, the shear resistance of the tested HMA mixes increased with test loading rate and decreased with test temperature. Both these behaviors are theoretically expected. At a higher loading rate, the mixes get less recovery time, thus increasing resistance to shear failure. At higher temperature, the mixes become softer, thus decreasing the shear resistance.

- The shear resistance of the tested mixes increased with asphalt-binder PG grading and decreased with asphalt-binder content. In general, any mix with higher PG grade traditionally performs well under shear loading in the field, whereas, shear performance of the mixes worsens with increased AC due to the increased softness of the mix.

- A statistical analysis at 95 percent confidence level showed the supremacy of the shear strength and SSE parameters over the shear strain and SSE Index in capturing the SPST sensitivity to input parameters and HMA mix-design variations, thus confirming the findings from the graphical plots. These findings also substantiate Chapter 4's recommendations to adapt the shear strength and SSE as the mix screening parameters for HMA shear resistance potential.

CHAPTER 6   LABORATORY TEST CORRELATIONS – SPST VERSUS HWTT, FN, RLPD, AND DM TESTS

As part of the HMA mix- and structural-design process to optimize field performance, several laboratory tests are routinely used by many agencies to characterize the HMA mix rutting and permanent deformation resistance potential. These tests include the Hamburg wheel tracking, the uniaxial repeated load permanent deformation, the dynamic modulus, and the flow number tests.

In this study, researchers have comprehensively studied the HWTT in an attempt to optimize the laboratory mix screening process to better capture the field rutting susceptibility of the HMA. Also, the SPST was developed in this study as a supplementary HMA shear test in order to generate HMA shear parameters, e.g., shear strength (τ_s), shear strain (γ_s), shear modulus (G_s), and shear strain energy (SSE). As a newly developed test, the SPST needs to be compared and correlated with the other existing HMA rutting tests. This chapter presents the comparison and the correlation of the SPST with these aforementioned HMA rutting/PD tests.

DESCRIPTION OF THE RUTTING AND PD TEST METHODS

The laboratory tests that were compared and correlated with the SPST include the following:

- The Hamburg wheel tracking test.
- The uniaxial repeated load permanent deformation test.
- The dynamic modulus test.
- The flow number test.

Brief descriptions of the test methods are presented below followed by the comparative analysis and discussions of the laboratory test results.

The Hamburg Wheel Tracking Test

The HWTT is used for characterizing the rutting resistance potential and stripping susceptibility (moisture damage potential) of HMA in the laboratory. The detailed discussion on the HWTT procedure and data analysis methods are covered in Chapter 3 of this report. In addition to the traditional HWTT parameters, namely, the HWTT rut depth (Rut_{max}) and the

number of cycles to failure (N_d), three new HWTT parameters are introduced in Chapter 3 in order to better optimize the HWTT in assessing HMA field rutting performance. The new parameters are: the HWTT rutting area (Δ), the normalized rutting area (Rut_Δ), and the shape factor (SF). However, to facilitate comparison with the SPST results in this chapter, the researchers attempted to evaluate HMA shear properties from the HWTT data through introducing the following additional parameters:

The HWTT-HMA Strength (τ_H)

The HWTT-HMA strength is defined as the ratio of the HWTT wheel load and the failure surface area and is calculated using the following formula:

$$\tau_H = \frac{HWTT\ wheel\ load}{Rutting\ surface\ area} = \frac{W}{A} \tag{6.1}$$

In the current HWTT test procedure (Tex-242-F), the specified wheel load is 158 lb.

The HWTT-HMA Strain (γ_H)

The HWTT-HMA strain is defined as the normalized deformation of the HMA samples under HWTT wheel loading relative to the sample thickness. Mathematically, it is calculated using the following formula:

$$\gamma_H = \frac{HWTT\ rut\ depth}{Sample\ thickness} = \frac{Rut_{max}}{t} \tag{6.2}$$

The HWTT-HMA Modulus (G_H)

The HWTT-HMA modulus is defined as the ratio of the HWTT-HMA strength and the HWTT-HMA strain. Mathematically, it is calculated using the following formula:

$$G_H = \frac{\tau_H}{\gamma_H} \tag{6.3}$$

The Flow Number Test

The FN test protocol was developed and introduced in the NCHRP project 9-19 (Witczak et al., 2002) as a simple performance test to evaluate the rutting susceptibility of HMA mixes. As

shown in Figure 6-1, the FN test was conducted in a repeated compressive Haversine loading (0.1 s loading time and 0.9 s resting time=1 cycle) mode to measure the vertical accumulated permanent strains as a function of the loading cycles.
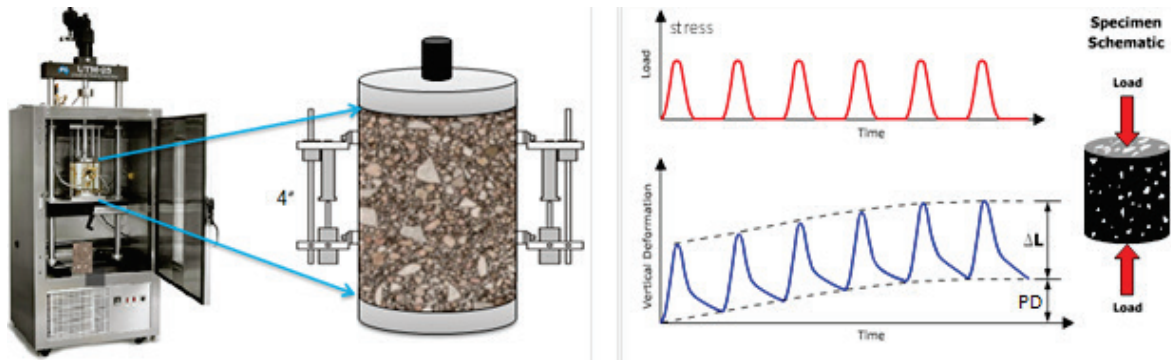
Figure 6-1. FN Test Setup and Configuration.

NCHRP project 9-19 recommended conducting the FN test at the effective pavement temperature in an unconfined mode with a vertical stress between 10 and 30 psi (Witczak et al., 2002). Accordingly, the deviator stress used in this study was 30 psi, which is also recommended in other studies (Witczak et al., 2002; Goh et al., 2011; Apeagyei, 2011). For consistency with the temperature of the traditional HWTT, and to closely simulate the Texas high summer pavement surface temperatures, the temperature selected for the FN test was 50°C. The test was set to terminate at 10,000 loading cycles or an accumulated 30,000 microstrains (με), whichever came first.

Figure 6-2 presents a typical plot of accumulated permanent strain versus number of loading cycles on a log-log scale. Three basic zones are identified:

- Primary: the portion in which the deformation rate decreases with loading cycles.
- Secondary: the portion in which the deformation rate is constant with loading cycles.
- Tertiary flow: the portion in which the deformation rate again increases with loading cycles.
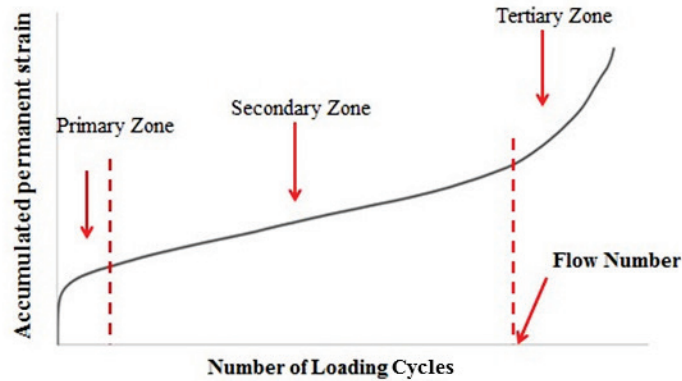
Figure 6-2. Plot of Accumulated Permanent Strain vs. Number of Loading Cycles.

The output data from the FN test include the following (Figure 6-2):

- Flow number (FN), in cycles, is the number of load cycles at which the HMA mix enters the tertiary zone (i.e., onset of tertiary flow) under vertical repeated loading, which corresponds to the minimum value of the strain rate (i.e., minimum value of the curve slope).
- Accumulated permanent strain at the onset of tertiary flow, $\varepsilon p(F)$, in microns.
- Time to the onset of tertiary flow, $t(F)$, in minutes.

In addition to the FN parameter, which has been widely accepted as a laboratory rutting performance indicator (Witczak et al., 2002; Goh et al., 2011; Apeagyei, 2011), a new concept of the FN Index (Equation 6.4) was introduced. The FN Index constitutes a balanced parameter for evaluating the HMA rutting resistance and takes into account both the strains and the number of load cycles sustained to reach tertiary flow. Lower values of the FN Index are related to higher rutting resistance of the HMA mix and vice versa.

$$FN\ Index = \frac{\varepsilon_p(F)}{FN} \qquad\qquad 6.4$$

The Dynamic Modulus Test

Unconfined DM testing is an AASHTO standardized test method for characterizing the stiffness, measured in terms of the dynamic complex modulus, |E*|, and visco-elastic properties of HMA mixes (AASHTO, 2003). The DM is a stress-controlled test involving application of a repetitive sinusoidal dynamic compressive-axial load (stress) to an unconfined specimen over a

range of multiple temperatures (i.e., −10 to 54.4°C) and loading frequencies (i.e., 0.1 to 25 Hz). The typical parameter that results from the DM test is the |E*|, which is computed as:

$$|E^*| = \frac{\sigma_o}{\varepsilon_o} \qquad\qquad 6.5$$

where σ_o is the axial (compressive) stress, and ε_0 is the axial (compressive) resilient strain. For graphical analysis and easy interpretation of the DM data, |E*| master-curves were also generated as a function of the loading frequency using Pellinen and Witczak's (2002) time-temperature superposition sigmoidal model shown in Equations 6.6 and 6.7:

$$Log\,|E^*| = \delta + \frac{\alpha}{1 + e^{\beta - \gamma \log(\xi)}} \qquad\qquad 6.6$$

$$Log(\xi) = \log(f) + \log(a_T) \qquad\qquad 6.7$$

where ξ is the reduced frequency (Hz), δ is the minimum |E*| value (MPa), α is the span of |E*| values, and β and γ are shape parameters. Parameters f and a_T are the loading frequency and temperature shift factor to temperature T, respectively. For this study, the reference temperature was 21.1°C.

The Uniaxial Repeated Loading Permanent Deformation Test

The RLPD test was used to characterize the permanent deformation properties of HMA mixes under repeated compressive Haversine loading, in an unconfined loading mode, at two test temperatures, namely 40 and 50°C (Zhou and Scullion, 2004). For the purpose of this study, the visco-elastic parameters α and μ were computed as a function of a log-log plot of the accumulated plastic strain (ε_p) versus the number of load cycles (N) as follows:

$$\varepsilon_p = aN^b \qquad\qquad 6.8$$

$$\alpha = 1 - b;\ \mu = \frac{ab}{\varepsilon_{p100}} \qquad\qquad 6.9$$

Parameters *a* and *b* are the intercept and slope of the linear portion of the ε_p-load cycles curve on a log-log scale. Alpha (α) and mu (μ) are rutting parameters, with μ computed using the ε_p at the 100th load cycle (i.e., ε_{p100}) (Zhou and Scullion, 2004).

RESULTS, ANALYSES, AND TEST CORRELATIONS

Up to nine mixes were tested using the HWTT, RLPD, DM, and FN test methods as described in the preceding sections and were compared and correlated with the SPST results. The mix-design details of these mixes are presented in Chapter 2.

However, caution needs to be exercised while directly comparing results from these test methods since the objective and the loading modes of the tests are fundamentally different. The HWTT, RLPD, DM, and FN are load controlled repeated loading tests, whereas the SPST is a displacement controlled monotonic loading test. However, all these tests are designed to predict and interpret the HMA's susceptibility to shear/rutting loading; hence, their performance can be objectively compared. The results and the graphical correlations are presented in the subsequent subsections.

SPST Correlation with HWTT Results

Table 6-1 presents the SPST and HWTT results for the nine mixes that were comparatively studied. The mixes are arranged in the order of decreasing SPST shear strength. However, this order of ranking is not replicated in terms of the HWTT rutting performance of the mixes. For example, the US 277 Type D and the APT Type B mixes have fairly high shear strength, whereas, both these mixes have failed in the HWTT. Data from Table 6-1 are used to draw correlation curves between the SPST and HWTT parameters and are presented in Figure 6-3.

72

Table 6-1. Comparison of the SPST and HWTT Results.

Mix Type	Hwy	τ_s (psi)	γ_s (in/in)	G_s (ksi)	SSE (kJ/m^2)	Rut_{max} (mm)	Rut_Δ (mm)	γ_H (in/in)	τ_H (psi)	G_H (ksi)
Type B	IH 35	456	0.120	3.82	63.0	2.84	2.18	0.034	85.41	2.49
Type C	Loop 480	321	0.108	2.97	43.0	3.59	3.01	0.047	85.41	1.80
Type D	US 277	319	0.087	3.67	36.0	12.5	8.22	0.129	85.41	0.66
Type B	APT	310	0.108	2.95	40.1	12.5	8.72	0.137	85.41	0.62
Type C	US 83	292	0.091	3.27	34.7	8.22	3.39	0.053	85.41	1.60
Type F	US 271	248	0.089	2.82	29.0	5.45	3.56	0.056	85.41	1.52
Type C	SH 21	228	0.114	2.00	18.6	9.39	5.15	0.081	85.41	1.05
SMA	IH 35	222	0.139	1.66	37.2	9.91	8.01	0.126	85.41	0.68
PFC	US 271	127	0.157	0.87	18.6	12.5	8.21	0.129	85.41	0.66
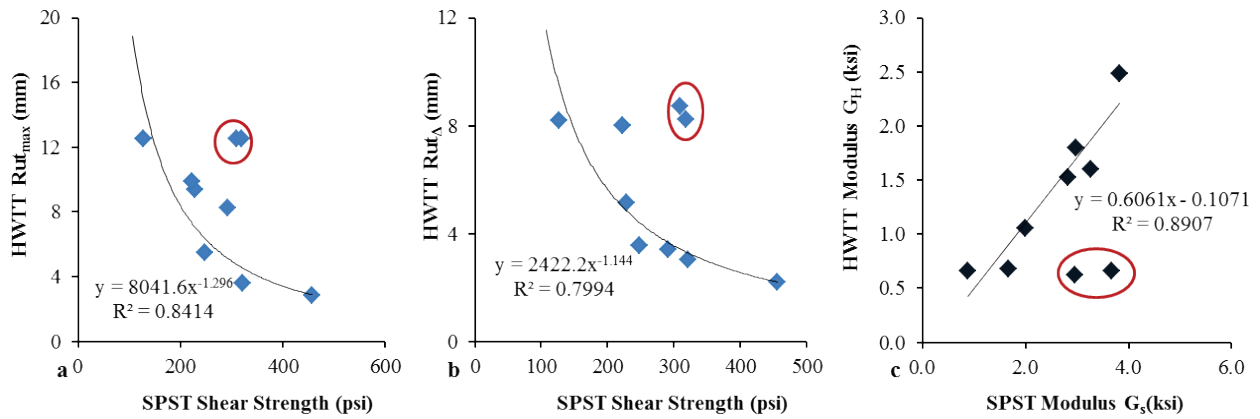
Figure 6-3. Correlation of SPST and HWTT Results.

Figure 6-3a shows that the HWTT rut depth (Rut_{max}) versus the SPST shear strength for the mixes has a fairly reciprocal correlation represented by a power function with a couple of outlying data points. A similar correlation trend is observed when the HWTT rutting is represented by the normalized rutting area parameter (Rut_Δ) (Figure 6-3b). The exhibited correlation is theoretically justified since a mix with higher shear strength is expected to be less susceptible to rutting and vice versa. Additionally, the HWTT modulus (G_H) and the SPST shear modulus (G_s) exhibited a fairly linear correlation, which is somewhat theoretically expected.

A preliminary comparison of the SPST to the HWTT is provided in Table 6-2 and shows that both tests use the same sample configuration and dimensions, all with the potential to readily test field cores.

Table 6-2. Comparison of the SPST and HWTT Protocols.

Item	SPST	HWTT
Sample preparation	Very easy (no cutting required)	Easy (cutting required)
Sample dimension	2.5" thick × 6.0" ϕ	2.5" thick × 6.0" ϕ
Overall test simplicity	Very simple	Very simple
Test equipment	UTM or IDT machine setup	Stand alone Hamburg
Test time	≤ 10 minutes*	≤ 8 hours
Data analysis and result interpretation	Fairly simple, needs post processing of data	Straight forward (machine reports rut depth)
Repeatability of test results	Very repeatable	Very repeatable
HMA mix screening ability	Good	Very good
Sensitivity to temperature	Very good	Very good
Data output	HMA shear parameters: shear strength, shear strain, shear modulus, SSE, and SSE Index	HMA rutting resistance potential: rut depth, cycles to failure, normalized rutting area, and shape factor
Routine application	Promising potential	Very good
Correlation to field data	Good, based on preliminary validation	Good
Practicality and implementation	Yes	Yes

*Requires about 1 hour temperature conditioning time of the specimens prior to testing.

As compared to the HWTT, one key benefit of the SPST is its ability to directly capture the HMA shear properties and resistance to shear deformation. While some element of cutting is needed on the HWTT samples, none is required on the SPST samples, thus allowing for a much simpler sample preparation. Also, the SPST has a considerably shorter test time with the potential to cost-effectively test numerous samples in a day. The multipurpose test equipment (UTM) with the ability to run several other test procedures as opposed to the stand-alone machine required for the HWTT is an additional benefit of the SPST protocol.

SPST Correlation with RLPD Results

Similar to the HWTT, the RLPD has a very good correlation to field rutting performance of mixes. The test also produces HMA material properties that can be used in mechanistic-empirical (M-E) pavement thickness design procedures. Therefore, a good correlation with the RLPD result will be beneficial for the validation and implementation of the SPST. Table 6-3 presents the SPST and RLPD results for the nine mixes that were comparatively studied. The

mixes are arranged in the order of decreasing SPST shear strength. Data from Table 6-3 are used to draw correlation curves between the SPST and RLPD parameters and are presented in Figure 6-4.

Table 6-3. Comparison of the SPST and RLPD Results.

Mix Type	Hwy	τ_s (psi)	γ_s (in/in)	G_s (psi)	SSE (J/m^2)	ε_p
Type B	IH 35	456	0.120	3.82	63.0	1270.0
Type C	Loop 480	321	0.108	2.97	43.0	3389.3
Type D	US 277	319	0.087	3.67	36.0	1811.0
Type D	US 59	269	0.115	2.37	37.0	6485.0
Type F	US 271	248	0.089	2.82	29.0	3246.0
Type C	SH 21	228	0.114	2.00	18.6	3735.0
SMA	IH 35	222	0.139	1.66	37.2	5440.0
CAM	SH 121	178	0.085	2.11	19.4	5359.0
PFC	US 271	127	0.157	0.87	18.6	11083.0
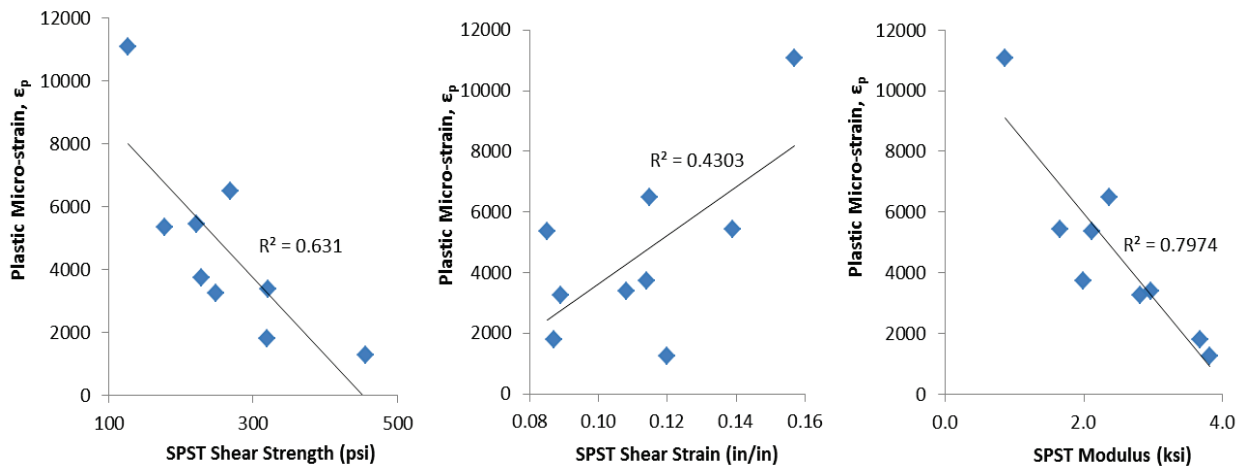
Figure 6-4. Correlation of SPST and RLPD Results.

In Figure 6-4, the plastic microstrain (ε_p) parameter obtained from the RLPD is correlated with three SPST shear parameters, namely the shear strength, shear strain, and the shear modulus. Overall, the correlation curves follow the theoretically expected trend, i.e., higher HMA shear strength and modulus corresponding to lower plastic microstrain and vice versa. However, the degree of correlation is not very pronounced. For example, the linear correlation of RLPD ε_p and SPST γ_s has an R^2 value of just above 43 percent. A preliminary comparison of the SPST to the RLPD test is provided in Table 6-4.

Table 6-4. Comparison of the SPST and RLPD Test Protocols.

Item	SPST	RLPD
Sample preparation	Very easy (no cutting required)	Complicated (requires cutting and coring)
Sample dimension	2.5" thick × 6.0"ϕ	6.0" thick × 4.0"ϕ
Potential to test field cores	Yes	Cannot readily test field cores
Overall test simplicity	Very simple	Complicated test (requires experienced operators)
Test equipment	UTM or IDT machine setup	UTM, AMPT, or MTS machine setup
Test time	≤ 10 minutes*	≤ 12 hours*
Data analysis & result interpretation	Fairly simple, needs post processing of data	Fairly simple, needs post processing of data
Repeatability of test results	Very repeatable	High variability at high test temperatures
HMA mix screening ability	Good	Good
Sensitivity to temperature	Very good	Good
Data output	HMA shear parameters: shear strength, shear strain, shear modulus, SSE, and SSE Index	HMA visco-elastic parameters: Accumulated plastic microstrain, α and μ
Routine application	Promising potential	Very good
Correlation to field data	Good, based on preliminary validation	Very good
Practicality & implementation	Yes	Yes

* Requires about 1 hour temperature conditioning time of the specimens prior to testing.

It is observed from Table 6-4 that the SPST is a considerably simpler test with easier sample preparation, shorter test time, and overall test simplicity and practicality. Several challenges of the RLPD test method are identified, including need for experienced operators, issues in maintaining the LVDT studs at high temperatures, and high variability at high test temperatures. However, proven field correlation and ability to produce HMA visco-elastic properties are some of the advantages of the RLPD over the SPST.

SPST Correlation with DM Results

Table 6-5 presents the SPST and DM test results for eight mixes that were comparatively studied. The mixes are arranged in the order of decreasing SPST shear strength. |E*| at 54.4°C at three different loading frequencies, namely 0.1, 5.0, and 10.0 Hz were compared to the SPST parameters. Although the DM results become less reliable at high test temperatures due to high variability, the DM results at 54.4°C were selected for comparison because HMA rutting-shear

failure is more critical at high temperatures. Also, the recommended default test temperature for the SPST is 50°C, thus DM results at 54.4°C facilitates a fair baseline comparison of the two test methods. Data from Table 6-5 were used to draw correlation curves between the SPST and DM parameters and are presented in Figure 6-5.

Table 6-5. Comparison of the SPST and DM Results at 54.4°C.

Mix Type	Hwy	τ_s (psi)	γ_s (in/in)	G_s (psi)	SSE (J/m^2)	$\|E^*\|_{0.1Hz}$	$\|E^*\|_{5Hz}$	$\|E^*\|_{10Hz}$
Type B	IH 35	456	0.120	3.82	63.0	16.4	80.3	105.5
Type C	Loop 480	321	0.108	2.97	43.0	24.0	71.0	102.0
Type D	US 277	319	0.087	3.67	36.0	29.0	92.0	125.3
Type D	US 59	269	0.115	2.37	37.0	10.3	52.9	59.7
Type F	US 271	248	0.089	2.82	29.0	10.1	39.5	51.9
Type C	SH 21	228	0.114	2.00	18.6	24.7	79.7	104.3
CAM	SH 121	178	0.085	2.11	19.4	11.7	35.3	44.7
PFC	US 271	127	0.157	0.87	18.6	15.3	39.0	58.7
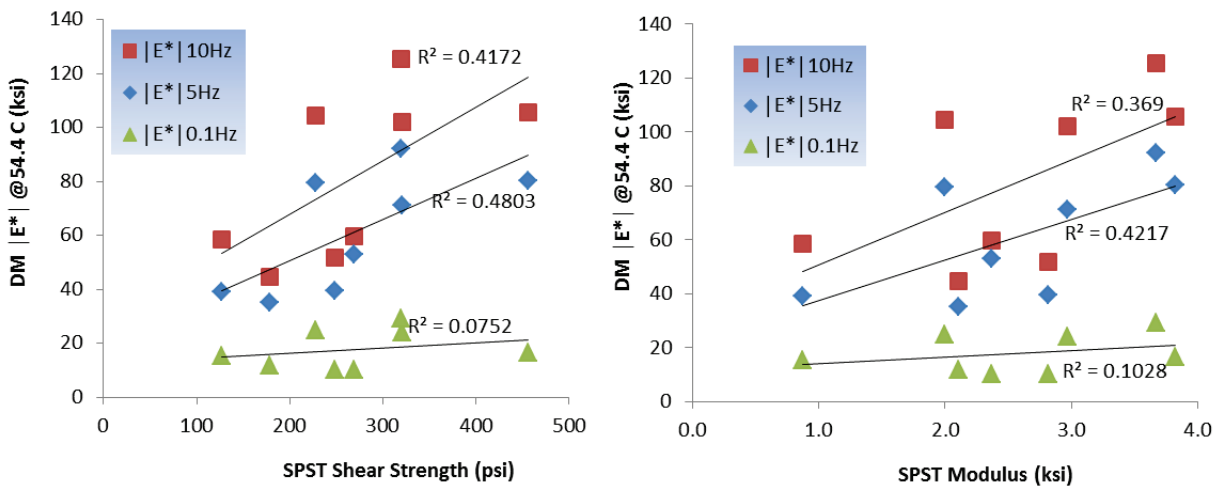
Figure 6-5. Correlation of SPST and DM Results.

The correlation curves presented in Figure 6-5 show that the dynamic modulus, $|E^*|$ at 54.4°C is increasing with increasing SPST shear strength and SPST modulus for all three frequencies. However, the correlation is not particularly strong with R^2 values below 50 percent. Also, the correlation is strongest when the $|E^*|$ at 5 Hz is compared with both the SPST shear strength and modulus.

A preliminary comparison of the SPST to the DM test is provided in Table 6-6. It is observed that the SPST is a considerably simpler test with easier sample preparation, shorter test

time, and overall test simplicity/practicality. Several challenges of the DM test method were also identified, including the need for experienced operators, issues in maintaining the LVDT studs at high temperatures, considerably long test duration, and high variability at high test temperatures.

Table 6-6. Comparison of the SPST and DM Test Protocols.

Item	SPST	DM
Sample preparation	Very easy (no cutting required)	Complicated (requires cutting and coring)
Sample dimension	2.5" thick × 6.0"ϕ	6.0" thick × 4.0"ϕ
Potential to test field cores	Yes	Cannot readily test field cores
Overall test simplicity	Very simple	Complicated test (requires experienced operators)
Test equipment	UTM or IDT machine setup	UTM, AMPT, or MTS machine setup
Test time	≤ 10 minutes*	≥ 3 days
Data analysis & result interpretation	Fairly simple, needs post processing of data	Needs post processing of data to obtain |E*| master curve
Repeatability of test results	Very repeatable	High variability at high test temperatures
HMA mix screening ability	Good	Not ideal for mix screening
Sensitivity to temperature	Very good	Good (test is run at multiple temperatures)
Data output	HMA shear parameters: shear strength, shear strain, shear modulus, SSE, and SSE Index	Dynamic Modulus |E*|, Master curve
Routine application	Promising potential	Not ideal for routine application
Correlation to field data	Good, based on preliminary validation	Good

* Requires about 1 hour temperature conditioning time of the specimens prior to testing.

SPST Correlation with FN Results

Table 6-5 presents the SPST and FN test results for the nine mixes that were comparatively evaluated. The mixes are arranged in the order of decreasing SPST shear strength. The comparison and correlation of the parameters from the two test methods are made with the fundamental assumption that a higher flow number (number of load repetition to onset of plastic flow) and a lower FN Index indicates better rutting resistance of a mix. On the other hand, for the SPST results, a good rut/shear resistant mix ideally would have higher shear strength, shear modulus, and SSE. Data from Table 6-7 were used to draw correlation curves between SPST and FN parameters and are presented in Figure 6-6.

Table 6-7. Comparison of the SPST and FN Results.

Mix Type	Hwy	τ_s (psi)	γ_s (in/in)	G_s (psi)	SSE (J/m^2)	FN $(x10^2)$	FN Index $(\mu\varepsilon/cycles)$
Type B	IH 35	456	0.120	3.82	63.0	15.78	4.39
Type C	Loop 480	321	0.108	2.97	43.0	147.00	1.84
Type F	US 271	248	0.089	2.82	29.0	41.39	39.50
Type C	SH 21	228	0.114	2.00	18.6	20.80	7.00
PFC	US 271	127	0.157	0.87	18.6	9.60	26.90
SMA	IH 35	222	0.139	1.66	37.2	55.30	0.94
Type D	US 277	319	0.087	3.67	36.0	60.30	3.60
CAM	SH 121	178	0.085	2.11	19.4	13.78	14.67
Type D	US 59	269	0.115	2.37	37.0	12.17	7.68
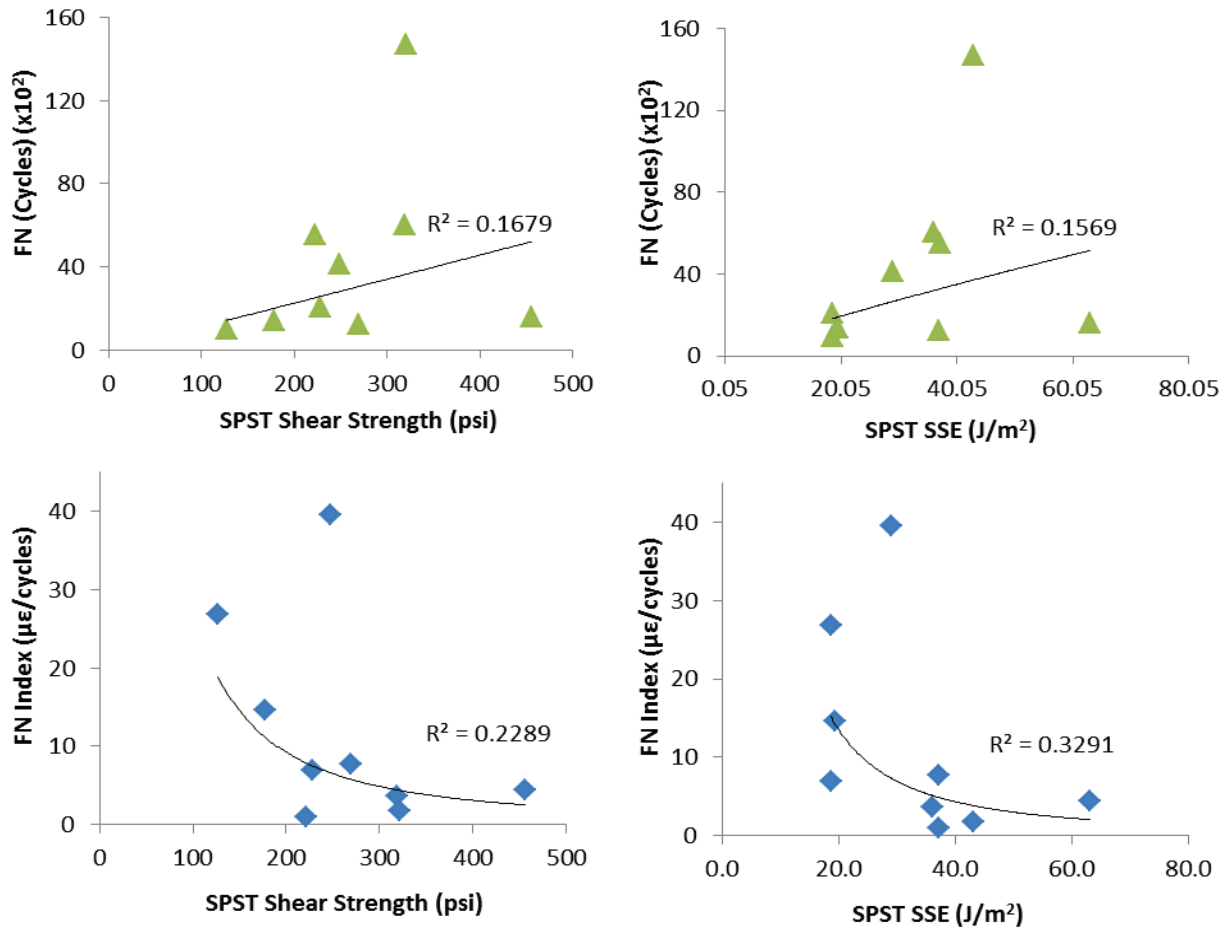
Figure 6-6. Correlation of SPST and FN Results.

Figure 6-6 shows that the correlation curves follow the expected trend, but with modest degrees of correlation. A preliminary comparison of the SPST to the DM test is provided in Table 6-8.

Table 6-8. Comparison of the SPST and FN Test Protocols.

Item	SPST	FN
Sample preparation	Very easy (no cutting required)	Complicated (requires cutting and coring)
Sample dimension	2.5" thick × 6.0"φ	6.0" thick × 4.0"φ
Potential to test field cores	Yes	Cannot readily test field cores
Overall test simplicity	Very simple	Complicated test (requires experienced operators)
Test equipment	UTM or IDT machine setup	UTM, AMPT, or MTS machine setup
Test time	≤ 10 minutes*	≤ 3 hours*
Data analysis & result interpretation	Fairly simple, needs post processing of data	Fairly simple, needs post processing of data
Repeatability of test results	Very repeatable	High variability at high test temperatures
HMA mix screening ability	Good	Fair
Sensitivity to temperature	Very good	Good
Data output	HMA shear parameters: shear strength, shear strain, shear modulus, SSE, and SSE Index	Flow number (FN), accumulated permanent strain $\varepsilon_p(F)$, time to the onset of tertiary flow t(F), FN Index
Routine application	Promising potential	Not ideal for routine application
Correlation to field data	Good, based on preliminary validation	Needs validation

* Requires about 1 hour temperature conditioning time of the specimens prior to testing.

The comparison in Table 6-8 indicates that the SPST is a considerably simpler test with easier sample preparation, shorter test time, and overall test simplicity/practicality. Some challenges of the FN test method were identified in Table 6-8 and include the need for experienced operators, issues in maintaining the LVDT studs at high temperatures, longer test duration, and high variability at high test temperatures.

SUMMARY

In this chapter, the newly developed SPST was compared and correlated with some of the more traditional HMA rutting and permanent deformation tests, namely the HWTT, RLPD, DM, and FN. The key findings from this chapter are summarized as follows:

- At 50°C, the SPST and HWTT do not provide a completely similar ranking of all the mixes. However, the graphical correlation plotting of the HWTT rut depths versus the

SPST shear strength for the mixes shows a fairly reciprocal correlation represented by a power function. The exhibited correlation is theoretically justified since a mix with higher shear strength is expected to be less susceptible to rutting and vice versa.

- A qualitative comparison of the RLPD plastic microstrain and the SPST shear strength and shear modulus follow an expected reciprocal trend, i.e., higher HMA shear strength and modulus corresponding to lower plastic microstrain and vice versa. The RLPD plastic microstrain values also show a fairly linear correlation with the SPST shear strain values.

- Correlation of the dynamic modulus, |E*| at 54.4°C with the SPST shear properties is strongest at 5 Hz loading frequency. Although the degree of linear correlation (R^2) is not particularly strong between the DM and SPST parameters, it follows the theoretically expected trend, i.e., higher |E*| corresponding to higher shear strength and shear modulus. On the other hand, no strong correlation was observed between the SPST and the FN test results.

- Comparative evaluation of the test protocols showed that the SPST is at close par with the HWTT and is a considerably simpler test with easier sample preparation, shorter test time, and overall test simplicity/practicality as compared to the DM, RLPD, and FN tests. Both the SPST and HWTT have the same sample configuration and dimensions, along with the potential to readily test field cores producing repeatable test results. On the other hand, the RLPD, DM, and FN test methods are relatively more complicated, requiring expert operators and having considerably longer test times. However, the HWTT and RLPD already have a proven history of good field correlation, whereas the SPST and the other cited test methods do not.

- Due to the fundamental differences between the test methods in terms of loading mode (displacement controlled monotonic loading versus stress controlled repeated loading), direct numerical pairwise comparisons of the SPST with the other test methods did not always produce strong correlations. However, qualitative trends observed from the correlation curves indicated that the SPST can be objectively compared to the other test protocols with reasonable degree of reliability.

Overall, the SPST is the only test method with the potential to directly measure and capture the HMA shear properties. This is one of the key benefits of the SPST among all the other lab test methods evaluated in this study.

CHAPTER 7 COMPUTATIONAL MODELING AND SHEAR STRESS-STRAIN ANALYSIS

As an integral component of this study, computational modeling was imperative, at a minimum, to address the following two key aspects:

- Shear stress-strain distribution analysis to determine the critical zones of plastic deformation and shear failure in a pavement structure.
- Sensitivity analysis to determine the critical factors that influence rutting and shear deformation when the pavement structure is subjected to the worst case scenario in terms of traffic loading (low speed/heavy trucks), intersections/turning traffic, traffic stop-go sections (i.e., at traffic lights), and extreme temperatures.

Overall, the ultimate intent is to be able to compare and relate the HMA shear strength properties to the shear stresses that heavy trucks produce on pavement structures under the aforementioned extreme conditions in order to mitigate HMA shear failures in the field. To accomplish these goals, the researchers used 2-D elastic and 3-D visco-elastic FE analyses with the PLAXIS and Abaqus software, respectively. The details of the 2-D PLAXIS analysis were documented in the year one report of this project (Walubita et al., 2013), and the details of the 3-D FE analysis using Abaqus, in a dynamic mode, are presented in this chapter.

Computational modeling and numerical analysis in 3-D dynamic mode was executed to help identify the critical factors that influence rutting and shear deformation in terms of:

- Stress-strain impacts on PVMNT response and performance.
- Generation of a matrix of critical factors to aid in establishing and verifying the lab test parameters.
- Establishment of preliminary limits and thresholds for critical shear deformation zones and occurrence of maximum plastic strains.
- Establishment and relation of the analytical displacements and shear stress-strain results to the lab tests and field data in terms of HMA shear resistance, PD, and rutting characterization.

To accomplish the aforementioned objectives, the research team undertook the following work plan/methodology:

- Establish input variables and modules for 3-D sensitivity analysis in Abaqus.

- Formulate FE models in Abaqus for shear, permanent deformation, and rutting analysis.

- Perform 3-D response and stress-strain sensitivity analyses in Abaqus.

- Establish critical loading parameters/conditions and shear deformation zones in PVMNT structures.

- Recommend preliminary threshold values for critical shear and plastic strains.

The overall modeling approach is schematically outlined in Figure 7-1.
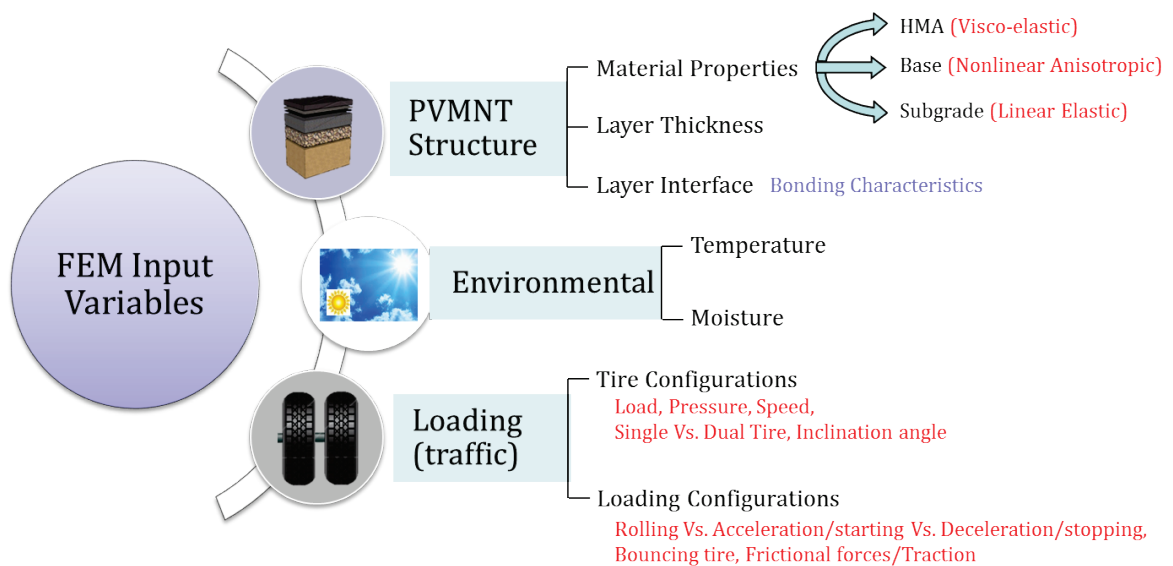
Figure 7-1. Schematic Outline of 3-D FE Modeling Approach.

The remainder of this chapter presents a step-by-step description of the modeling approach and the results obtained, starting with a brief description of the Abaqus software.

THE ABAQUS SOFTWARE

Abaqus is a suite of FE analysis modules used for stress, heat transfer, and other types of analyses in mechanical, structural, civil, and related engineering applications. The Abaqus system consists of several modules, and the key modules for mechanical purposes are Abaqus/Standard and Abaqus/Explicit, which are complementary and integrated analysis tools:

- Abaqus/Standard: a general purpose finite element module.

- Abaqus/Explicit: an explicit dynamic finite element module.

- Abaqus/CAE: an analysis module designated as the Complete Abaqus Environment (CAE) for modeling, managing, and monitoring Abaqus analysis and visualizing results.

- Integrated Abaqus/Standard and Abaqus/Explicit.

The FE program used in this study was Abaqus/CAE, which has an intuitive and consistent user interface throughout the system. Figure 7-2 shows the main user interface screen for the Abaqus/CAE software.
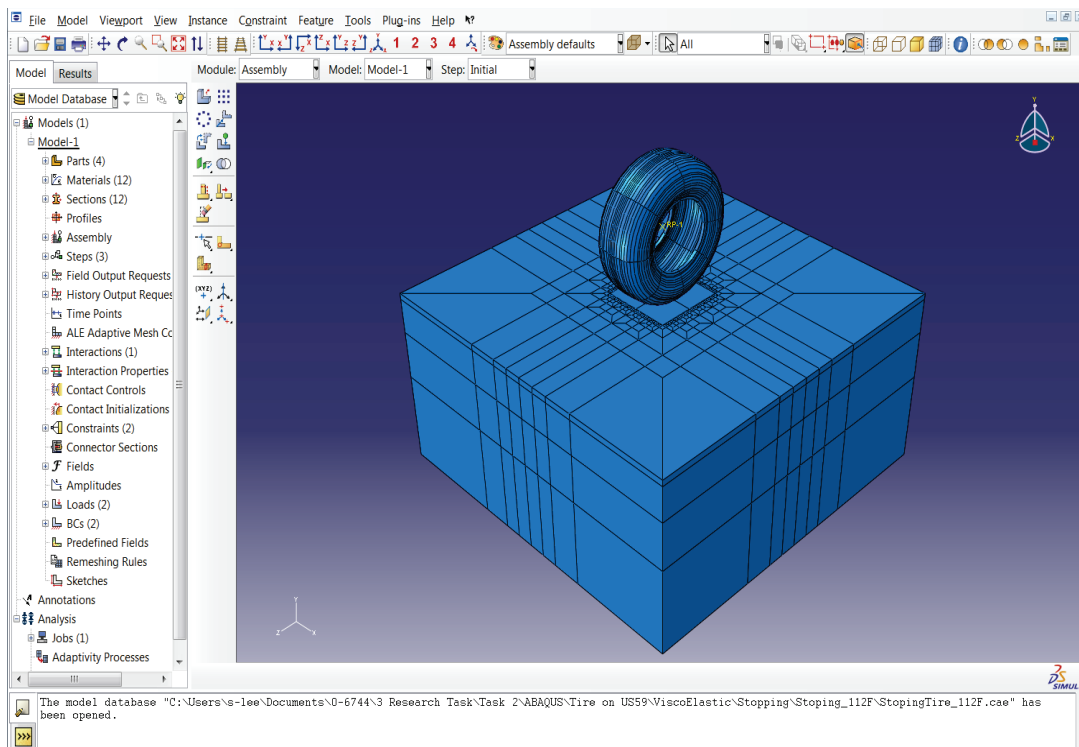
Figure 7-2. Abaqus/CAE Main Screen – User Interface.

ABAQUS 3-D DYNAMIC MODELING

In this study, the Abaqus FE modeling and stress-strain analyses were executed in a 3-D dynamic mode to simulate real-time traffic loading and environmental conditions. Details of the modeling approach are discussed in the subsequent sections.

Pavement Structure

For the 3-D FE visco-elastic modeling, the US 59 highway in the Atlanta District—a test section in Study 0-6658, with known material properties, traffic, and climatic data—was utilized as the reference PVMNT structure (see Figure 7-3).

Layer#	Thickness (Inches)	Layer Material	Year Constructed
7	2.0	Type D (PG 64-22 with 20% RAP)	2011
3-6	~11.5	Existing HMA	-
1-2	~16.0	LFA Base (8″ + 8″ = 16″)	-
0	∞	Compacted Subgrade Soil	-
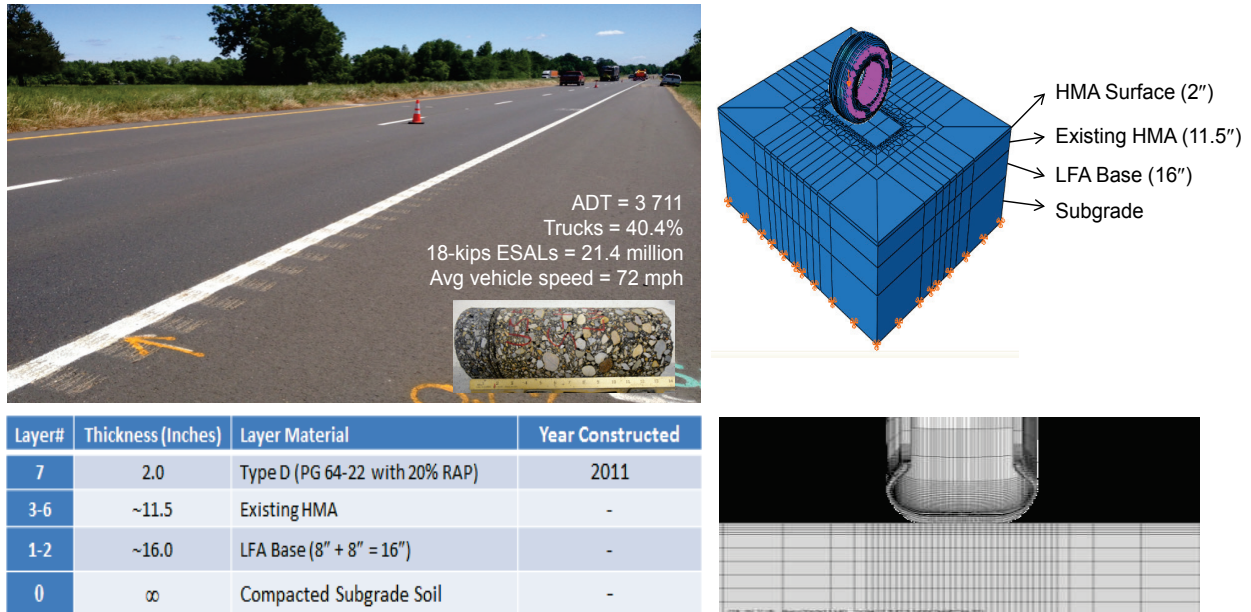
Figure 7-3. US 59 PVMNT Structure and Abaqus 3-D Modeling.

Table 7-1 shows the variations of layer thickness and HMA modulus influenced by field temperature. The temperatures 112 and 92°F represent actual measured field temperatures in summer and fall, respectively, in 2013 at 1 inch PVMNT depth. The following equation was used to correct the HMA back-calculated modulus to 77°F (Walubita et al., 2012):

$$E_{77^o F} = \left(T^{2.81}/200\,000\right) \times E_{FWD} \qquad\qquad 7.1$$

where, $E_{77°F}$ is the corrected HMA modulus to 77°F in ksi, E_{FWD} is the back-calculated FWD modulus in ksi without any temperature corrections, and T is the pavement temperature in °F measured at 1-inch depth during FWD testing.

86

Table 7-1. Pavement Structure and Moduli Values.

Layer	Thickness (in.)			Modulus (ksi) by Temperature (°F)		
HMA Overlay (Type D)	1.5	2.0	2.5	147.7 (112°F)	256.7 (92°F)	423.3 (77°F)
Existing HMA	11.5			478.5		
LFA Base (Lime fly-ash treated)	16.0			129.8		
Subgrade	-			44.0		

In this preliminary study, the HMA surface layer was modeled as an isotropic visco-elastic medium, and the other layers, i.e., the existing HMA, the base, and the subgrade, were modeled as elastic medium as shown in Figure 7-3. For simulating traffic loading on the PVMNT, the tire was modeled inclusive of the rubber and steel wires, assuming a smooth tire without any discrete consideration of the treads or ribs. Evaluation of treaded tires and/or ribs can be considered in possible future follow-up studies.

However, in order to obtain a better representation of the material properties of the PVMNT, visco-plastic and damage properties of both the overlay and the existing HMA need to be considered. Also, the non-linear anisotropic behavior of the base and subgrade layers needs to be properly modeled. Nonetheless, the simplified material characteristics assumed in this study give a general insight to the stress-strain responses of the PVMNT structure, as well as serve as an initial step toward a more detailed sensitivity evaluation study.

Material Properties

The time- and temperature-dependent behavior of the HMA is captured in Abaqus through modeling the visco-elastic properties of the HMA. The generalized Maxwell model available in Abaqus was used for this modeling. The generalized Maxwell model in Abaqus is represented by the following equations:

$$s = \int_{-\infty}^{t} 2G(t-\tau)\frac{de}{d\tau}d\tau \qquad\qquad 7.2$$

$$p = \int_{-\infty}^{t} K(t-\tau)\frac{d\left(tr[\varepsilon]\right)}{d\tau}d\tau \qquad\qquad 7.3$$

where, s and e are the deviatoric stress and strain, respectively; p and $tr[\varepsilon]$ are the volumetric stress and trace of volumetric strain, respectively; and t is the relaxation time.

K and G, in Equations 7.2 and 7.3, are the bulk and shear moduli of the HMA, respectively, and are calculated from the DM test data of the HMA. However, the frequency-dependent DM data need to be converted to the moduli values in the time domain using the prony series as illustrated in Equations 7.4 and 7.5:

$$G(t) = G_o\left[1 - \sum_{i=1}^{n} G_i\left(1 - e^{-t/\tau_i}\right)\right] \qquad\qquad 7.4$$

$$K(t) = K_o\left[1 - \sum_{i=1}^{n} K_i\left(1 - e^{-t/\tau_i}\right)\right] \qquad\qquad 7.5$$

G_o and K_o are the instantaneous shear and elastic moduli, respectively. The G_i, K_i, and τ_i are prony series parameters. Linear elastic behavior is assumed for existing HMA, granular base, and subgrade.

Input Variables

In order to perform the sensitivity analysis, the researchers identified the critical input variables and studied the model predicted responses by varying each of these input parameters. The main input parameters that were studied are listed in Table 7-2.

Note that although the overall average vehicle speed as indicated in Figure 7.3 is 72 mph on this Hwy (US 59), the measured average truck speed was actually 63.5 mph. For simplicity and for the purposes of conservatism, 60 mph was utilized in the Abaqus FE 3-D dynamic modeling; see Table 7.2.

Table 7-2. Model Input Variables for FE Sensitivity Study.

Input Variable	Parametric Values
Overlay thickness	1.5", 2.0", and 2.5"
Tire pressure	80, 100, and 120 psi
Temperature	77, 92, and 112°F
Tire inclination angle	0, 5, and 10 degrees
Tire configuration	Single and dual tires
Traffic movement condition	Accelerating (22 fps^2), steady rolling (88 fps), and decelerating or braking (22 fps^2) traffic
Vehicle (truck) speed	60 mph (88 fps)
Layer interface condition	No slip

ABAQUS FE ANALYSIS RESULTS

The output results for each of these variables are discussed in the subsequent sections.

Overlay Thickness

One of the commonly used rehabilitation practices for pavements with excessive rutting failure is to apply an overlay. The overlay thickness of the reference PVMNT structure (US 59, Atlanta District) is 2 inches. However, in this computational study, the overlay thickness was varied to study its effect on shear stress and vertical strains. The modeling results are presented in Figure 7-4 through Figure 7-6.

1.5" thick Overlay   2.0" thick Overlay   2.5" thick Overlay
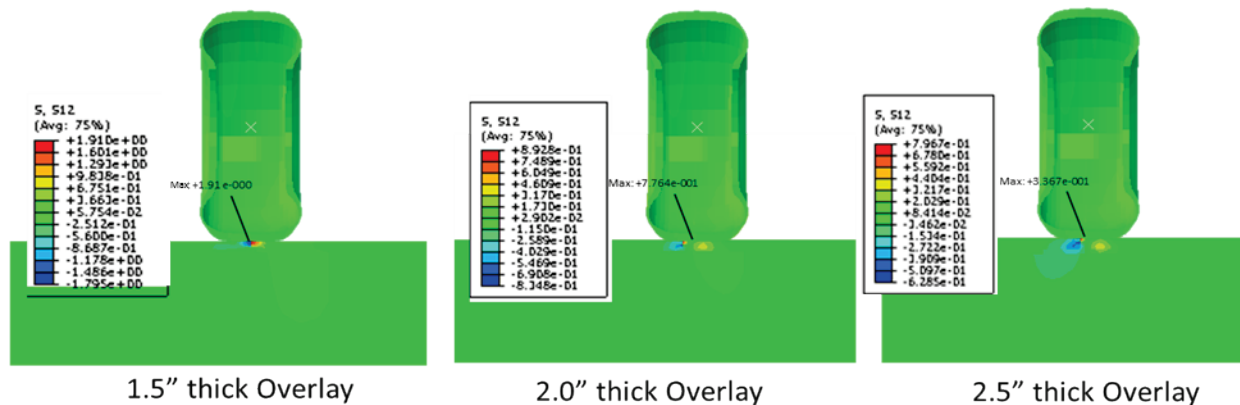
Figure 7-4. Shear Stress Response for Overlay Thickness Variation.

| 1.5" thick Overlay | 2.0" thick Overlay | 2.5" thick Overlay |
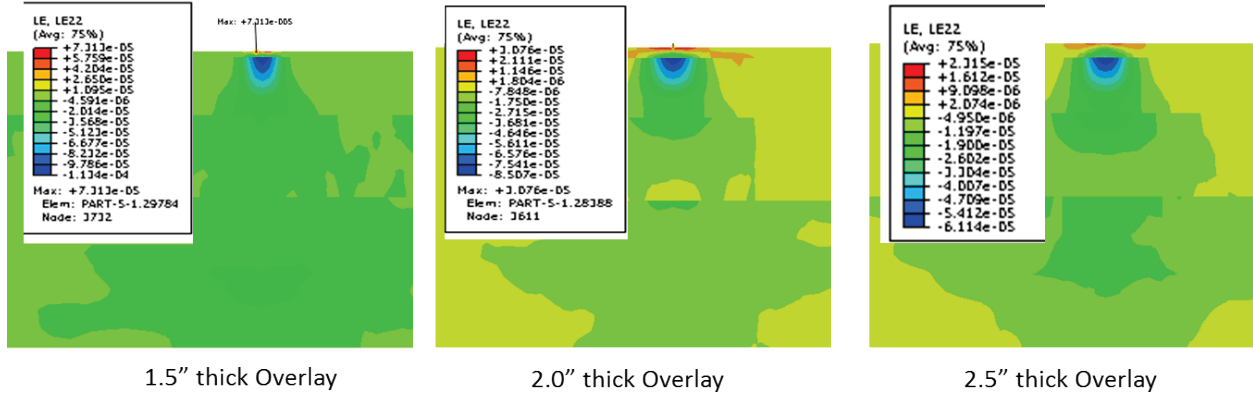
Figure 7-5. Vertical Strain Response for Overlay Thickness Variation.

Overlay Thickness (inch)	Shear Stress (MPa)	Vertical Strain (mm/mm)
1.5	1.91	5.32E-05
2.0	0.77	4.34E-05
2.5	0.33	3.56E-05
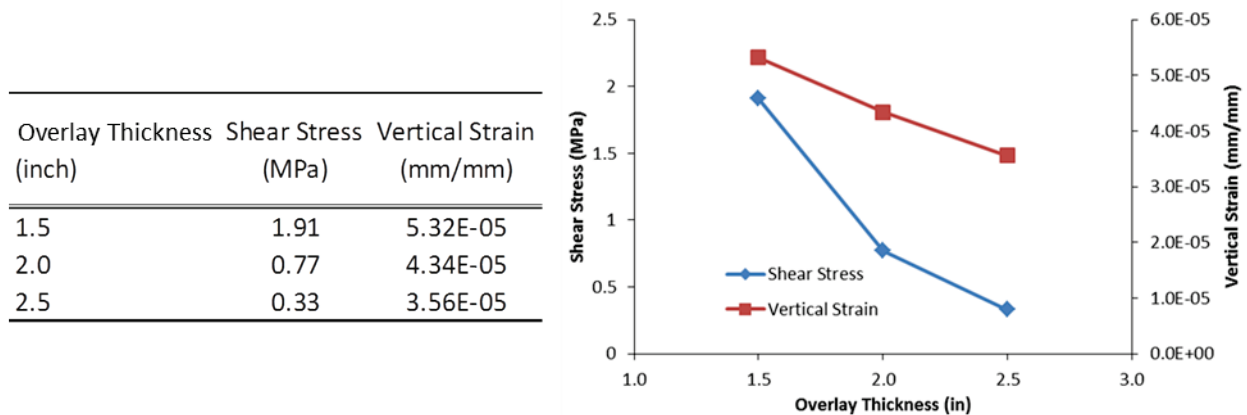
Figure 7-6. Maximum Shear Stress and Vertical Strain Variation.

The modeling shows clear sensitivity of the shear stress and vertical strain responses to overlay thickness. Both the maximum shear stress and vertical shear strain decrease with increasing overlay thickness. This finding is easily correlated to practical observations. The maximum shear stress for the 1.5-inch thick overlay has the highest shear stress value (1.91 MPa), which is less than the laboratory-tested SPST shear strength of this mix (2.90 MPa). Therefore, based on this study, it can be argued that a 1.5-inch thick overlay would have sufficed for this PVMNT structure in terms of shear stress considerations. The distributions of the shear stresses and the vertical strains across the PVMNT thickness are presented in Figure 7-7 and Figure 7-8.
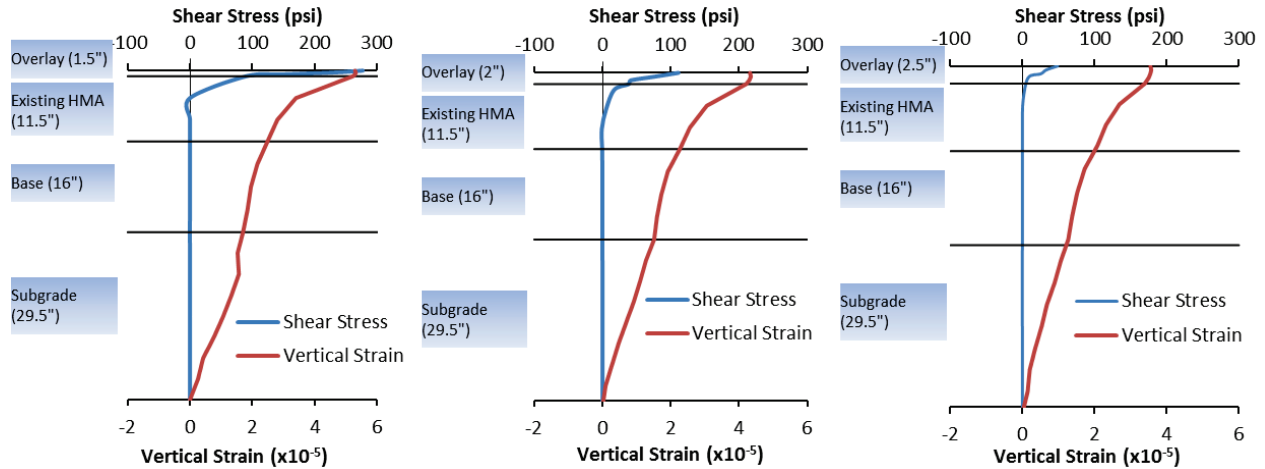
Figure 7-7. Shear Stress and Vertical Strain Distribution for Overlay Thickness Variation (across Full Thickness of the Pavement).
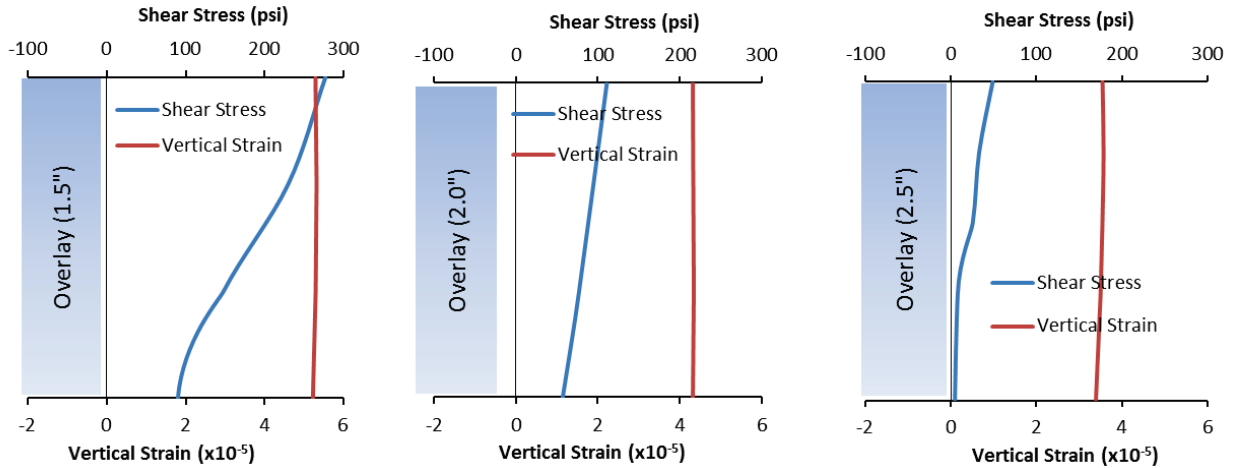
Figure 7-8. Shear Stress and Vertical Strain Distribution for Overlay Thickness Variation (across the Thickness of the Overlay).

From Figure 7-7 and Figure 7-8 it is evident that the model predicted that shear stress is most critical in the top HMA layer. The bottom layers show little to no shear stress. This is partly due to the fact that the bottom layers were all modeled as linear elastic materials. Also, proper modeling of the interfaces between the PVMNT layers is critical for effective stress transfer. However, the vertical strain is nicely distributed across the PVMNT thickness. The figures also indicate that, though the maximum shear stress and vertical strain values are greatly sensitive to overlay thickness variation, the distribution shapes do not show any significant sensitivity. The strain is fairly constant across the thickness of the overlay regardless of the overlay thickness, whereas the shear stress is consistently decreasing.

91

Overall, the findings from this study confirm that thicker overlays reduce maximum shear stress and vertical strain in the PVMNT structure, thus reducing the susceptibility to premature rutting/shear failures.

Tire Inflation Pressure

The effect of tire inflation pressure variation on the PVMNT shear stress and vertical strain response was studied, and the corresponding results are presented in Figure 7-9 through Figure 7-11.

| 80 psi | 100 psi | 120 psi |
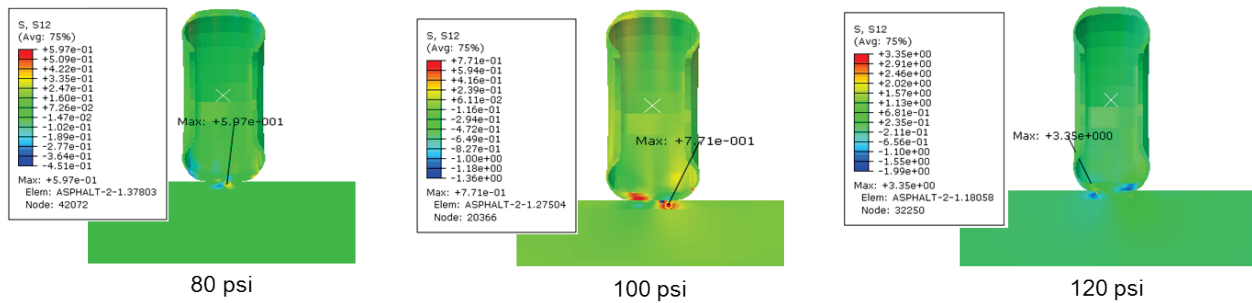
Figure 7-9. Shear Stress Response for Tire Pressure Variation.

| 80 psi | 100 psi | 120 psi |
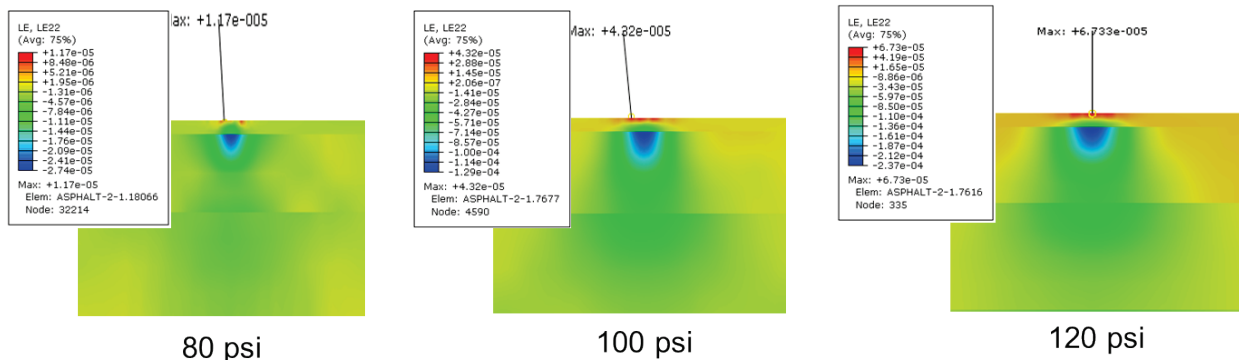
Figure 7-10. Vertical Displacement Response for Tire Pressure Variation.

Tire Pressure (psi)	Shear Stress (MPa)	Vertical Strain
80	0.597	1.17E-05
100	0.771	4.32E-05
120	3.350	6.73E-05
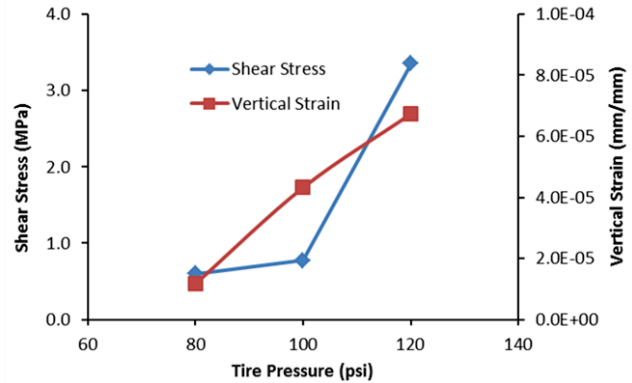
Figure 7-11. Maximum Shear Stress and Vertical Strain Variation.

As was theoretically expected, both the shear stress and vertical strain increase with increasing tire pressure. The maximum shear stress at 120 psi tire pressure (3.35 MPa) is significantly higher than the lab-predicted shear strength of the HMA overlay (2.90 MPa). Therefore, based on this study, it can be concluded that the tire inflation pressure of trucks travelling on this highway section should be around the standard 100 psi and never exceed 115 psi so as to minimize any potential effects of premature shear failures due to high tire inflation pressures.

The distributions of the shear stress and the vertical strain across the PVMNT thickness are presented in Figure 7-12 and Figure 7-13.
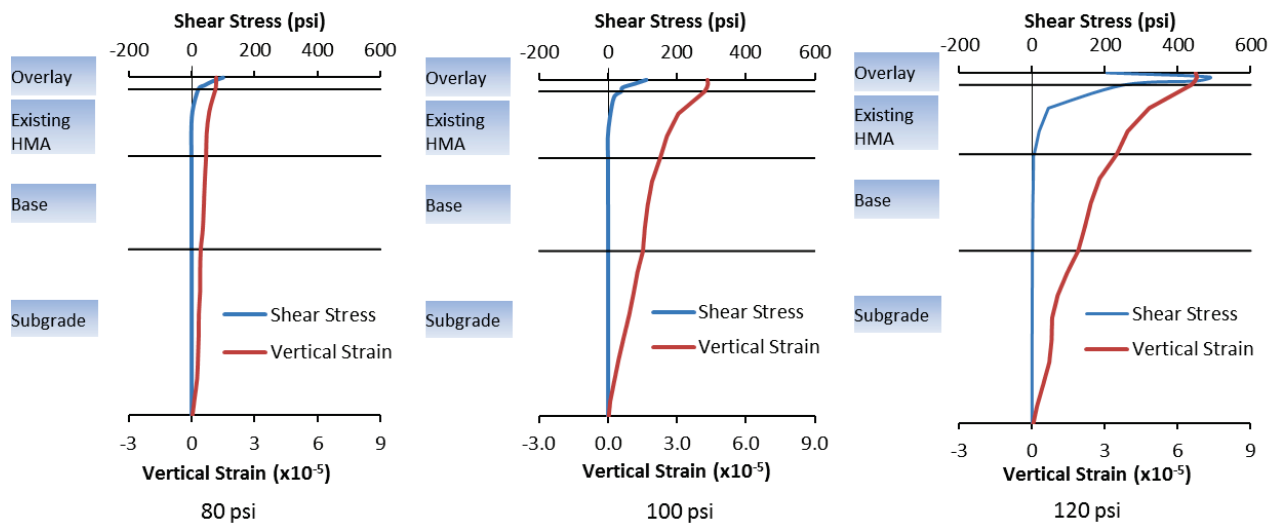
Figure 7-12. Shear Stress and Vertical Strain Distribution for Tire Pressure Variation (across Full Thickness of the Pavement).
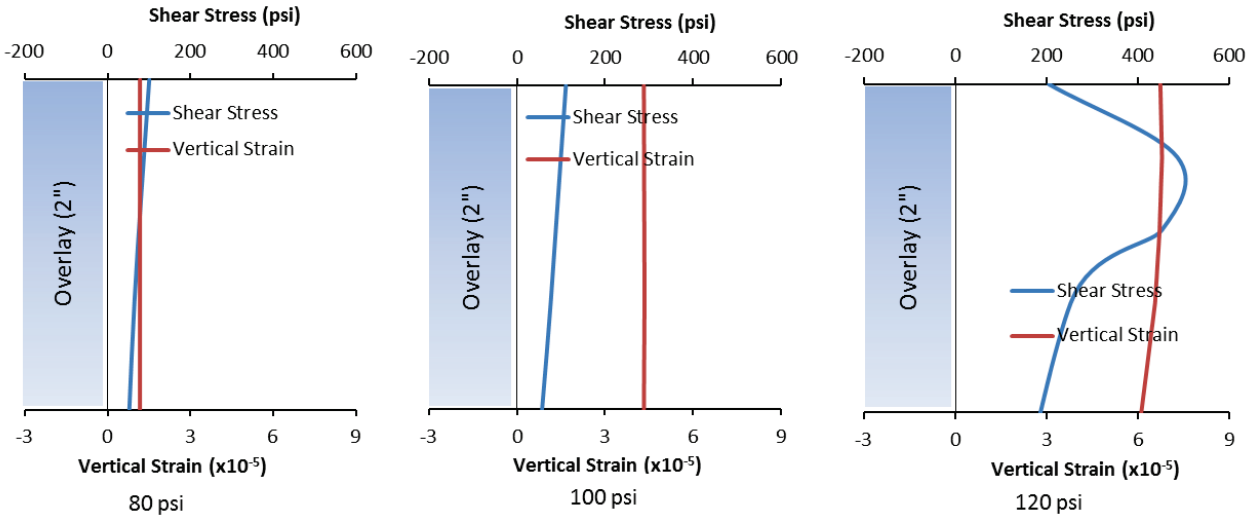
Figure 7-13. Shear Stress and Vertical Strain Distribution for Tire Pressure Variation (across the Thickness of the Overlay).

As in the thickness variation study shown in Figure 7-7 and Figure 7-8, the shear stress in this analysis seems to be most dominant in the topmost layer of the PVMNT. The location of the maximum shear stress in the cases of 80 and 100 psi tire pressure is at the PVMNT surface underneath the tire. However, in the case of 120 psi tire pressure, the maximum shear stress seems to be occurring a little below the top surface (at the depth of 0.67 inch). The vertical strain is fairly consistent throughout the thickness of the overlay.

Overall, the findings from this study confirm that higher tire inflation pressures (exceeding 100 psi) increase shear stress and vertical strain in the PVMNT structure, thus increasing susceptibility to rutting/shear failures.

Temperature Variation

Current high summer temperature trends often result in high pavement temperatures that are sustained for multiple hours each day, sometimes for weeks on end. Thus, it is critical that the shear stresses and strains within the PVMNT structure are properly studied and understood over a wide range of temperatures. In this modeling study, the researchers evaluated the PVMNT temperature effect through variation of the HMA moduli for the top layer (overlay). The primary objective of this particular task was to investigate how the maximum shear stress that the HMA mix can sustain or endure varied as a function of temperature and HMA modulus when subjected to traffic loading. The corresponding results are presented in Figure 7-14 through Figure 7-16.

94
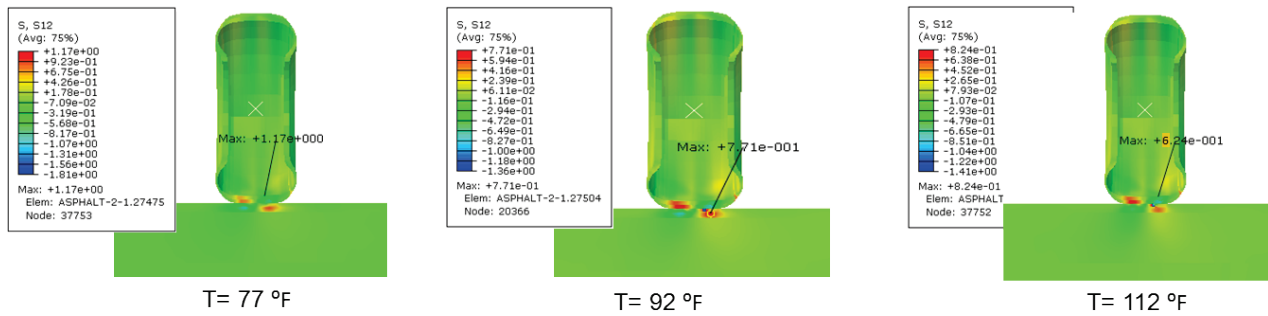
Figure 7-14. Shear Stress Response for Temperature Variation.
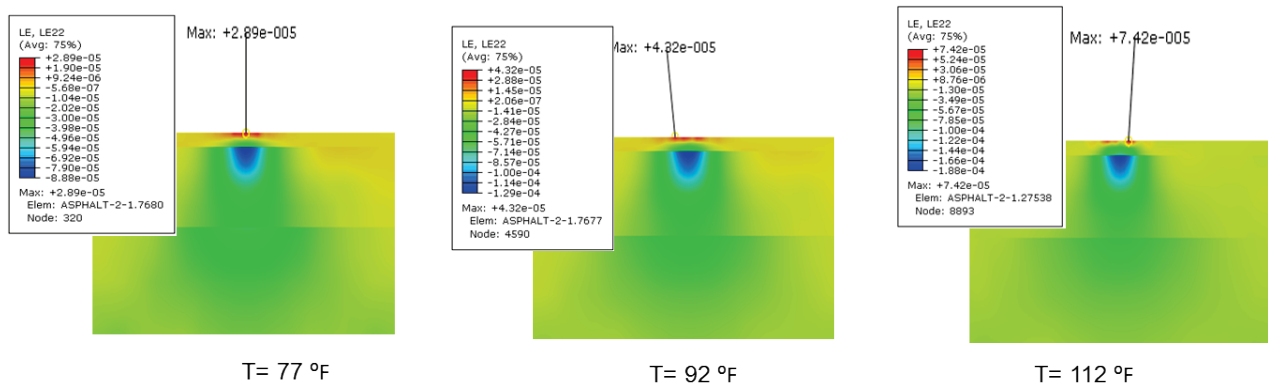
Figure 7-15. Vertical Strain Response for Temperature Variation.

PVMNT Temp (°F)	Shear Stress (MPa)	Vertical Strain
77	1.17	2.89E-05
92	0.77	4.32E-05
112	0.62	7.42E-05
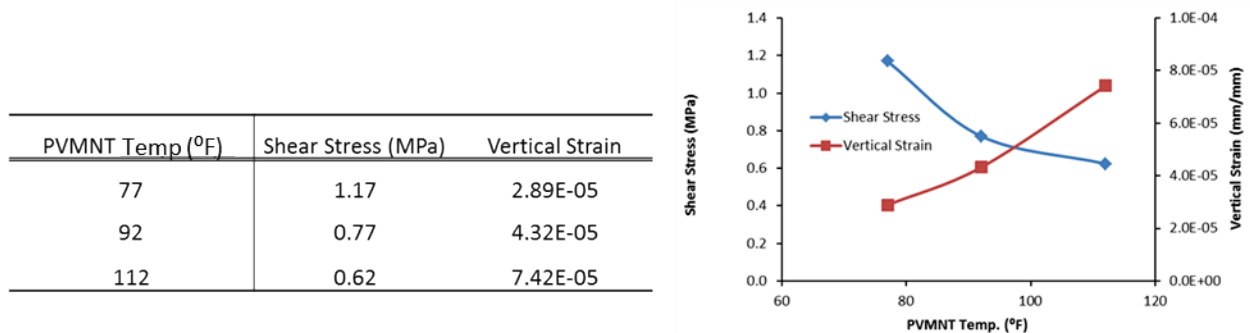
Figure 7-16. Maximum Shear Stress and Vertical Strain Variation.

The above figures show that the shear stress sustained by the top HMA layer decreases with increasing temperature. This might seem counter-intuitive since from field experience it is well documented that the rutting/shear failures of the HMA are most critical at high PVMNT temperatures. However, due to the visco-elastic nature of the HMA, the mix's shear strength is also reduced drastically with increasing temperature. Due to this decrease in the HMA strength with increasing temperature, the sustainable shear stress or the maximum shear stress that the

HMA mix can endure prior to shear failure also decreases, as evident in Figure 7-16. Quite often, the shear stress exerted on the PVMNT (due to traffic loading or at intersections, stop-go sections, etc.) exceeds the shear strength of the HMA, thus leading to more rutting and shear failures. This is particularly evident at elevated temperatures where the HMA shear strength deteriorates even further. Indeed, the vertical strain is found to be increasing with increasing temperature as a result of this complex interaction.

The distributions of the shear stress and the vertical strain across the PVMNT thickness are presented in Figure 7-17 and Figure 7-19 with varying temperatures.
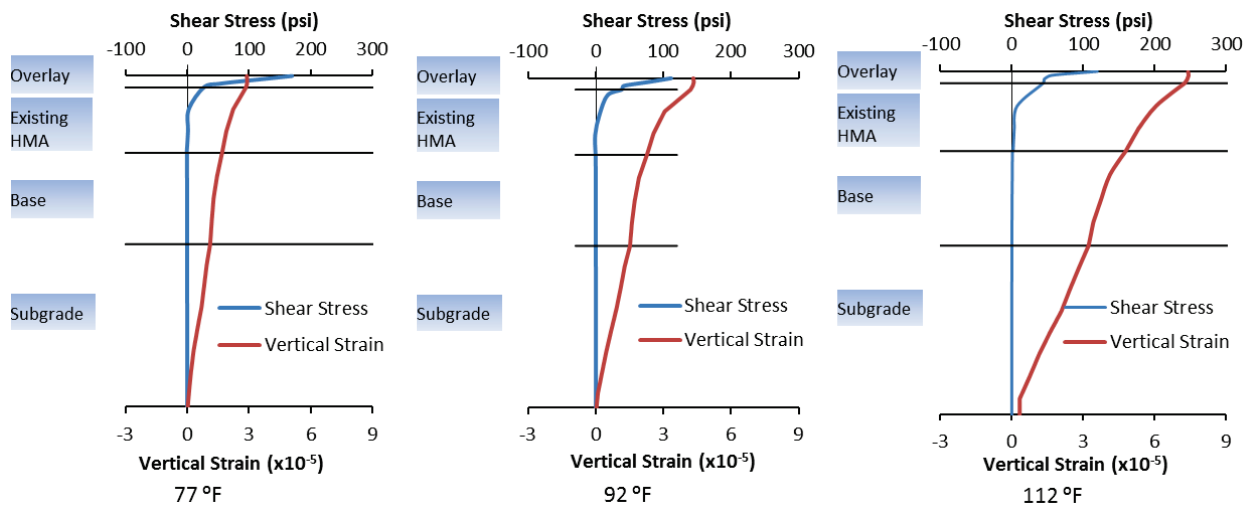
Figure 7-17. Shear Stress and Vertical Strain Distribution for Temperature Variation (across Full Thickness of the Pavement).
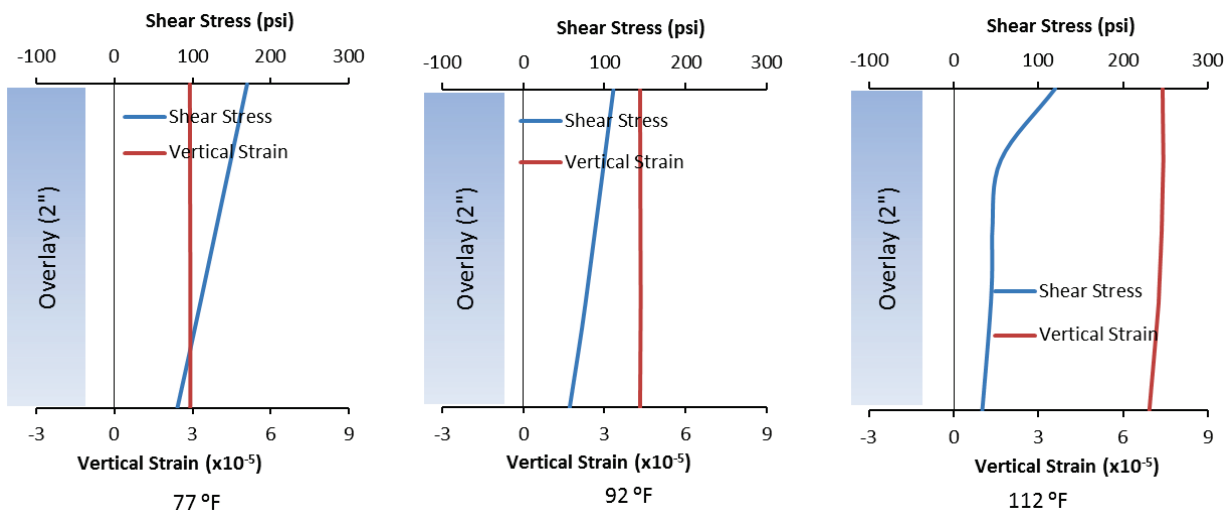
Figure 7-18. Shear Stress and Vertical Strain Distribution for Temperature Variation (across the Thickness of the Overlay).

From the shear stress and vertical strain distribution curves, it is observed that the shear stress is mostly confined to the top layer of the HMA. Even so, with increasing temperature (at 112°F), the existing HMA layer seems to be more affected with shear stress, thus making it susceptible to shear/rutting failures. However, proper modeling of the interface conditions between the layers, through defining proper interfacial properties (i.e., interfacial strength, temperature gradient, and modulus parameters) is critical for effective stress transfer. Therefore, caution needs to be exercised while interpreting these results, especially for the existing underlyng HMA layers. In this study, the interfacial condition was simply assumed as "no slip" condition. The strain distribution for the top layer (overlay) is fairly consistent.

Tire Inclination Angle

To simulate the effect of turning traffic at the intersections, the researchers modeled the tires with varying tilting angle, up to 10 degrees. The results are presented in Figure 7-19 through Figure 7-21.

Angle = 0º   Angle = 5º   Angle = 10º
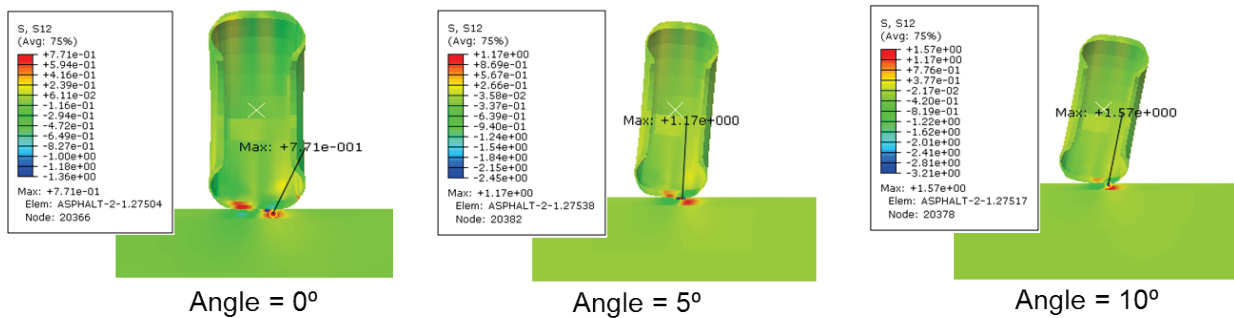
Figure 7-19. Shear Stress Response for Tire Tilting Angle Variation.

Angle = 0º   Angle = 5º   Angle = 10º
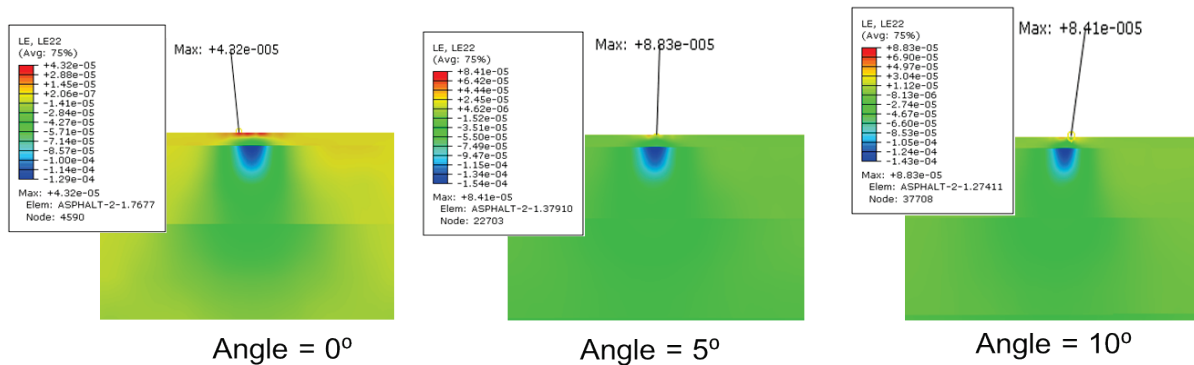
Figure 7-20. Vertical Strain Response for Tire Tilting Angle Variation.

97

Tire Inclination Angle	Shear Stress (MPa)	Vertical Strain
0 °	0.77	4.32E-05
5°	1.17	8.83E-05
10°	1.57	8.41E-05
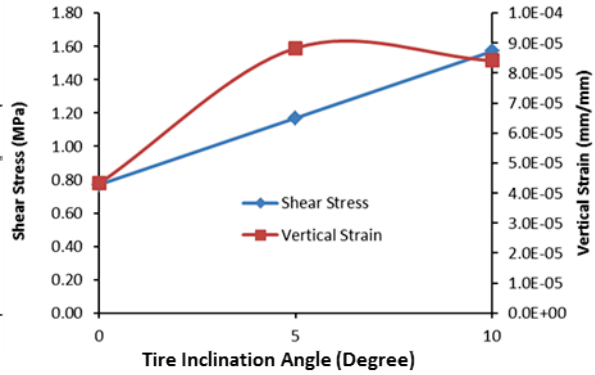
Figure 7-21. Maximum Shear Stress and Vertical Strain Variation.

From the results shown in these figures, it is clear that shear stress increases with increasing tire tilting angle. These results confirm the assumption that turning traffic causes more shear stresses, and more likely shear failure, as well. However, the vertical strain seems to have a peak value at 5° tilting angle for this particular PVMNT structure. Therefore, based on this study finding, it is argued that the geometric design of the Hwy section should be carefully done so as to ensure that tire inclination angles is below 5 degrees. Similarly, the HMA shear strength design should also be based on the maximum possible inclination angle that generates the most critical strains; for this particular Hwy section that angle would be 5 degrees.

The distributions of the shear stress and the vertical strain across the PVMNT thickness are presented in Figure 7-22 and Figure 7-23 with varying tire tilting angle.
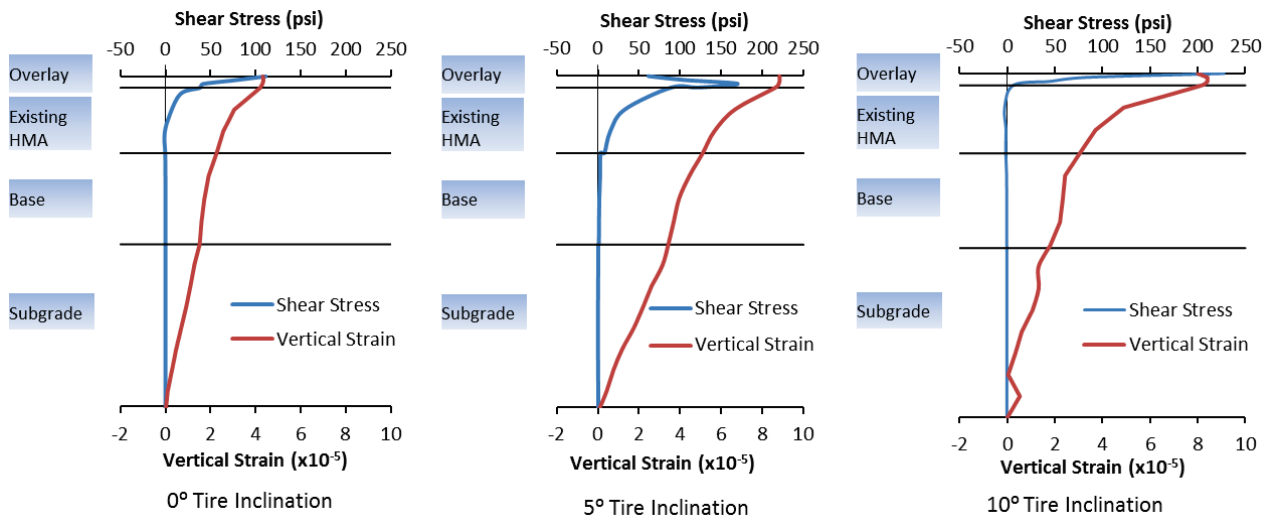
Figure 7-22. Shear Stress and Vertical Strain Distribution for Tire Inclination Angle Variation (across Full Thickness of the Pavement).

98
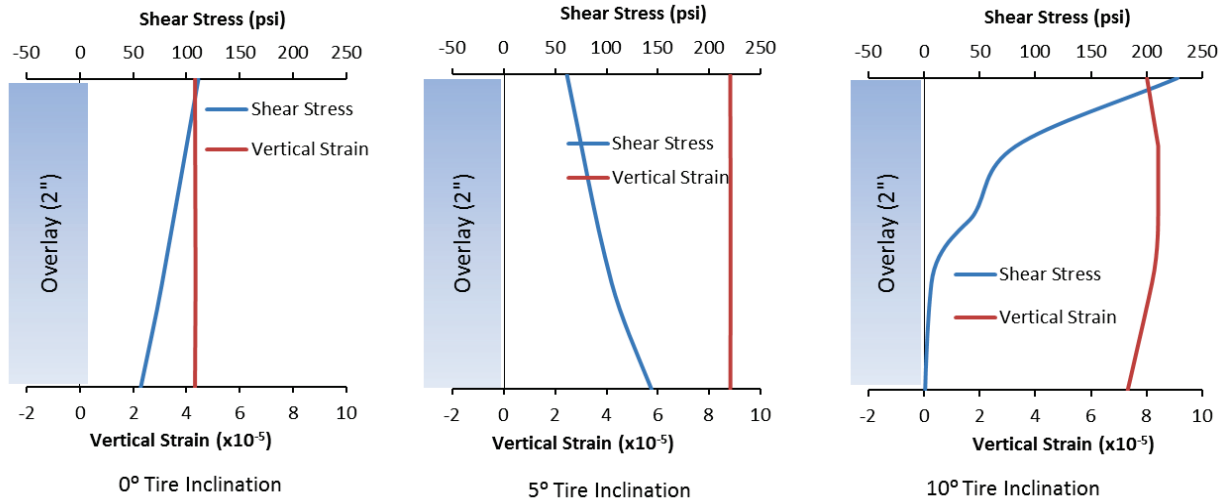
Figure 7-23. Shear Stress and Vertical Strain Distribution for Tire Inclination Angle Variation (across the Thickness of the Overlay).

Figure 7-22 and Figure 7-23 show that at a tilting angle of 5 degrees, the existing HMA experiences more shear stresses as compared to the other two tilting angles (0 and 10 degrees). This, in part, might contribute to the higher vertical strain observed in the case of the 5-degree tilting angle.

Overall, the findings from this study confirm the field observations that turning traffic at critical locations such as intersections or horizontal curves increases shear stress and vertical strain in the PVMNT structure—with a considerably higher potential for shear failure compared to straight sections of a Hwy. Also worth noting is that the impact of the shear stress and vertical strains are not only confined to the surface "overlay," but it also penetrates deep enough to affect the underlying HMA materials that may also be vulnerable to rutting/shear failures. However, as discussed in the preceding paragraphs regarding the interfacial conditions/properties, caution needs to be exercised while interpreting these results, especially for the underlying layers. For this particular Hwy section and the variables considered, 5 degrees appears to be the critical tilting angle for maximum vertical strains.

Tire Configuration: Single versus Dual Tires

The single and dual tire configurations were compared using the developed models, and the results are presented in Figure 7-24 and Figure 7-25.

99
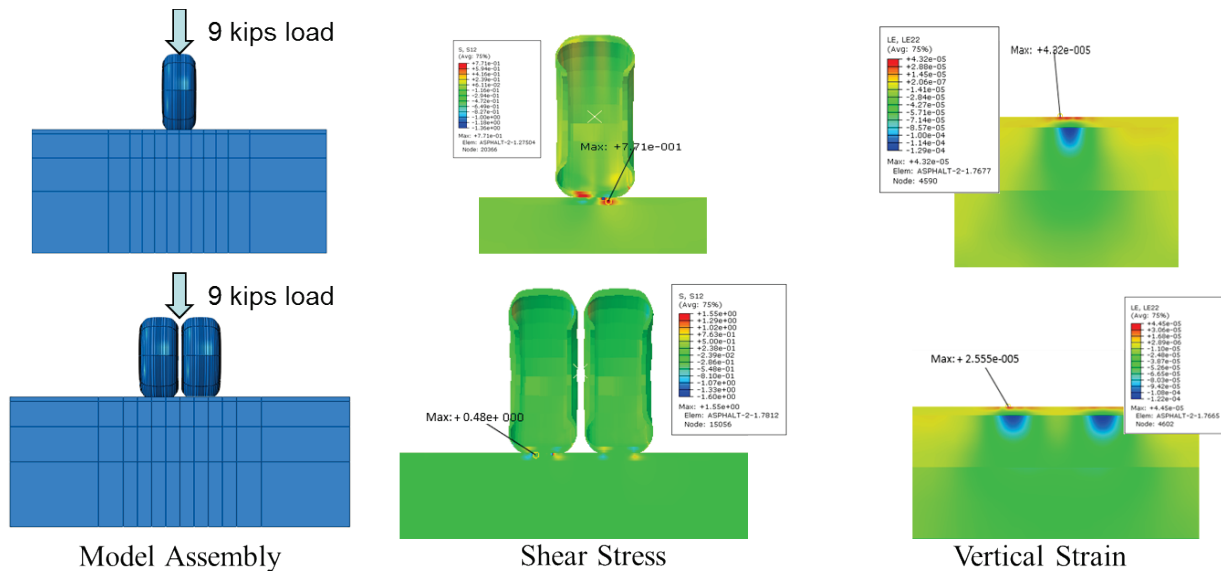
Figure 7-24. Shear Stress and Vertical Strain Response for Single vs. Dual Tires.

Tire Configuration	Shear Stress (MPa)	Vertical Strain
Single	0.77	4.32E-05
Dual	0.48	2.55E-05
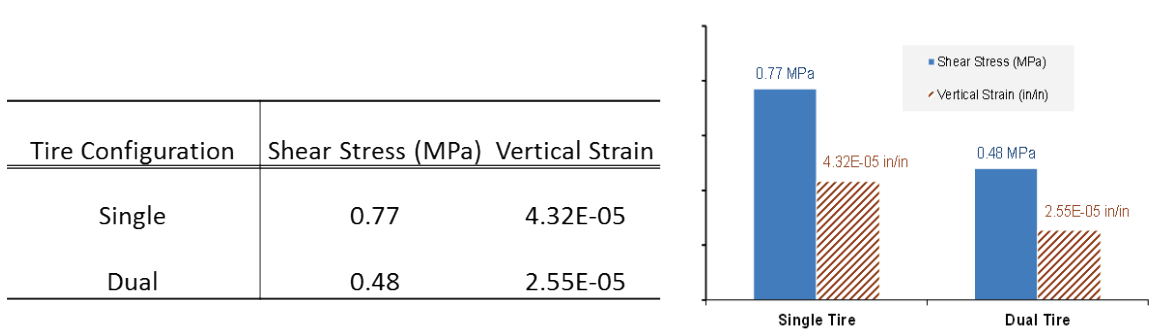
Figure 7-25. Shear Stress and Vertical Strain Comparison for Single vs. Dual Tires.

From the results in Figure 7-25, it is evident that both shear stress and vertical strains are least in magnitude under dual tire configuration for the same traffic loading. Thus, the theoretically expected response behavior is confirmed from this study, i.e., dual tire configuration for the same traffic loading, PVMNT structure, and environmental conditions is beneficial to pavement performance due to lower shear stresses and vertical strains compared to a single tire configuration.

Accelerating, Steady Rolling, and Decelerating Traffic

In the limited scope of this study, the researchers conducted preliminary dynamic modeling to study the shear stress-strain behavior of the PVMNT structure under different traffic conditions, i.e., accelerating, steady rolling, and decelerating (stopping) traffic. The modeled tire was simulated to move on a 40-ft-long stretch of PVMNT. The model assembly and the obtained

100

results are presented in Figure 7-26 and Figure 7-27. For this analysis, the following parametric values were used: PVMNT temperature = 77°F, tire inflation pressure = 100 psi, inclination angle = 0°, acceleration = 22 fps^2, steady rolling = 88 fps (60 mph), deceleration (braking) = 22 fps^2, and configuration = single tire.
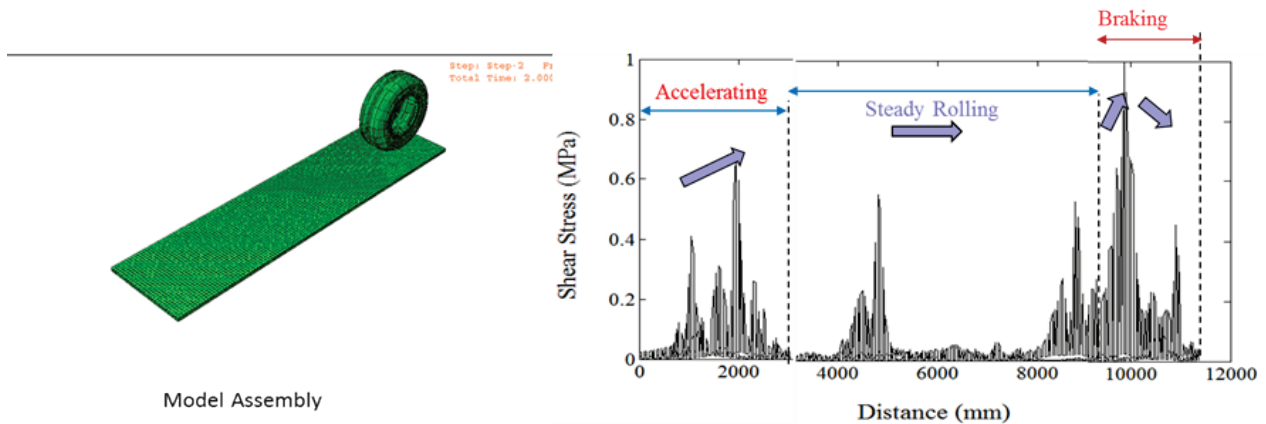
Figure 7-26. Dynamic PVMNT Shear Stress Response for Accelerating → Rolling → Decelerating (Stopping) Tire.

Loading Phase	Max Shear Stress (MPa)
Accelerating	0.65
Steady **Rolling**	0.54
Decelerating	1.00
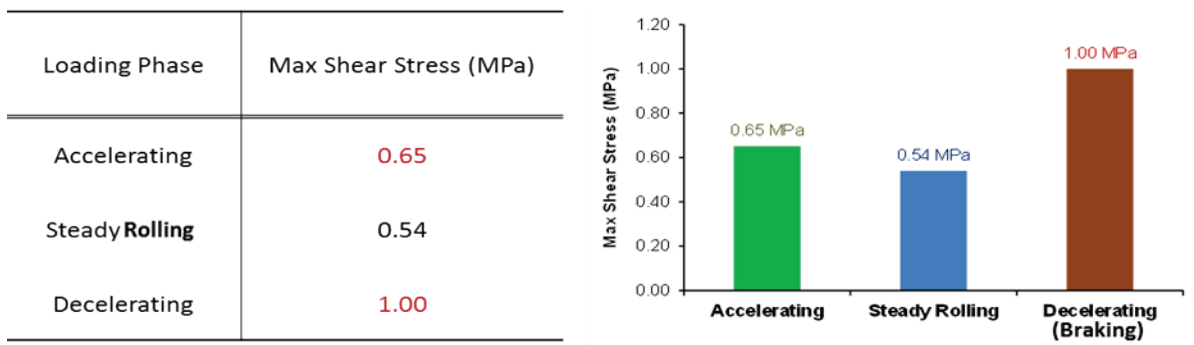
Figure 7-27. Maximum Shear Stress for Accelerating → Rolling → Decelerating Tire.

From the results in Figure 7-26 and Figure 7-27, it is evident that the maximum shear stress occurs at the onset of tire braking, indicating that intersections and stop-go sections may be more susceptible to shear deformation and rutting. In Figure 7-27, the maximum shear stress (1.00 MPa) is indicated for braking and the least (0.54 MPa) for steady rolling when comparing an accelerating, steady rolling, and braking tire. Thus, for PVMNT design purposes, the following critical Hwy areas should always be given due consideration with respect to the HMA shear strength properties and mitigation of shear failure:

- Intersections and junctions.

- Urban stop-go sections.

- Speed hump areas.

Based on these results, the maximum computed shear stress due to vehicle braking for this particular PVMNT structure (US 59) and for the parametric values described earlier is only 1.00 MPa (Figure 7-27) while the HMA shear strength of the Type D surfacing mix is 2.90 MPa. Assuming all other influencing parameters remain equal or constant, no shear failures related to the surfacing mix are theoretically expected on this Hwy, which is consistent with the visual performance observations made in the summer of 2014; see Figure 7-28 below. In reality, however, this may not be so if the combined effects of all the other elevated shear situations such as higher tire inflation pressure, high temperature, deceleration, etc., are interactively considered. That is, in order to effectively compare the modeling results with the field performances, combinations of critical parameters producing maximum shear damage need to be evaluated interactively; i.e., high temperature, high tire inflation pressure, and high tire inclination angle combined with the decelerating tire effects. However, this aspect could not be executed within this initial study's timeframe due, partly, to the complexity and computational intensive nature of the 3-D dynamic FE modeling with Abaqus. Thus, future studies warrant the holistic consideration of all the combined and interactive effects of these severe shear conditions.

Also, noteworthy is that the evaluated test section on US 59 does not include a controlled intersection, with the closest controlled intersection being about 1.5 miles ahead. Therefore, the effects of decelerating traffic might not be as severe for this particular section as compared to a PVMNT section approaching a controlled intersection. These are aspects that need to be given attention in future studies.

Layer#	Thickness (Inches)	Layer Material	Year Constructed
7	2.0	Type D (PG 64-22 with 20% RAP)	2011
3-6	~11.5	Existing HMA	-
1-2	~16.0	LFA Base (8" + 8" = 16")	-
0	∞	Compacted Subgrade Soil	-
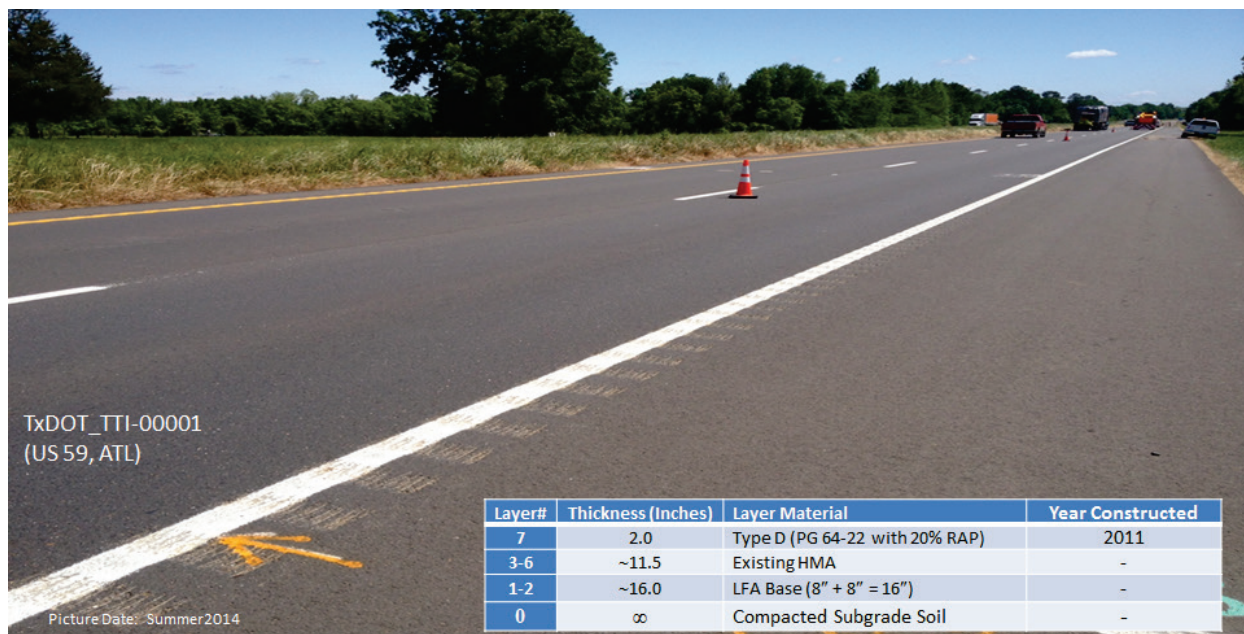
Figure 7-28. US 59 (Sec01) in Summer 2014.

SUMMARY

In this study, Abaqus FE modeling and stress-strain analyses, in 3-D dynamic mode to simulate real-time traffic loading and environmental conditions, were conducted using an in-service Hwy pavement structure on US 59 (Atlanta District). The input for the Abaqus FE 3-D dynamic modeling consisted of actual lab and field data, including material properties (i.e., modulus), traffic, climate (i.e., temperature), in-service PVMNT structure, etc. The maximum shear stress and vertical strains were then analyzed and correlated to the HMA material shear strength and the actual measured/observed field performance. The conclusions drawn from this chapter can be summarized as follows:

- Thicker overlays reduce maximum shear stress and vertical strains in the PVMNT structure, thus reducing the susceptibility to premature rutting/shear failures. However, for the analyzed PVMNT structure, the maximum shear stress for the 1.5-inch thick overlay was 1.91 MPa, which was less than the laboratory HMA shear strength (2.9 MPa). Thus, it is predicted that a thinner cost-effective 1.5-inch thick overlay would have sufficed for this particular PVMNT section for the considered loading conditions in terms of maximum shear stress. Nonetheless, the 2-inch thick overlay is structurally sound and conservatively safe based on these analyses, which are also in concurrence with field performance observations as at the time of this report.

103

- The shear stresses and vertical strains exhibited an increasing trend with an increase in the tire pressure and inclination angle. Considering the 420 psi (2.90 MPa) HMA shear strength of the Type D surfacing mix on US 59, the results suggest that the truck tire pressures should be kept below 120 psi on this highway, preferably at about 100 psi.

- Due to HMA's visco-elastic nature, modulus tends to be inversely related to temperature. Thus, due to reduced HMA stiffness (modulus), the HMA mix sustains less shear stress with increased vertical strains (deformation) at elevated temperatures.

- As theoretically expected, dual tire configuration for the same traffic loading, PVMNT structure, and environmental conditions is beneficial to pavement performance due to lower shear stresses and vertical strains compared to a single tire configuration.

- For turning traffic, 5 degrees appears to be the critical tire inclination or tilting angle producing maximum vertical strains on this particular highway. Therefore, special attention is required for minimizing tire inclination for turning traffic. This can be achieved by reducing the suggested speed limit at curvatures and increasing the turn radius during the design phase to limit the tire inclination angle. The results further indicate that intersections and horizontal curves that are subjected to turning traffic may be more vulnerable to shear failure than straight sections of the highway.

- FE 3-D dynamic modeling of the US 59 PVMNT section with tire rolling showed that the maximum shear stress occurs at the onset of tire braking, indicating that intersections, stop-go sections, and speed hump areas may be more critical to shear deformation and rutting.

CHAPTER 8   CORRELATION OF LABORATORY, FIELD, AND COMPUTATIONAL MODELING RESULTS

In an attempt to develop laboratory test procedures that are able to effectively characterize HMA rutting-shear performances under field loading conditions, a new HMA rutting-shear test method, the SPST, is introduced in this study (Chapters 4 and 5) along with some modification proposals to the HWTT method (Chapter 3). One of the primary challenges of developing a new laboratory test procedure is to calibrate and validate it through comparison and correlation with actual field performance data.

The primary focus of the work presented in this chapter was to validate the SPST procedure by comparing and correlating the laboratory test results of commonly used Texas HMA mixes with their respective field performance. The HWTT, which traditionally has a proven history of field correlation, was also evaluated alongside the SPST results to comparatively study the two lab test methods. The correlation and validation studies were executed following three approaches, namely:

- Correlation with conventional in-service field Hwy PVMNTs.
- Correlation with APT data.
- Correlation with computational model predictions.

The detailed discussions on each of these approaches, along with the corresponding results, are presented in the subsequent sections of this chapter.

CORRELATION WITH CONVENTIONAL IN-SERVICE FIELD HIGHWAY PAVEMENTS

Five in-service Hwy sections were selected that have different climate, traffic, and PVMNT structural conditions. The details of these test sections are described in Table 8-1 and Figure 8-1. For each test section, the work plan entailed testing the HMA mixes in the lab to obtain the SPST and HWTT data and comparing it to the field rutting data collected from the respective field Hwy sections.

Table 8-1. Description of the Selected In-Service Highway Test Sections.

Hwy	PVMNT Type	Mix Type	Date of Construction	Climatic Region	Max PVMNT Temperature	AADTT*
US 59	Overlay-HMA-LTB	Type D	Apr '11	Wet-Cold	135.5°F	1502
Loop 480	New Construction	Type C	June '12	Dry-Warm	145.5°F	60
SH 121	Overlay-HMA-CTB	CAM	Oct '11	Wet-Cold	137.5°F	468
SH 21	Overlay-HMA-FB	Type C	July '12	Wet-Warm	127.5°F	560
IH 35**	New Construction	Type B	Oct '11	Moderate	131.3°F	53

* AADTT = Average Annual Daily Truck Traffic

** Frontage (service) road

US 59 (Atlanta)   Loop 480 (Laredo)

SH 121 (Paris)   SH 21 (Bryan)   IH 35 (Waco)

Figure 8-1. Current Field Conditions of the Selected In-Service Highway Test Sections.

While comparing the laboratory rutting performance (SPST and HWTT) of the mixes with their respective field performance, it needs to be considered that the five in-service Hwy test sections selected for this study vary widely in terms of the traffic, climatic, and PVMNT structural conditions to which they are subjected. Also, since all five test sections are at different

stages of their service lives, the field rutting performances at 7 months after construction of each test section was considered for baseline comparison of all the test sections.

In order to compare the laboratory versus field performance of the mixes, it is vital that only the field rutting contribution of the relevant HMA layer is taken into account. Since a full-scale forensic study was beyond the scope of this study, the contributions of the respective layers were estimated through M-E modeling (using M-E PDG software) of the in-service Hwy pavement structures, as shown in Figure 8-2. Each highway section was modeled using the M-E PDG design software to calculate the percentage contribution of each layer toward the total surface rut depth. These estimated percentages were then used to estimate the rutting contribution of the relevant layers from the total surface rut depth measured from field surveys.
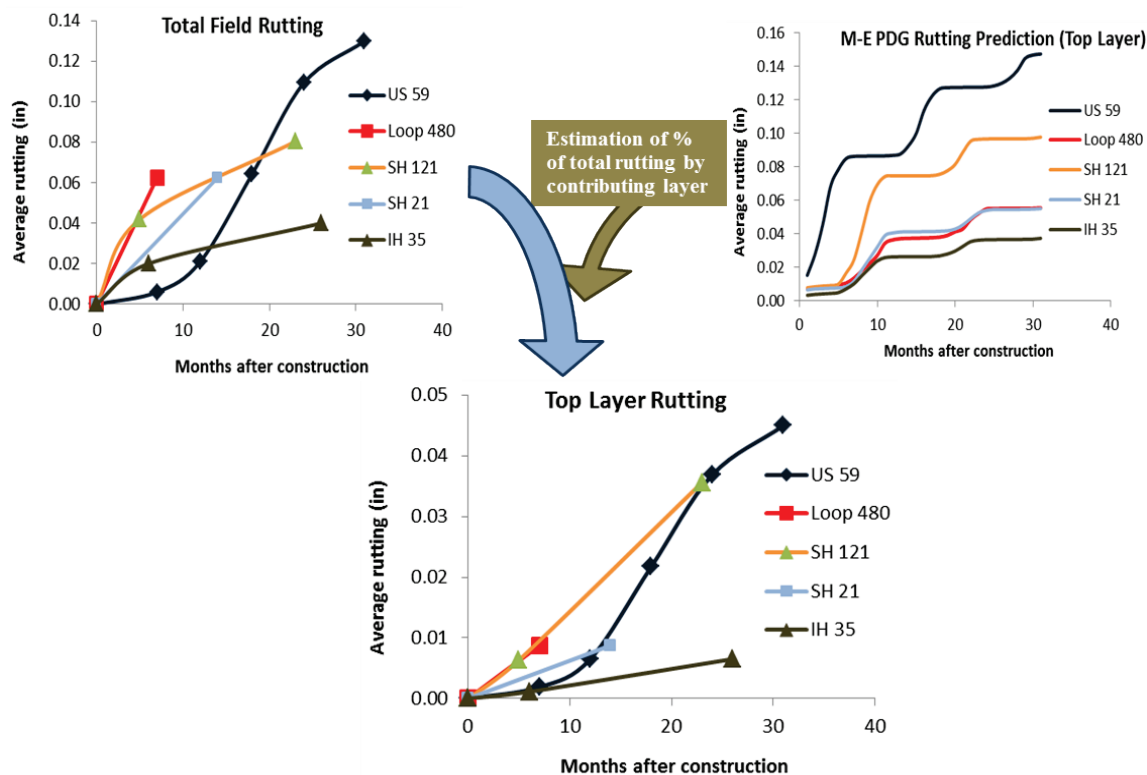
Figure 8-2. Estimation of Field Rutting of the Contributing Layer through M-E PDG Model Predictions.

Field Rutting Correlation with the SPST

Following the correlation methodology described in the preceding sections, the SPST results of the mixes were compared and correlated to their respective field rutting performances.

The SPST L-D curves for the five mixes are presented in Figure 8-3 alongside their respective field rutting curves.
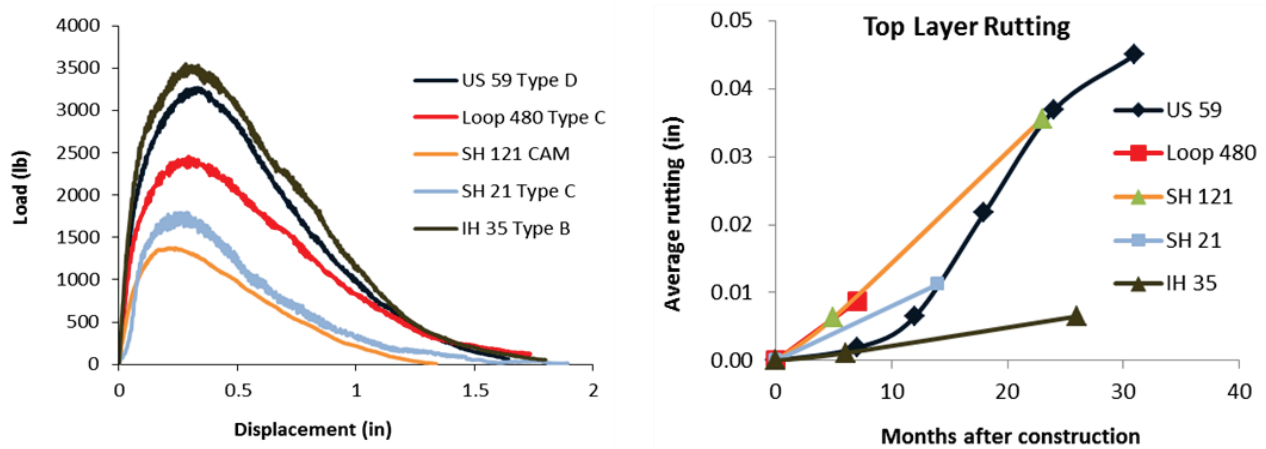
Figure 8-3. Comparison of SPST Load-Displacement Output with Field Rutting.

From Figure 8-3, it is observed that the SPST shear L-D curves present a good indication of a mix's field rutting performance. For example, the IH 35 Type B and the US 59 Type D mixes have the best SPST L-D curves in terms of high peak load and larger strain energy (area under the L-D curve). Indeed, these two mixes also show the best performance in the field in terms of rutting resistance. On the other hand, the SPST output of the SH 121 CAM mix gives a fair indication of the mix's poor rut resistance performance in the field. To better quantify the rutting performance correlation of these, Table 8-2 comparatively presents the SPST parameters and the field rutting measurements of these mixes.

Table 8-2. Comparison of SPST Lab Results with Field Rutting Performance.

Hwy	SPST				Total Field Rutting (in)		Top Layer Field Rutting (in)	
	τ_s (psi)	γ_s (in/in)	G_s (ksi)	SSE (kJ/m^2)	August 2014	After 7 months	Current	After 7 months
US 59	420 (11%)	0.135 (3.0%)	3.11 (9.2%)	55.8 (17%)	0.130	0.006	0.045	0.002
Loop 480	321 (1.8%)	0.108 (1.9%)	2.97 (3.5%)	42.9 (7.4%)	0.063	0.063	0.009	0.009
SH 121	178 (4.9%)	0.085 (15%)	2.11 (19%)	19.4 (6.6%)	0.080	0.046	0.036	0.012
SH 21	228 (4.5%)	0.114 (9.2%)	2 (12.4%)	18.6 (5.7%)	0.060	0.030	0.011	0.002
IH 35	456 (7.0%)	0.12 (5.9%)	3.82 (0.7%)	62.6 (1.2%)	0.040	0.020	0.007	0.001

Coefficient of Variation (COV) values are in parentheses.

108

The data in Table 8-2, it is observed indicates that the SPST has a fairly promising correlation with field performance. The US 59 Type D and the IH 35 Type B mixes have higher shear strength and shear strain energy than the other mixes and this is also reflected in their respective field performance, when considering the 7-month rutting performance data. Indeed, the early-life rutting performance of these two mixes is very similar. Due to a considerably higher level of traffic loading (Table 8-1), however, US 59 appears to be accumulating more rutting with time. Correlation curves were drawn from the results presented in Table 8-2 and are presented in Figure 8-4.
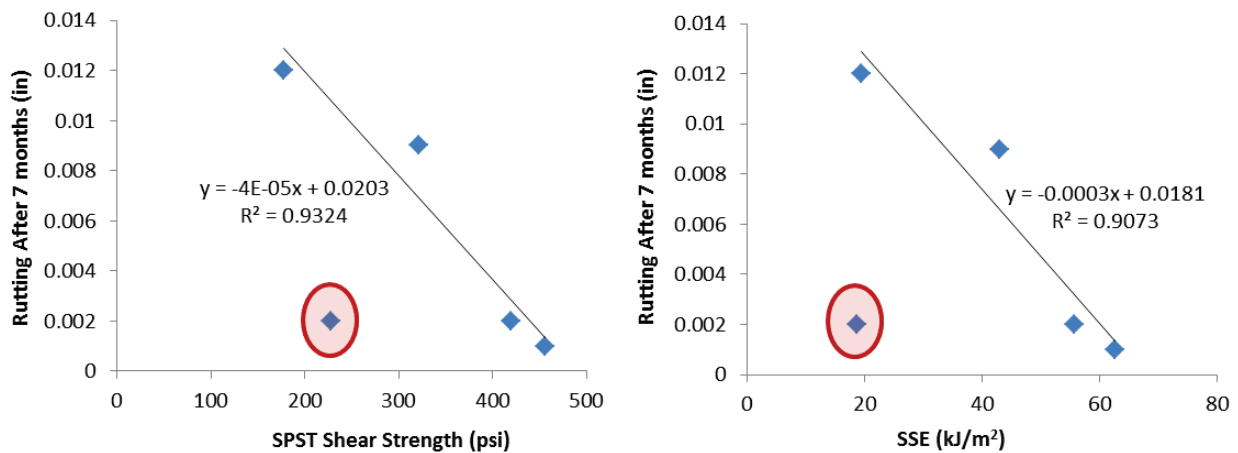
Figure 8-4. Correlation of SPST with Field Rutting Performance.

Except for one outlying mix (SH 21 Type C), Figure 8-4 shows good correlation between the laboratory SPST and field rutting performance of the mixes. The linear correlation strongly supports the hypothesis that higher HMA shear strength and shear strain energy results in less rutting in the field and high resistance to PD. However, caution needs to be exercised while drawing conclusions from such correlations between laboratory and field performance of in-service test sections to properly account for the diverse traffic, climatic, and PVMNT structural conditions for each of these field test sections.

Field Rutting Correlation with the HWTT

The HWTT results traditionally have good correlation with field rutting performance of HMA. However, to investigate the underlying reasons behind the number of recently observed field rutting failures, the research team decided to revisit the field correlation/validation aspect of the HWTT. Along with the traditional parameters, the new HWTT data analysis approaches,

described in Chapter 3, were also utilized in this correlation study. Figure 8-5 presents the HWTT rutting curves of the five mixes along with their respective field rutting performances.
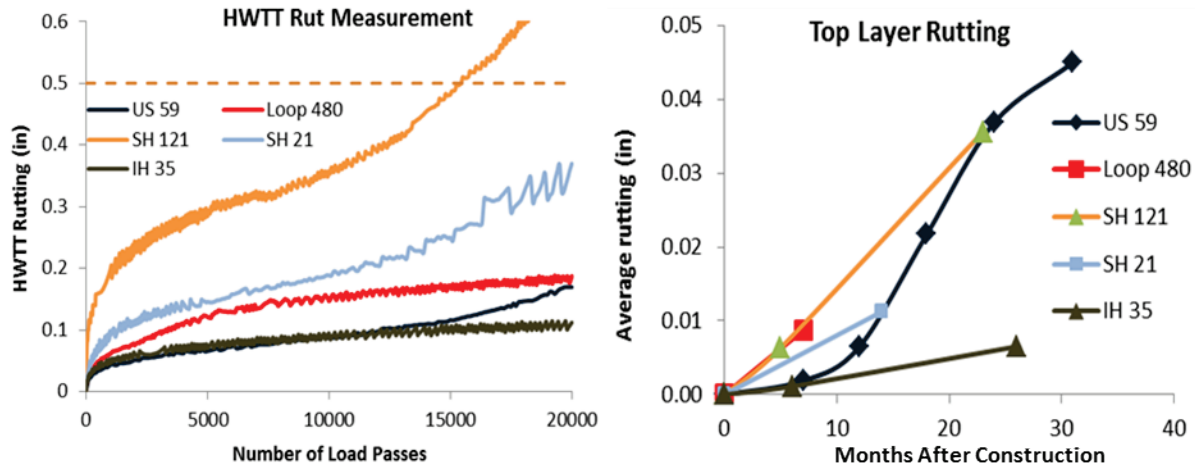
Figure 8-5. Comparison of HWTT Output Rutting Curves with Field Rutting.

Figure 8-5 indicates that the HWTT rutting curve shape can be a critical tool in estimating the field rutting performance of a mix. For example, the US 59 and the IH 35 HWTT and field rutting history curves up to 7 months follow a similar pattern and, in fact, overlap. HWTT rutting parameters were calculated for these mixes and are presented in Table 8-3 along with their respective field rutting performances.

Table 8-3. Comparison of HWTT Lab Results with Field Rutting Performance.

Hwy	HWTT (Tex-242-F)				Field Rutting (in)		Top Layer Rutting (in)	
	Rut_{max} (in)	Δ (in-cycle)	Rut_{Δ} (in)	SF	August 2014	After 7 Months	Current	After 7 Months
US 59	0.170	1865	0.090	1.099	0.130	0.006	0.045	0.002
Loop 480	0.190	2700	0.130	1.433	0.063	0.063	0.009	0.009
SH 121	0.500	4928	0.320	1.316	0.063	0.026	0.036	0.012
SH 21	0.370	4050	0.200	1.096	0.060	0.030	0.011	0.002
IH 35	0.110	1708	0.090	1.496	0.040	0.020	0.007	0.001

Based on the comparison between the HWTT and the field rutting performance presented in Table 8-3, it is observed that the traditional HWTT rut depth may at times not be sufficient to accurately predict the field rutting performance of a mix. For example, the US 59 Type D and the

Loop 480 Type C mixes have very similar HWTT rut depth (Rut_{max} = 0.17 inch and 0.19 inch, respectively), whereas, the early-life field rutting performance of these two mixes are widely different. However, considering the HWTT rutting path-history of the mixes can lead to a better prediction of their field rutting performance. Though not very pronounced, the Loop 480 Type C mix has a somewhat undesirable convex-like shape for the HWTT rutting response curve, indicating that the mix will be more prone to early-life rutting as compared to the US 59 Type D mix, which exhibits a concave-like shape for the HWTT rutting response curve.

Correlation curves were drawn comparing the top layer field rutting (after 7 months) of the mixes with their respective HWTT rutting parameters, namely, Rut_{max}, rutting area (Δ), and Rut_Δ, and are presented in Figure 8-6.
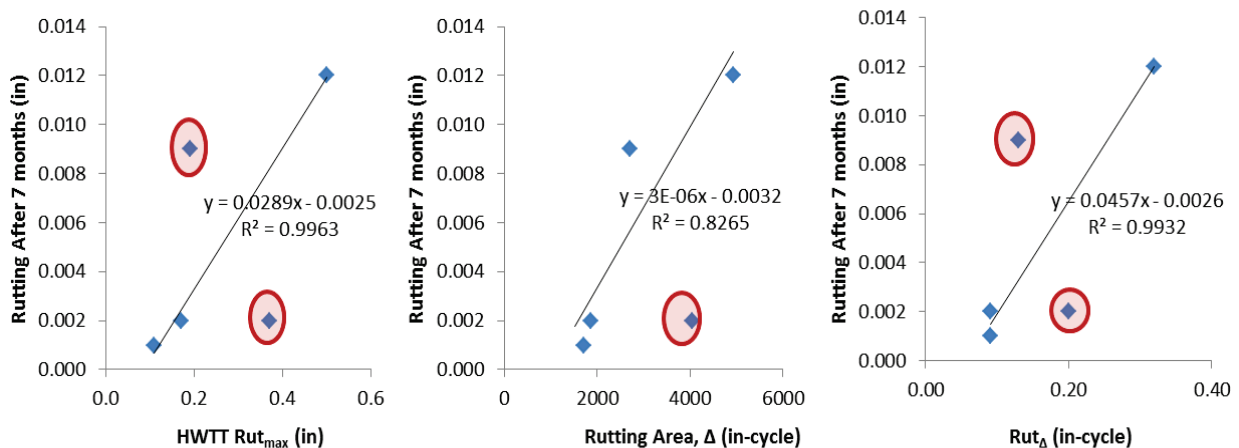
Figure 8-6. Correlation of HWTT with Field Rutting Performance.

From the three correlation curves presented in Figure 8-6, it is observed that for each pair of laboratory versus field rutting parameters, fairly linear correlations exist if outlier sections are ignored. For field rutting versus HWTT rutting area, one such outlier section exists (SH 21) and the rest of the mixes show a linear correlation with R^2=83 percent. In the case of the field rutting versus Rut_{max} and the field rutting versus Rut_Δ correlation curves, two outlier mixes are present. However, the remaining mixes show impressive linear correlation ($R^2 \cong 99$ percent).

The presence of the outlying sections is arguably due to the varying traffic, environmental, and PVMNT structural conditions of these sections. To obtain a truly objective correlation between laboratory and field rutting performance, it is imperative that these conditions are kept uniform among the sections to be compared.

CORRELATION WITH APT TEST SECTIONS

One of the key challenges in comparing and correlating laboratory test results with in-service field test sections, as was discussed in the preceding section of this chapter, is the diversity in traffic, environmental, and PVMNT structural conditions of the test sections. One possible way of obtaining uniform field conditions when comparing test sections is through APT in an accelerated loading facility (ALF). In this study, HMA mixes from the ALF-APT site located in Arlington, Texas, were tested in the lab to compare with the APT data. However, due to the unavailability of the APT field rutting data at this time, comparisons were only made with the M-E model predicted rutting performances of the respective APT sections, using PLAXIS, TxACOL, and M-E PDG software. The PVMNT structures and mix descriptions for the APT test site are presented in Figure 8-7.
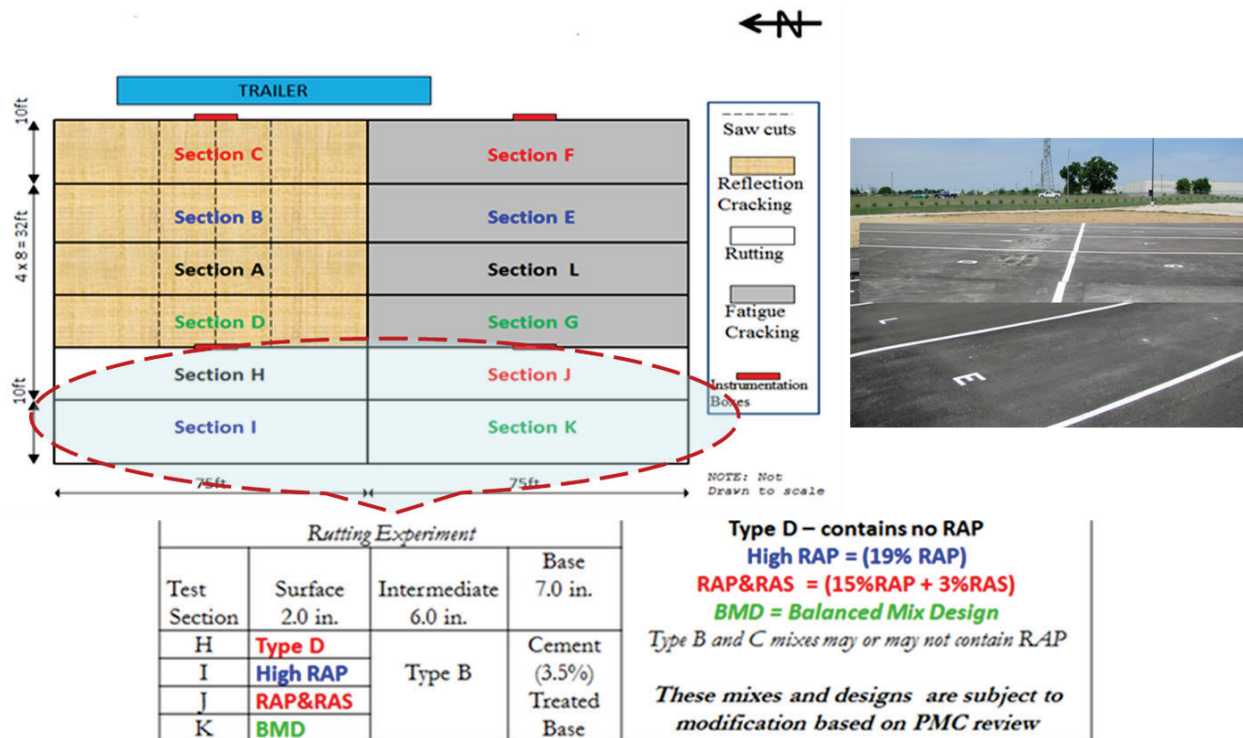
Figure 8-7. APT Test Sections Description (PG 64-22 on All the Rutting Experiment).

SPST results for the APT mixes are presented in Table 8-4 and Figure 8-8, along with their respective model performance predictions.

Table 8-4. Comparison of APT Rutting Performance: SPST vs. M-E Model Predictions.

APT Section	Mix Designation	SPST				Model Performance Prediction		
		τ_s (psi)	γ_s (in/in)	G_s(ksi)	SSE (kJ/m^2)	PLAXIS Vertical Displ. (mils)	TxACOL* Rutting (in)	M-E PDG* Rutting (in)
Sec H	Type D	313 *(3.7%)*	0.092 *(1.1%)*	3.4 *(2.7%)*	33.9 *(7.8%)*	12.58	1.01	0.50
Sec I	High RAP	333 *(5.9%)*	0.095 *(2.2%)*	3.53 *(9.1%)*	36.7 *(6.0%)*	12.20	0.15	0.29
Sec J	RAP & RAS	359 *(4.2%)*	0.094 *(4.9%)*	3.82 *(9.0%)*	38.2 *(1.2%)*	12.36	0.24	0.31
Sec K	BMD	295 *(5.8%)*	0.099 *(5.7%)*	2.99 *(7.4%)*	36.3 *(3.2%)*	12.79	0.84	0.54

Coefficient of Variation (COV) values in parenthesis   * Rutting prediction after 500k ESALs
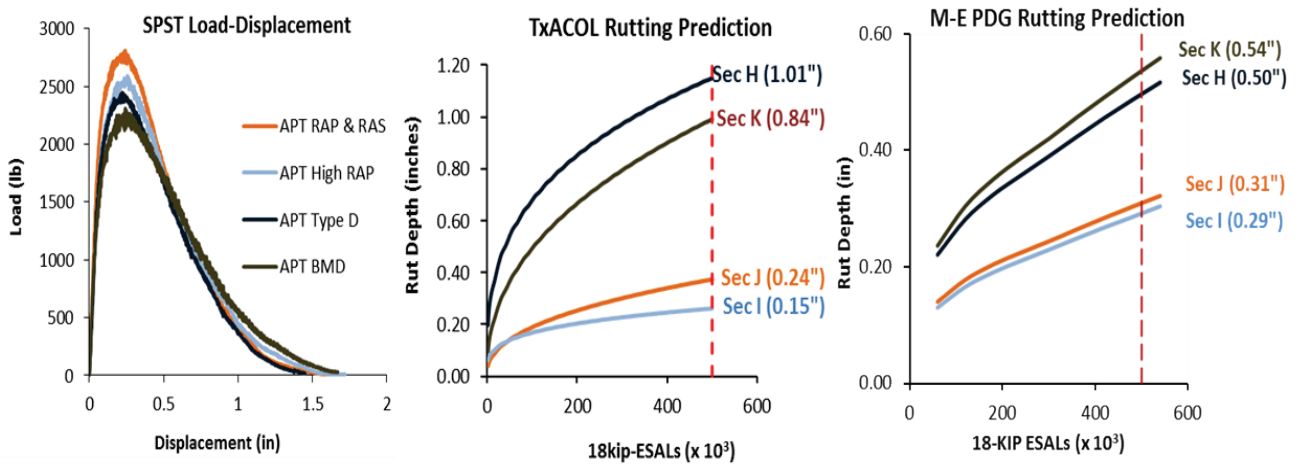
Figure 8-8. SPST L-D vs. Model Rut Predictions (TxACOL and M-E PDG).

As shown in Table 8-4 and Figure 8-8, the SPST lab test results show good correlation with the M-E model predicted rutting performance of the HMA mixes. As expected, the HMA mixes with RAP and RAS (Sections I and J) have low predicted rutting from both TxACOL and M-E PDG modeling. These HMA mixes, from Sections I and J, also have good shear resistance in the SPST with higher shear strength (τ_s > 300 psi). However, the SSE values of all four mixes are reasonably high (> 30kJ/m^2) and do not show significant difference to act as an effective screening parameter for these mixes. Figure 8-9 shows the correlation between the M-E model predicted rut performances of the mixes with their respective SPST parameters.
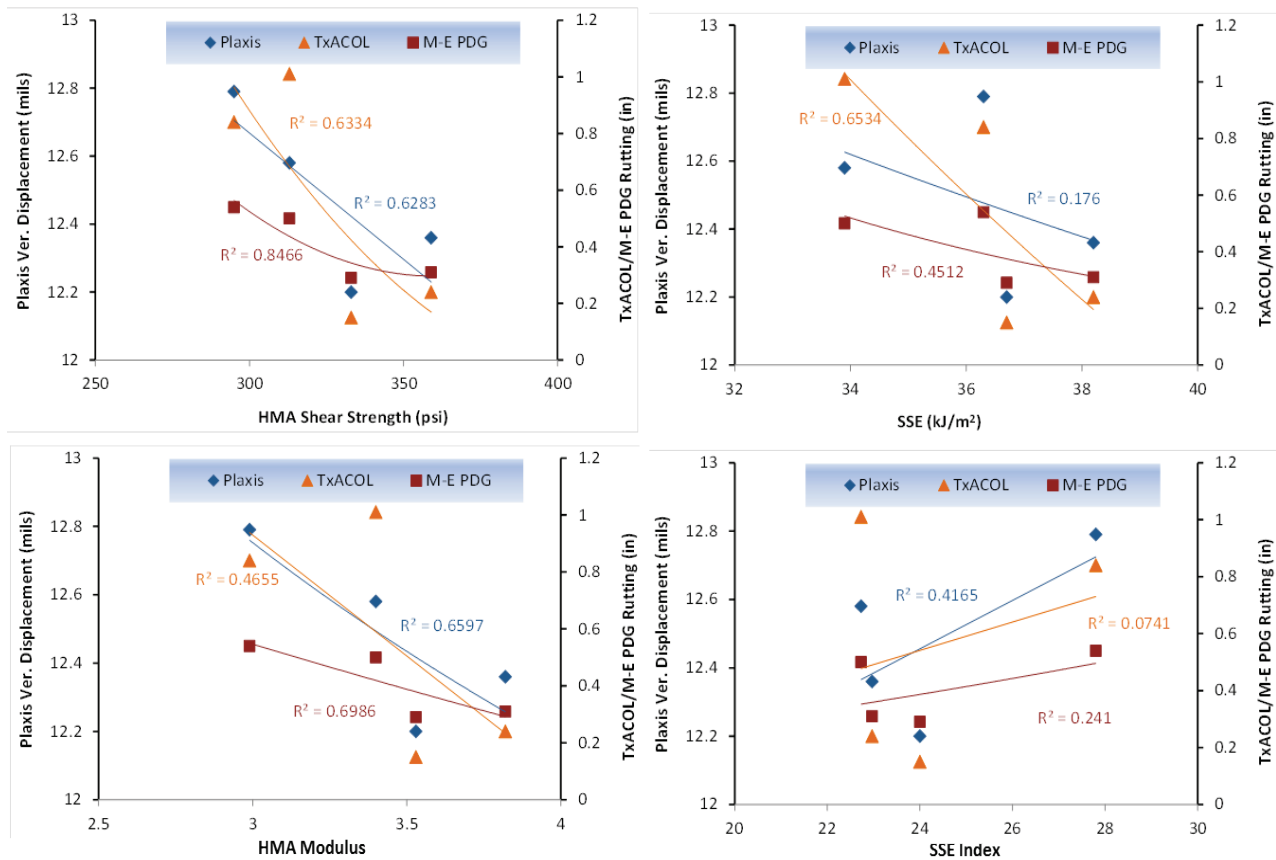
Figure 8-9. Plot of SPST Correlation with M-E Modeling.

From the correlation curves presented in Figure 8-9, it is evident that HMA shear strength and the modulus parameters gave better correlations with the model predicted rutting performances than the SSE and SSE Index. Especially, the M-E PDG rutting prediction has an 85 percent correlation with the SPST shear strength for the four APT mixes. HWTT results for the APT mixes are presented in Table 8-5 and Figure 8-10, along with their respective model performance predictions.

Table 8-5. Comparison of APT Rutting: HWTT vs. M-E Model Predictions.

APT Section	Mix Designation	SPST				Model Performance Prediction		
		Rut_{max} (in)	N_d	Rut_Δ (in)	SF	PLAXIS Vertical Displ. (mils)	TxACOL* Rutting (in)	M-E PDG* Rutting (in)
Sec H	Type D	0.50	12152	0.22	0.9	12.58	1.01	0.50
Sec I	High RAP	0.22	20000	0.12	1.1	12.20	0.15	0.29
Sec J	RAP- RAS	0.50	16773	0.20	0.8	12.36	0.24	0.31
Sec K	BMD	0.50	15102	0.23	0.9	12.79	0.84	0.54

* Rutting prediction after 500k ESALS

114
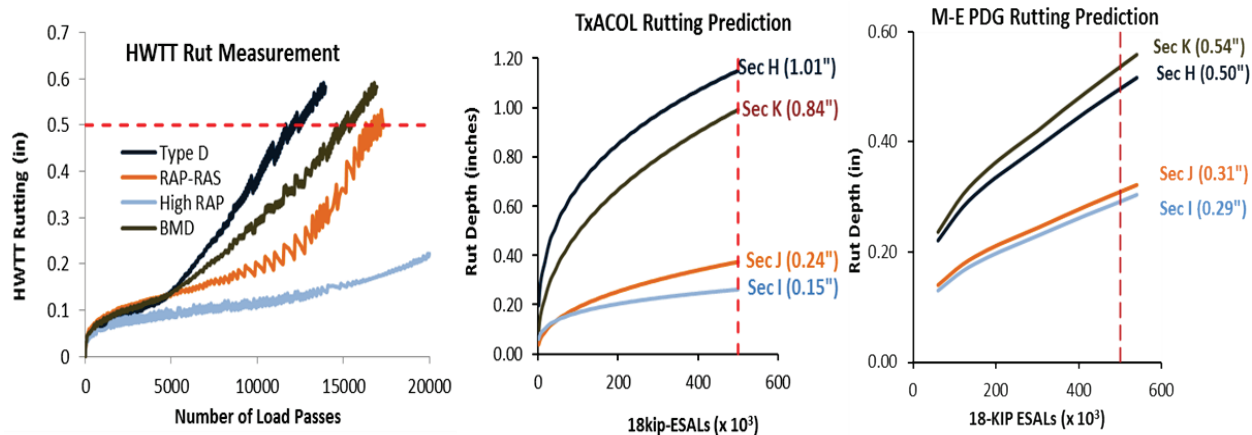
Figure 8-10. HWTT Rutting Curves vs. Model Rut Predictions (TxACOL and M-E PDG).

With the exception of Section J (RAP and RAS mix), the HWTT lab results also agree with the M-E model rut predictions of the HMA mixes for all the other APT test sections. The Section J mix failed (0.5-inch rut depth) after 16,773 load passes in the HWTT (Table 8-5), whereas, the M-E model rutting performance of this mix is in the same order as that of Section I (High RAP) for both PLAXIS and M-E PDG model predictions. Figure 8-11 presents the correlation between the M-E model predicted rut performances of the mixes with their respective HWTT parameters.
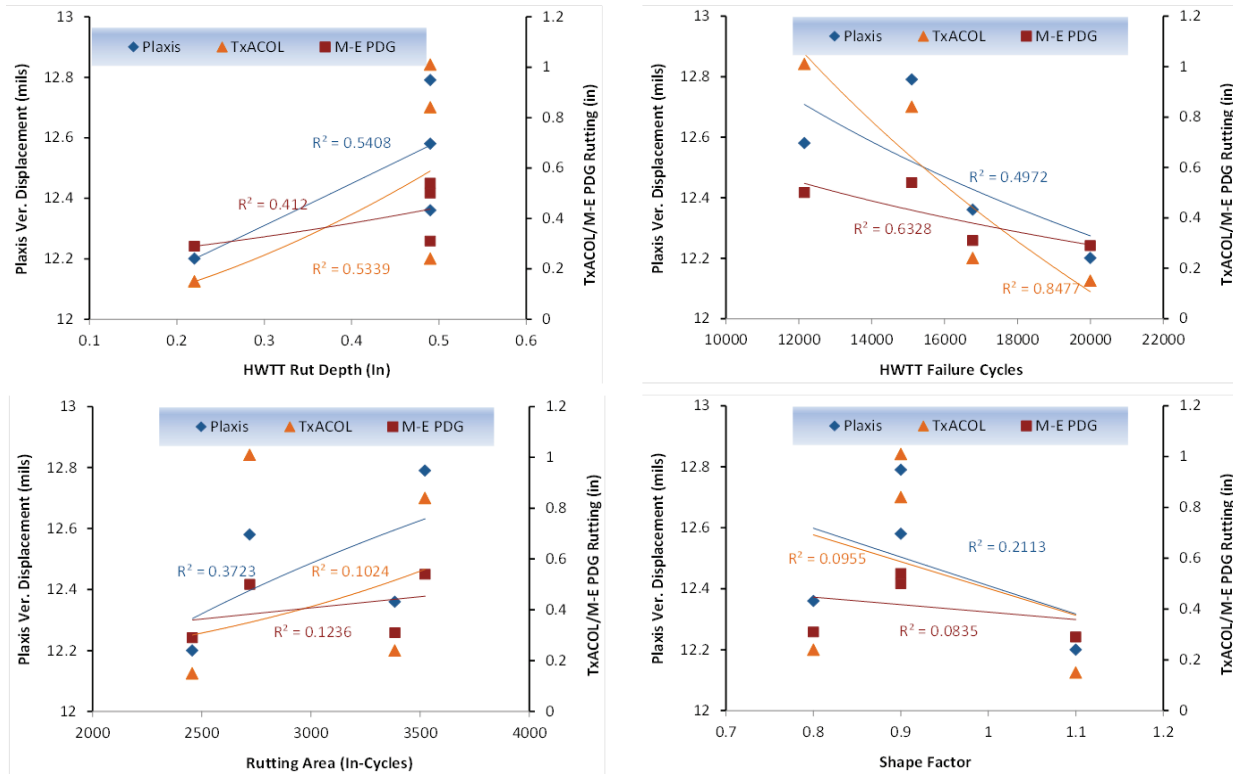
Figure 8-11. Plot of HWTT Correlation with M-E Modeling.

It is evident from Figure 8-11 that the failure cycles parameter shows superior correlation with the model prediction as compared to the other HWTT parameters. Overall, the HWTT correlation with the model predicted rutting performance is not as good as the correlation of the SPST results with the same.

CORRELATION WITH COMPUTATIONAL MODEL PREDICTIONS

As a means to further validate and establish some preliminary pass-fail screening criteria for the SPST method, laboratory test data were correlated to computational model predictions and actual measured/observed field performance on in-service Hwy sections. Abaqus FE modeling and stress-strain analyses, in a 3-D dynamic mode to simulate real-time traffic loading and environmental conditions, were conducted using an in-service Hwy pavement structure on US 59 (Atlanta District). The structural details of the test section are presented in Figure 8-12. The input for the Abaqus FE 3-D dynamic modeling consisted of actual measured lab and field data, including material properties (i.e., modulus), traffic, climate (i.e., temperature), in-service PVMNT structure, etc.

116

Layer#	Thickness (Inches)	Layer Material	Year Constructed
7	2.0	Type D (PG 64-22 with 20% RAP)	2011
3-6	~11.5	Existing HMA	-
1-2	~16.0	LFA Base (8" + 8" = 16")	-
0	∞	Compacted Subgrade Soil	-
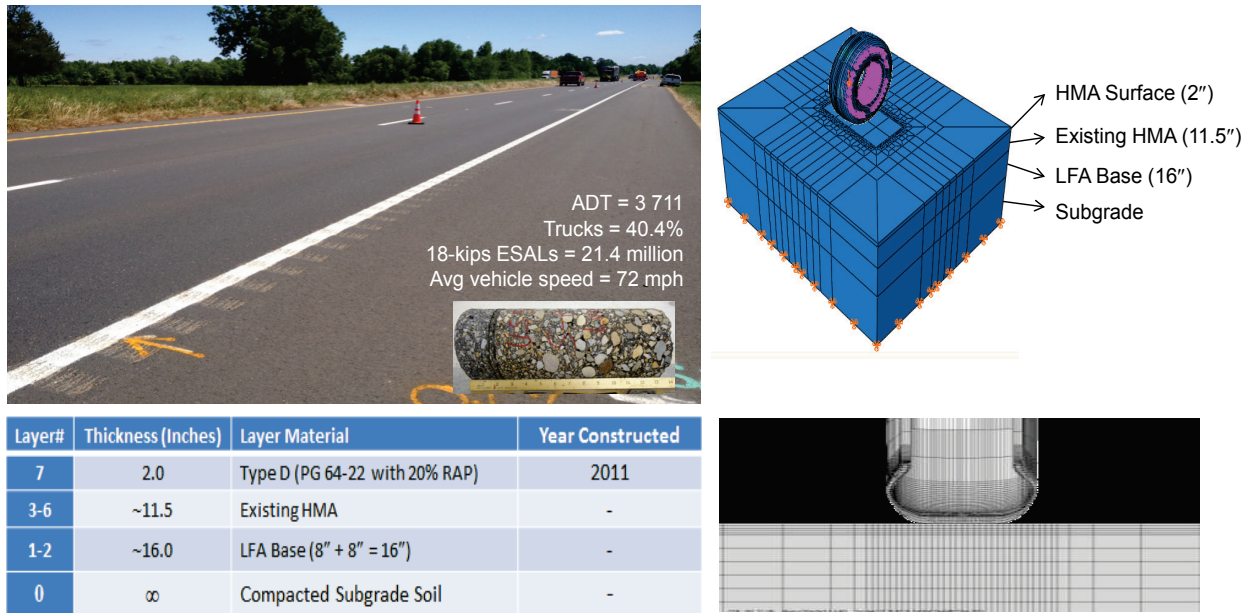
Figure 8-12. US 59 PVMNT Structure and Abaqus 3-D Modeling.

Abaqus FE modeling and 3-D dynamic simulations incorporated variations of the following factors that are considered critical to the HMA shear response, PD behavior, and rutting performance when subjected to Hwy traffic loading:

- Tire pressure.
- Temperature (in terms of the HMA modulus).
- Tire inclination angle (effects of turning traffic).
- Single versus dual tire configuration.
- Accelerating versus decelerating tire and braking effects.

The maximum shear stress and vertical strains were then analyzed and correlated to the HMA material shear strength and the actual measured/observed field performance. The obtained FE analysis responses are presented in Figure 8-13 through to Figure 8-17.
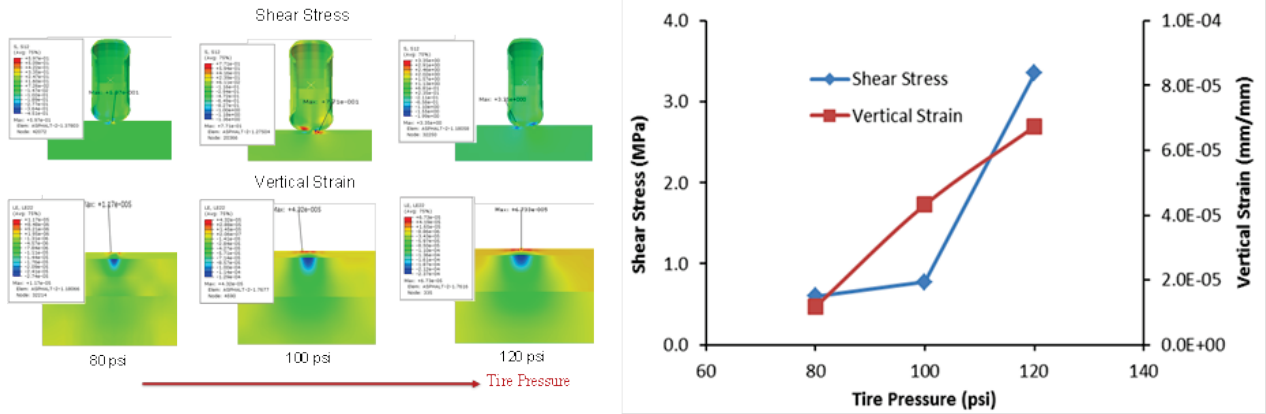
Figure 8-13. FE Modeling Results for Tire Pressure Variation (80–120 psi).
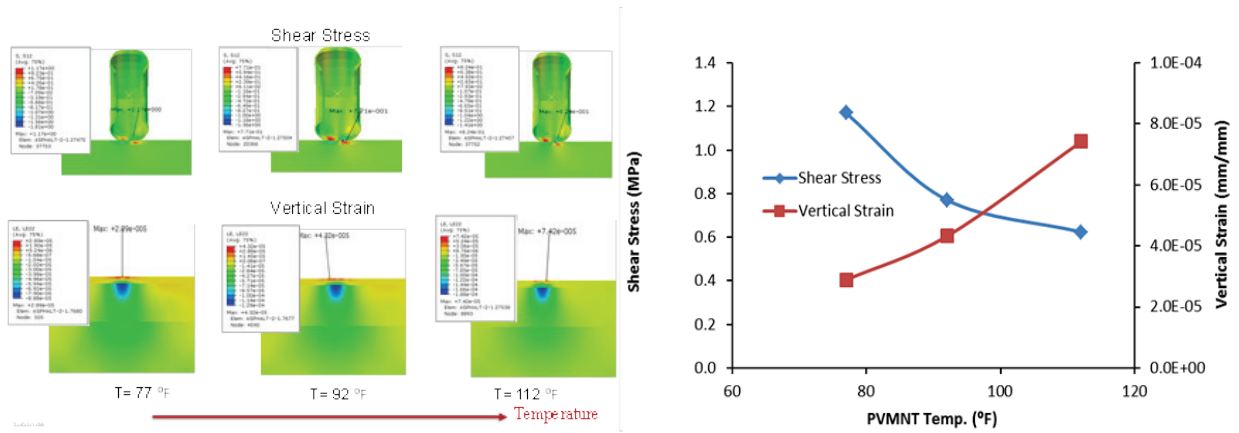
Figure 8-14. FE Modeling Results for Temperature Variation (77–112°F).
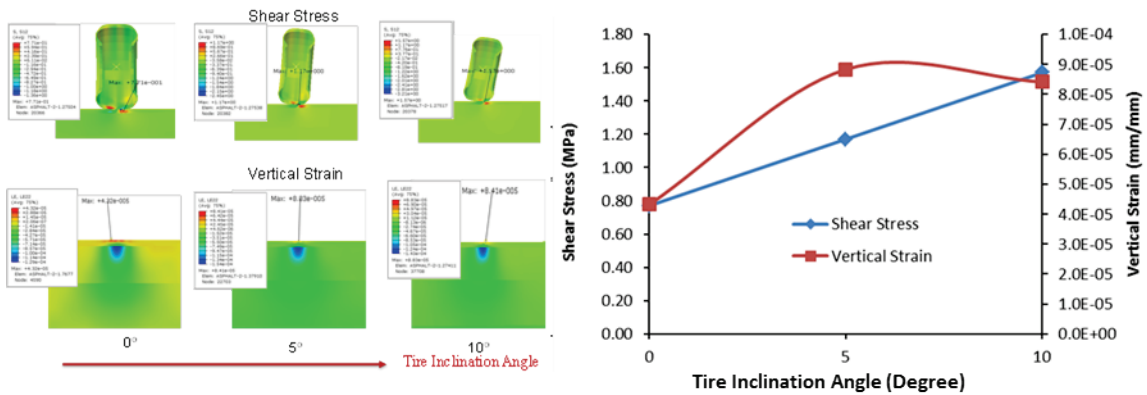
Figure 8-15. FE Modeling Results for Tire Inclination Angle Variation (0–10°).

118
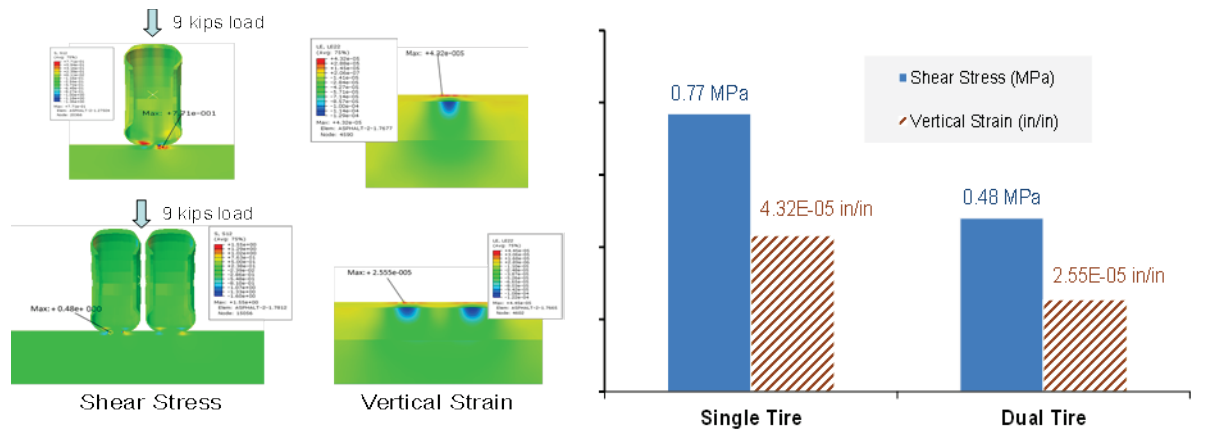
Figure 8-16. FE Modeling Results for Single vs. Dual Tire (9 kips Total Vertical Load).
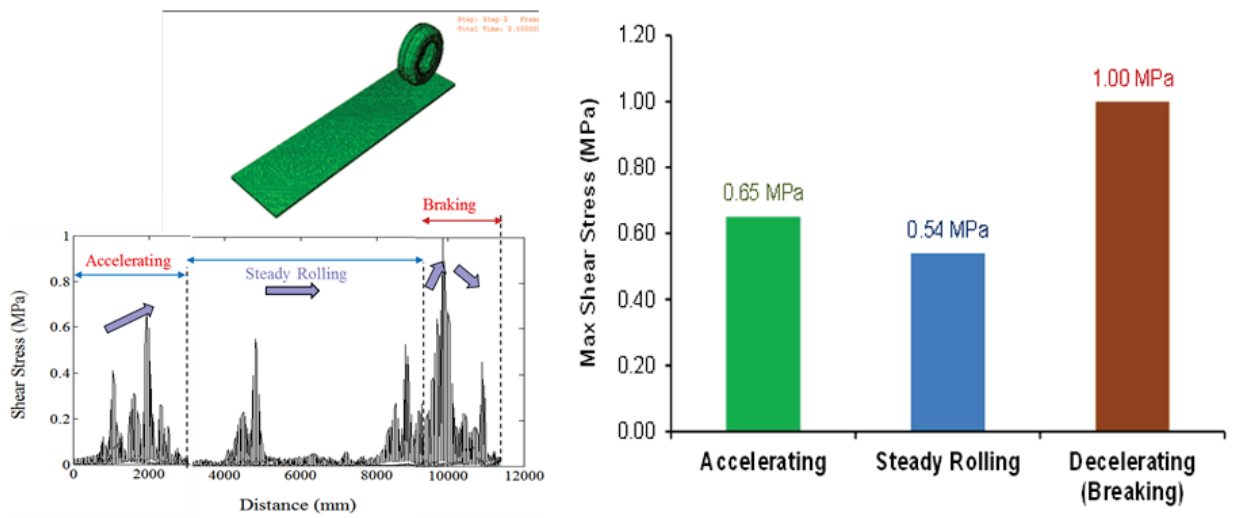
Figure 8-17. FE Modeling Results for Tire Accelerating–Steady Rolling–Decelerating.

The 3-D dynamic FE modeling responses were compared to the material properties obtained from the laboratory rutting-shear tests, namely the SPST and HWTT, as well as the current field rutting conditions for the particular Hwy section. The laboratory and the field test results are presented in Figure 8-18 and Figure 8-19, respectively.

119
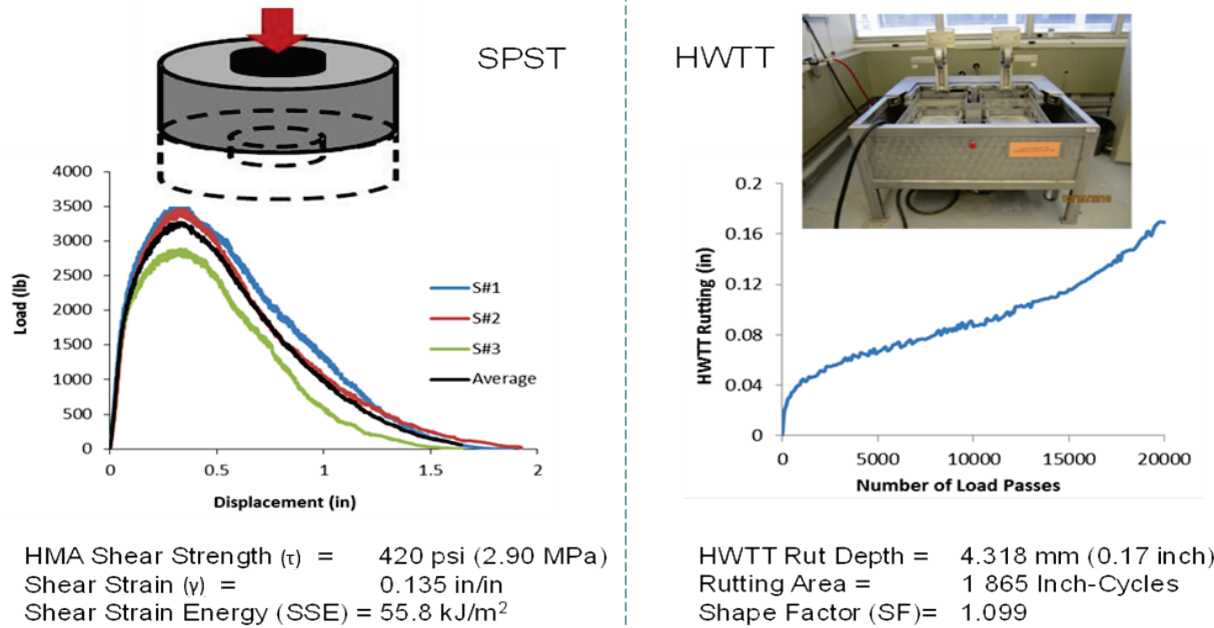
Figure 8-18. SPST and HWTT Lab Test Results for Type D Surfacing Mix Used on US 59.
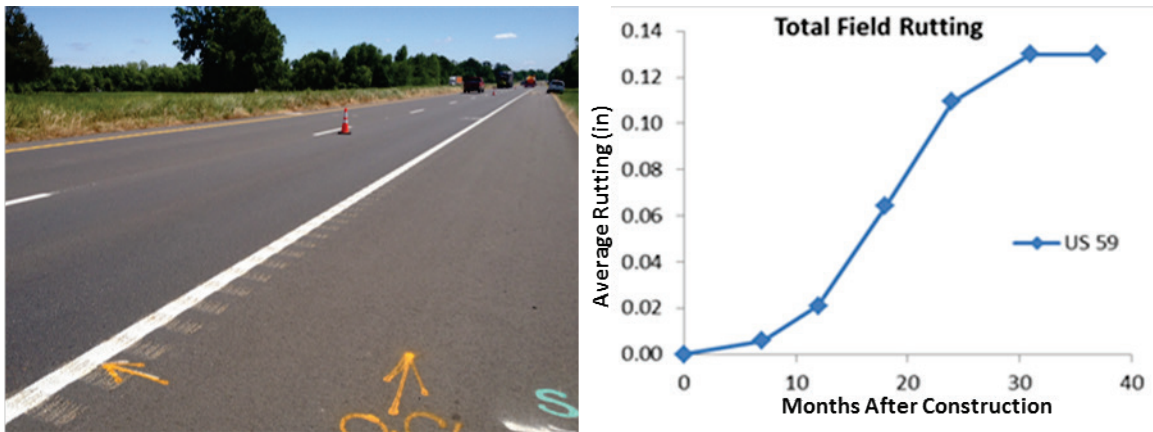
Figure 8-19. Visual Outlook and Measured Field Surface Rutting on US 59.

The findings from this correlation study are outlined in the following bullet listed paragraphs:

- The shear stresses and vertical strains exhibited an increasing trend with an increase in the tire pressure and inclination angle (Figure 8-13 and Figure 8-15, respectively). Considering the 420 psi (τ_s = 2.90 MPa) shear strength of the Type D surfacing mix on US 59, as presented in Figure 8-18, the results suggest that the truck tire pressures should be restricted to below 120 psi on this Hwy, preferably at around 100 psi. At the prevailing conditions, a tire pressure of 120 psi, with a resulting shear stress of 3.35 MPa cannot be

sustained by the Type D surfacing mix ($\tau_s = 2.90$ MPa). For turning traffic, 5 degrees appears to be the critical tire inclination or tilting angle for maximum vertical strains on this Hwy (Figure 8-15), suggesting that geometric design (banking and horizontal curve radius) of the highway should be carefully conducted so as to minimize the tire tilting angles below 5 degrees.

- Due to HMA's visco-elastic nature, modulus tends to be inversely related to temperature. Thus, due to reduced HMA stiffness (modulus), the HMA mix sustains less shear stress with increased vertical strains (deformation) at elevated temperatures; see Figure 8-14.

- As theoretically expected, dual tire configuration for the same traffic loading, PVMNT structure, and environmental conditions is beneficial to pavement performance due to lower shear stresses and vertical strains compared to a single tire configuration; see computational results in Figure 8-16.

- FE dynamic modeling of the US 59 PVMNT section with a rolling tire showed that the maximum shear stress occurs at the onset of tire braking, indicating that intersections and stop-go sections may be more critical to shear deformation and rutting. In Figure 8-17, the maximum shear stress (1.00 MPa) is indicated for braking and the least (0.54 MPa) for steady rolling when comparing accelerating, steady rolling, and braking tire.

- Considering 100 psi tire pressure, the maximum of the maximum shear stresses for each of the individual scenarios above occurs during vehicle turning and braking, most likely at intersections and stop-go areas. The computed maximum of the maximum shear stress (1.57 MPa) under these extraneous conditions is less than 2.90 MPa, the SPST measured shear strength of the mix. Thus, the Type D surfacing mix has sufficient shear strength to sustain the impacted traffic loading, which perhaps, has partly contributed to the satisfactory performance of US 59 evident in Figure 8-19, with very marginal surface rutting. However, the modeling results did not consider the interactive and simultaneous combination of the critical parameters (i.e., high temperature, high tire inflation pressure, high tire inclination angle combined with the decelerating tire effects, etc.), which is likely to produce higher shear stresses and vertical strains. Therefore, the aforementioned conclusions may not be exhaustive.

SUMMARY

This chapter documented the efforts undertaken by the research team to correlate and validate the newly developed test method for SPST against field rutting-shear performance. Laboratory-obtained shear and rutting properties of commonly used Texas mixes were compared with their respective field performance, along with inputs from 3-D dynamic FE modeling. Two approaches were followed in order to correlate lab data with field performance data, namely, correlating with in-service field Hwy test sections and correlating with field data from APT test sections. The overall findings from this chapter can be summarized as follows:

- The SPST showed promising correlation with field rutting performance for the mixes and Hwy test sections evaluated. The HMA shear strength (τ_s) and shear strain energy (SSE) parameters, in particular, seem to give good indication of the mixes' field performance.

- In addition to the traditional HWTT outputs (rut depth), consideration of the HWTT rutting path-history (i.e., the HWTT curve shape) can lead to better prediction of field performance, especially for mixes in high shear stress locations. These additional HMA mix screening parameters (Rut_Δ and SF) should be considered for possible inclusion in the Tex-242-F test procedure, along with appropriate mix screening criteria.

- Both the SPST (τ_s and SSE) and HWTT results (HWTT rut depth and rutting area) showed promising correlation with M-E model predictions for the APT test sections.

- For the APT test sections, both the lab test results and the M-E model predictions yielded similar ranking of the HMA mixes in terms of their rutting/shear performances. However, the M-E model predictions showed higher discrimination between the good and poor mix pairs. Between the two lab test methods, the SPST shear strength exhibited superior correlation with the M-E model predictions. Nonetheless, verification with actual APT field rut measurements is imperative to validate these results.

- Based on the lab, computational modeling, and field data presented in this chapter, preliminary SPST pass-fail screening criteria for HMA mixes at 50°C (122°F), with a 1.5-inch diameter punching head at a monotonic loading rate of 0.20 mm/sec under confined sample conditions, are tentatively proposed:

a) Shear strength (τ_s) $\geq$ 300 psi (2.07 MPa).

b) Shear strain energy (SSE) $\geq$ 25 kJ/m^2.

- SPST repeatability was also concurrently assessed in terms of variability in the test results for both the US 59 Type D and APT mixes, through computation of the COV values. Overall, the lab data showed good repeatability for the SPST method, with variability in the test results having COV values less than 30 percent. In fact, the maximum registered COV was only 16.8 percent, surprisingly for a dense-graded Type D mix.

- SPST lab testing and FE Abaqus 3-D dynamic modeling indicated that the Type D surfacing mix, used on US 59, has sufficient shear strength to withstand the traffic-load induced shear stresses including turning and braking vehicles at controlled intersections or stop-go traffic conditions. The computed shear stresses at 100 psi tire pressure and PVMNT temperature of 77 to 112°F were all less than the 420 psi (2.90 MPa) shear strength of the mix. Evidently, these analyses also highlight the fact that the SPST method can be directly related to both FE modeling and field performance, i.e., the parameters (shear strength) measured in the lab from the SPST, can be directly correlated to Abaqus FE model predictions (shear stresses) and field performance.

CHAPTER 9   PRELIMINARY LABORATORY TEST SPECIFICATION MODIFICATION AND DEVELOPMENT

This chapter summarizes the findings of the preceding chapters to propose modifications to the existing test procedure Tex-242-F for HWTT, as well as the new test specification for the SPST. Complete drafts of the proposed modification to the HWTT specifications and the newly proposed SPST specifications are presented in Appendices A and B, respectively. The key components of these two specifications are discussed in this chapter.

MODIFICATIONS TO THE HWTT SPECIFICATION

The researchers proposed modifications to the current HWTT test procedure Tex-242-F based on the sensitivity evaluation of the critical HWTT steps in Chapter 3 and experience gained from past studies. Also, alternate data analysis procedures were developed in order to make the HWTT more effective in evaluating the HMA rutting resistance and are included as proposed modifications to the Tex-242-F test procedure. Discussions of the proposed modifications are presented below:

- From the HWTT sensitivity evaluation, it was observed that the HWTT rutting of most commonly used Texas mixes increased significantly with temperature, with most mixes failing at temperatures exceeding 60°C. Based on this finding, the researchers proposed testing at multiple temperatures up to 60°C, especially for mixes that are to be placed in high temperature areas and/or "urban stop-go environments." Furthermore, field PVMNT temperatures in the past two Texas summers averaged around 58.3°C, which is considerably higher than the current Tex-242-F testing temperature of 50°C. Inevitably, this justifies the need to consider 60°C as a supplementary test condition in the Tex-242-F test procedure.

- Although, the current specification is conservative in terms of sample air voids, inconsistency in the test sample density often results in misleading HWTT rutting performance of the mixes. Therefore, the modified Tex-242-F test procedure recommends undertaking a "pre-molding" procedure consisting of molding some trial/preliminary samples to ensure that the desired sample density can be consistently achieved.

- The current HWTT machines have some challenges that include wheel load variations and testing in dry conditions under varying temperatures. To accommodate circumstances where these test conditions may be needed, modification or use of HWTT machines with capabilities for changeable wheel loads and testing under dry conditions at varying temperatures is suggested. This will allow for a re-evaluation of these particular sections of the Tex-242-F test procedure and propose modifications, if necessary.

- The current Tex-242-F test procedure does not have any guidelines regarding the amount of time the sample can be stored between fabrication and actual testing (sample sitting time). However, from this study, the research team has identified that a longer sitting time significantly increases the HWTT rutting resistance potential of the mixes through short-term oxidative aging of the asphalt-binder, thus posing the threat of misleading laboratory rutting performance of the mixes. To mitigate this effect, the research team proposed that the modified Tex-242-F test procedure would require samples to be consistently tested within five days of molding/fabrication.

- The current Tex-242-F test procedure does not specify any instructions for the analysis of the reported test data. The primary output (automatically reported by the machine) includes the number of load passes to failure and rut depth. In this study, the researchers found that the HWTT rutting path-history is a critical indication of the field performance of a mix, especially in terms of early-life field rutting, and have, accordingly, proposed some analysis procedures to capture these aspects through two newly introduced HWTT parameters, namely the "normalized rutting area (Rut_Δ)" and the "shape factor (SF)."

- The Rut_Δ parameter accounts for the rutting path-history of the sample/mix, whereas, the SF parameter accounts for the shape of the HWTT rutting curve (HWTT rut depth vs. number of load repetition curve). In general, the following are the tentatively proposed HMA screening/evaluation criteria when using these two HWTT parameters:
  - Higher Rut_Δ: signifies poor rutting resistance of the sample/mix.
  - SF > 1.25: less desirable for high temperature and high shear stress locations such as intersections, urban stop-go sections, etc., particularly with respect to the early-life rutting of the HMA mix.

o SF $\leq$ 1.25: more suitable for high temperature and high shear stress sections such as intersections, urban stop-go sections, etc.

• For mixes to be used in slow vehicle-speed areas such as intersections, urban city roads, etc., testing at lower and/or multiple HWTT wheel speeds should be considered as a supplement to the currently specified 50 ± 2 passes/minute, i.e., from 50 down as low as 35 passes/minute. For these special slow vehicle-speed areas, any or all of the following HWTT wheel speeds can be considered: 50, 45, 40, and/or 35 passes/minute.

The proposed modifications/additions to the Tex-242-F test procedure are summarized in Table 9-1 and also shown in <mark>yellow</mark> highlighted *italic font* in Appendix B.

Table 9-1. Proposed Modifications and Additions to Tex-242-F.

#	Tex-242-F	Proposed Modification/Addition	Comment
1	Item 4.1 (Note 2)	To ensure consistency, testing all the lab-molded HWTT specimens within five days of sample molding/fabrication is recommended.	Helps to minimize the possible effects of oxidative aging that can stiffen up the HMA.
2	Item 4.1.1 (Note 4)	The current HWTT protocol is conservative in terms of test sample air voids, thus no modifications are suggested in this aspect. However, to ensure consistency of the sample density, a pre-molding should be considered where necessary.	Although optional, pre-molding aids in improving HMA density accuracy and consistency, and saves both time and material wastage during molding.
3	Item 5.7 (Note 7)	The HWTT at lower wheel speeds (as low as 35 passes/minute) should be considered to supplement the specified 50 ± 2 passes/minute, particularly for mixes to be placed in slow vehicle-speed areas, e.g., intersections, and urban stop-go zones.	Critical for slow vehicle speed areas such as intersections, urban stop-go sections, speed hump zones, etc.
4	Item 5.8 (Note 8)	Higher or multiple HWTT temperatures should be considered for HMA mixes to be placed in high temperature areas up to 60°C, i.e., testing the mixes at 50, 55, and 60°C, respectively.	Current summer PVMNT temperatures are very high, averaging 58°C, and sustained for longer periods.
5	Item 6	To effectively capture the rutting path-history of the tested HMA samples, two additional HWTT parameters are proposed, namely, the "normalized rutting area (Rut_Δ)" and the "shape factor (SF)" with the following proposed failure criteria: a) $Rut_\Delta < 8.0$. b) SF $\leq$ 1.25.	These parameters are particularly very critical for assessing HMA's potential and susceptibility to early-life rutting.

THE PROPOSED DRAFT TEST SPECIFICATION FOR SPST

As presented in the preceding chapters, the researchers developed the SPST specification based on the laboratory tests undertaken to identify the test input parameters, sensitivity evaluation of the critical test parameters, loading conditions, modeling, and the preliminary field correlation studies performed to validate the test results.

The proposed SPST specification is included as Appendix C of this report. A discussion of the key features of the proposed test method is presented below:

- The SPST method determines the HMA shear properties of the compacted bituminous mixtures. The measurable and calculable shear parameters include: shear strength (τ_s), shear strain (γ_s), shear modulus (G_s), shear strain energy (*SSE*), and shear strain energy index (*SSE Index*).

- The proposed test protocol was developed such that commonly used Texas mixes can be routinely tested using commonly available material testing apparatus and fixtures, e.g., the universal testing machine (UTM), IDT testing jigs. For practicality, the sample size and test temperature for the SPST were devised to be similar to those of the HWTT and other HMA rutting tests in order to facilitate easy comparison of results.

- Fast, simple, and reasonably practical test procedure.

- The proposed SPST specification outlines the data analysis procedures and formulae to be used for calculating the HMA shear properties/parameters. The primary output of the test is the HMA shear load versus shear displacement response curve. These output data can be used to evaluate the HMA shear parameters, including HMA shear strength, shear strain at peak load, shear modulus, shear strain energy, SSE Index, etc.

- Following a series of laboratory sensitivity evaluation tests and a preliminary field validation study through performance correlation with in-service Hwy test sections and APT site, the researchers proposed a preliminary screening criteria for HMA shear resistance properties at 50°C SPST temperature as follows:

    a) *HMA shear strength (τ_s) $\geq$ 300 psi.*

    b) *SSE $\geq$ 25 kJ/m^2.*

If testing at 60°C, the following should tentatively be considered as a preliminary guidance for screening mixes:

a) *HMA shear strength (τ_s) $\geq$ 200 psi.*
b) *SSE $\geq$ 17 kJ/m^2.*

SUMMARY

This chapter listed the focal points of the modifications that are proposed to the current HWTT specification. These modifications were based on a thorough study of the testing procedure for the HWTT, which is comprised of extensive laboratory testing and subsequent data analysis. The proposed modifications are expected to improve the overall consistency and effectiveness of the test method for the HWTT in predicting the field rutting performances of HMA mixes. Also included in this chapter was a discussion of the proposed (draft) specification of the newly developed SPST. The test specifications are included as Appendices B and C of this report.

CHAPTER 10   CONCLUSIONS AND RECOMMENDATIONS

Traditionally run at one test temperature (122°F), the HWTT has a proven history of identifying hot-mix asphalt mixes that are moisture susceptible and/or prone to rutting. However, with the record summer temperatures of the recent years, several shear and rutting failures have occurred with HMA mixes that had passed the HWTT in the laboratory. Most of these failures occurred in high shear locations, in particular with slow-moving (accelerating/decelerating) traffic at controlled intersections, stop-go sections, in areas of elevated temperatures, heavy/high traffic loading, and/or where lower PG asphalt-binder grades have been used.

This study was undertaken by these researchers as a step toward improving the HWTT performance in simulating the field rutting conditions of the HMA and exploring new supplementary and/or surrogate HMA rutting/shear tests. The findings of this study are presented in detail in the preceding chapters of this report. This final chapter provides a summary of the overall findings and the recommendations drawn from this study.

EVALUATION OF THE HWTT PROTOCOL (TEX-242-F)

The current HWTT protocol was comprehensively evaluated in this study in order to improve the HWTT performance in simulating the field rutting conditions of the HMA, and the key findings are listed below:

- Current HWTT protocol specifies rutting performance of any mix at the end of the test without considering the rutting path-history. To address this issue and to capture the HWTT rutting path-history, three new HWTT parameters were introduced, namely the rutting area (Δ), the normalized rutting area (Rut_Δ), and the shape factor (SF). Among these, the Rut_Δ and the SF parameters showed promising potential to capture the HWTT rutting response and path-history. Therefore, the researchers recommended that these two parameters should be considered in the HWTT protocol and Tex-242-F test procedure, with the following tentative HMA mix screening criteria:

    1) $Rut_\Delta < 8.0$.

    2) $SF < 1.25$.

- HWTT rutting increases significantly with temperature with most mixes failing at 70°C. Therefore, considering the recent sustained elevated summer temperatures, higher or multiple HWTT temperatures should be considered for mixes to be placed where

pavement temperatures are in excess of 60°C. For example, testing could be conducted at 50, 55, and 60°C, respectively.

- Rutting performances of mixes worsen at lower wheel speeds. Based on this, it is argued that the HWTT should be tested at lower speeds (as low as 35 passes/minute) than the currently specified 50 ± 2 passes/minute, particularly for mixes to be placed in slow vehicle-speed zones such as intersections or urban stop-go zones.

- HWTT rutting-resistance performance of HMA improves with increased sample sitting time, i.e., the time between sample molding/fabrication and testing due to short-term aging of the asphalt. Therefore, allowing long and inconsistent sitting times for HWTT samples can lead to misleading rutting performance prediction of mixes, thus increasing the risk of premature early-life rutting failures in the field. To ensure consistency, and based on the results of this study, the researchers recommend testing all HWTT specimens within five days of sample molding/fabrication.

- The current HWTT protocol is conservative in terms of test sample air voids, thus no modifications are suggested in this aspect.

DEVELOPMENT OF THE SIMPLE PUNCHING SHEAR TEST

The SPST was developed as a supplementary HMA shear test method to potentially serve as a surrogate to the HWTT. The proposed preliminary SPST parameters are listed below:

- HMA specimen dimensions: 2.5-inch thick by 6.0-inch diameter
- HMA sample sitting time: Test lab-molded samples within 5 days of molding
- Monotonic compressive-loading rate: 0.2 mm/sec
- Punching loading head: 1.5 inches
- Test temperature: 50°C (test at 50, 55, and 60°C for mixes to be used in high temperature locations, high shear stress areas, urban stop-go sections, intersections, etc.)
- Sample restraint: Confined
- Output and measurable data: Peak shear failure load, shear failure displacement at peak load, HMA shear strength (τ_s), shear strain (γ_s), HMA shear modulus (G_s), shear strain energy

- HMA mix screening parameters:

(SSE), and SSE Index

Shear strength and SSE. These two parameters also exhibited superior repeatability with very low variability and COV values less than 30 percent.

- Confining torque

25 in-lb

A sensitivity study was conducted on the SPST, and the findings can be summarized as follows:

- The SPST was found to be reasonably sensitive to test input parameters (e.g., loading rate and temperature) and HMA mix variables (e.g., asphalt-binder type and content).

- Among the five HMA shear parameters calculated from the SPST, the shear strength was found to be the most sensitive to the test input variables, followed by the shear strain energy and shear modulus.

- For the mixes evaluated, the shear strain and the SSE Index parameters did not show any definitive trend with changing test input parameters and HMA mix-design variables.

- Based on the observed SPST results, the shear resistance of the tested HMA mixes increased with test loading rate and decreased with test temperature. Both these behaviors are theoretically expected. At a higher loading rate, the mixes get less recovery time, thus increasing resistance to shear failure; whereas, at higher temperature, the mixes become softer, thus decreasing the shear resistance.

- The shear resistance of the tested mixes increased with asphalt-binder PG grading and decreased with asphalt-binder content (AC). In general, any mix with higher PG grade traditionally performs well under shear loading in the field, whereas, shear performance of the mix worsens with increased AC due to the increased softness of the mix.

- A statistical analysis at 95 percent confidence level showed the supremacy of the shear strength and SSE parameters over the shear strain and SSE Index in capturing the SPST sensitivity to input parameters and HMA mix-design variations, thus confirming the findings from the graphical plots. These findings also substantiate Chapter 4's recommendations to adapt the shear strength and SSE as the mix screening parameters for HMA shear resistance potential.

CORRELATION OF LABORATORY, FIELD, AND COMPUTATIONAL MODELING

The HWTT and the SPST results were compared with field and computational data to validate both test procedures, as well as to establish some preliminary pass-fail screening criteria for the SPST method. The findings are summarized as follows:

- The SPST showed promising correlation with field rutting performance for the mixes and Hwy test sections evaluated. The HMA shear strength (τ_s) and shear strain energy (SSE) parameters, in particular, seem to give good indication of the mixes' field performance.

- In addition to the traditional HWTT outputs (rut depth), consideration of the HWTT rutting path-history, (i.e., the HWTT curve shape), can lead to better prediction of field performance, especially for mixes in high shear stress locations. These additional HMA mix screening parameters (Rut_Δ and SF) should be considered for possible inclusion in the Tex-242-F test procedure, along with appropriate mix screening criteria.

- Both the SPST (τ_s and SSE) and HWTT results (HWTT rut depth and rutting area) showed promising correlation with M-E model predictions for the APT test sections.

- For the APT test sections, both the lab test results and the M-E model predictions yielded similar ranking of the HMA mixes in terms of their rutting/shear performances. However, the M-E model predictions showed higher discrimination between the good and poor mix pairs. Between the two lab test methods, the SPST shear strength exhibited superior correlation with the M-E model predictions. Nonetheless, verification with actual APT field rut measurements is imperative to validate these results.

- Based on the lab, computational modeling, and field data presented in this chapter, the tentatively proposed preliminary SPST pass-fail screening criteria for HMA mixes at 50°C (122°F), with a 1.0-inch diameter punching head at a monotonic loading rate of 0.20 mm/sec under sample confined conditions, are:

  a) Shear strength (τ_s) $\geq$ 300 psi (2.07 MPa).
  b) Shear strain energy (SSE) $\geq$ 25 kJ/m^2.

PRACTICALITY OF THE KEY FINDINGS

The work conducted in this study showed potential in optimizing the performance of the HMA shear resistance and rutting/PD tests to better simulate the field rutting conditions of the

HMA. HMA mix screening and material selection will thus be cost-effectively optimized and premature rutting failures minimized if the following steps are properly followed:

- The recommended Tex-242-F updates and modifications for the HWTT should be properly implemented.

- The SPST concept should be investigated further as a supplementary and/or surrogate test to the standard HWTT procedure (Tex-242-F).

- Abaqus FE modeling in 3-D dynamic mode indicated that critical Hwy areas such as intersections or urban stop-go sections with decelerating and turning vehicles, as well as zones of sustained elevated temperatures, experience high shear stresses from traffic loading. HMA mixes used in these locations are, thus, more prone to shear failure if they do not have sufficient shear strength. Therefore, these critical Hwy sections should be given special attention during the materials (HMA) selection and PVMNT design phases.

RECOMMENDATIONS FOR IMPLEMENTATION

In consideration of the findings and conclusions drawn from this study, the following activities and tasks are recommended for implementation:

1) Parallel laboratory testing with TxDOT CST lab for:
   - Setting up and familiarizing TxDOT personnel with the SPST protocol.
   - Joint lab testing of more mixes to aid in the refinement of the SPST protocol for practical applications in routine HMA mix design and mix screening. This task will include evaluating more SMA (at 7 ± 1 percent AV) and PFC (AV at N_{design}) mixes in the lab test matrix, as well as investigating the effects of aggregate size and gradation on the SPST results.
   - Verifying and consolidating the proposed Tex-242-F modifications with additional HWTT lab testing and mixes.
   - Comparatively evaluating the SPST and HWTT for routine HMA mix design and screening, particularly for mixes to be used in high shear-stress locations such as intersections or urban stop-go sections, etc., or where a low PG grade asphalt-binder is used.

2) Additional FE modeling with Abaqus in 3-D dynamic mode to verify and refine the critical shear stresses and plastic strains for SPST lab testing, PVMNT design, and performance prediction. As a minimum, this task will also include the following:

- Investigating the interactive and combined effects for severe shear conditions such as high temperature, decelerating (braking), turning traffic, vehicle speed variations, etc.

- Investigating the interfacial properties such as variations in the layer interface conditions, tack coat, temperature gradients, etc.

- Evaluating threaded tires, ribs, etc.

- Evaluating more PVMNT structures with different layer combinations, traffic levels, and environmental exposure.

- Comparative modeling of PVMNT sections along straight Hwy sections versus controlled intersections and stop-go sections.

3) Further verification and validation of the SPST and modified HWTT protocol by correlating with field and APT data.

REFERENCES

AASHTO (1999). AASHTO PP2: Standard Practice for Mixture Conditioning of Hot Mix Asphalt (HMA). Washington, D.C.

AASHTO (2003). AASHTO T320-03: Standard Method of Test for Determining the Permanent Shear Strain and Stiffness of Asphalt Mixtures Using the Superpave Shear Tester; Procedure C Repeated Shear Test at Constant Height. Washington, D.C.

AASHTO (2005). AASHTO TP 62-03: Standard Method of Test for Determinng Dynamic Modulus of Hot-Mix Asphalt Concrete Mixtures. Washington D.C.

Apeagyei, A. K. (2011). Rutting as a Function of Dynamic Modulus and Gradation. *Journal of Materials in Civil Engineering*, Vol. 23, No. 9, pp. 1302–1310.

Brown, E. R., Kandhal, P. S., and Zhang, J. (2001), Performance Testing for Hot Mix Asphalt. In *National Center for Asphalt Technology, NCAT Report 01-05*. Auburn, Alabama.

Chen, X., H. Huang, and Z. Xu. (2006). Uniaxial Penetration Testing for Shear Resistance of Hot-Mix Asphalt Mixtures. In *Transportation Research Record: Journal of the Transportation Research Board, No. 1970*, Transportation Research Board of the National Academies, Washington, D.C.

Goh, S. W., Z. You, R. C. Williams, and X. Li. (2011). Preliminary Dynamic Modulus Criteria of HMA for Field Rutting of Asphalt Pavements: Michigan's Experience. ASCE *Journal of Transportation Engineering*, Vol. 137, No. 1, pp. 37–45.

Pellinen, T. K., and M. W. Witczak. (2002). Stress-Dependent Master Curve Construction for Dynamic (Complex) Modulus. *Journal of the Association of Asphalt Paving Technologists*, Vol. 71, 2002.

Texas Department of Transportation. (2004). *Standard Specifications for Construction and Maintenance of Highways, Streets, and Bridges*. Austin, Texas.

Texas Department of Transportation. (2009). *Test Procedure for Hamburg Wheel-Tracking Test*. TxDOT Designation: Tex-242-F, Texas Department of Transportation, Austin, Texas.

Texas Department of Transportation. (2005). *Laboratory Method of Mixing Bituminous Mixtures*. TxDOT Designation: Tex-205-F, Texas Department of Transportation, Austin, Texas

Tukey, J. W. (1953). *The Problem of Multiple Comparisons*. Draft Manuscript. Princeton University, Princeton, New Jersey.

Van de Ven, M. F. C., and L. F. Walubita. (2000). *Test Result of the Micropave ZM12 Mix, Draft ITT Report 4/2000*. Institute for Transport Technology, University of Stellenbosch, Stellenbosch, South Africa.

Walubita L. F., G. Das, E. Espinoza, J. Oh, T. Scullion, S. Nazarian, I. Abdallah, and J. L. Garibay. (2011). *Texas Flexible Pavements and Overlays: Data Analysis Plans and Reporting Format*. Technical Report 0-6658-P3, Texas Transportation Institute, Texas A&M University, College Station, Texas. http://tti.tamu.edu/documents/0-6658-P3.pdf.

Walubita, L. F., E. M. Espinoza, G. Das, J. H. Oh, T. Scullion, J. L. Garibay, S. Nazarian, I. Abdallah, and S. Lee. (2012). *Texas Flexible Pavements and Overlays: Year 1 Report–Test Sections, Data Collection, Analyses, and Data Storage System*. Technical Report 0-6658-1, Texas Transportation Institute, Texas A&M University, College Station, Texas. http://d2dtl5nnlpfr0r.cloudfront.net/tti.tamu.edu/documents/0-6658-1.pdf

Walubita, L., S. Lee, J. Zhang, A. N. M. Faruk, S. Nguyen, T. Scullion (2013). *HMA Shear Resistance, Permanent Deformation, and Rutting Tests for Texas Mixes: Year 1 Report*. Technical Report FHWA/TX-13/0-6744-1. Texas A&M Transportation Institute, College Station, Texas. http://d2dtl5nnlpfr0r.cloudfront.net/tti.tamu.edu/documents/0-6744-1.pdf

Witczak, M. W., K. Kaloush, T. Pellinen, M. El-Basyouny, and H. V. Quintus. (2002). *Simple Performance Test for Superpave Mix Design*. NCHRP Report 465. National Cooperative Highway Research Program.

Zeinali, A. (2014). "Preparing the AMPT Tests for Routine Use." *The Magazine of the Asphalt Institute*. 08/05/2014 Issue.

Zhou, F., and T. Scullion (2001). *Laboratory Results from Heavy Duty Asphalt Mixes*. Technical Memorandum to TxDOT, Texas Transportation Institute, College Station, Texas.

Zhou, F., and T. Scullion. (2004). *Input Parameters of Enhanced VESYS5*. Implementation
Report 9-1502-01-4, Texas Transportation Institute, College Station, Texas.
http://d2dtl5nnlpfr0r.cloudfront.net/tti.tamu.edu/documents/9-1502-01-4.pdf Zhou, F., E.
G. Fernando, and T. Scullion. (2009). *Laboratory and Field Procedures Used to
Characterize Materials*. FHWA/TX-09/0-5798-P1, Texas Transportation Institute,
College Station, Texas. http://d2dtl5nnlpfr0r.cloudfront.net/tti.tamu.edu/documents/0-
5798-P1.pdf

Zhou, F., E. G. Fernando, and T. Scullion. (2010). *Development, Calibration, and Validation of
Performance Prediction Models for the Texas M-E Flexible Pavement Design System.*
Technical Report 0-5798-2, Texas Transportation Institute, Texas A&M University,
College Station, Texas. http://tti.tamu.edu/documents/0-5798-2.pdf.

APPENDIX A: HMA MIX-DESIGN DATA

Note: Tex-210-F must be removed

TEXAS DEPARTMENT OF TRANSPORTATION

HMACP MIXTURE DESIGN : COMBINED GRADATION

Refresh Workbook   File Version: 06/07/10 10:24:04

SAMPLE ID: 3463852		SAMPLE DATE: 07-06-2011	
LOT NUMBER:		LETTING DATE:	
SAMPLE STATUS:		CONTROLLING CSJ: 0238-06-025,NH2011(801)	
COUNTY: Sherman, US-54		SPEC YEAR: 2004	
SAMPLED BY: Dale Winfield		SPEC ITEM:	
SAMPLE LOCATION:		SPECIAL PROVISION:	
MATERIAL CODE:		MIX TYPE: ITEM341_D_Fine_Surface	
MATERIAL NAME:			
PRODUCER: Miller Pit, XIT pit		WMA Included in Design?	Yes
AREA ENGINEER:	PROJECT MANAGER:	WMA TECHNOLOGY:	Double Barrel Green
COURSE\LIFT:	STATION:	DIST. FROM CL:	CONTRACTOR DESIGN # : 3463852

Recycled Binder, %

Bin No.8 :	1.1
Bin No.9 :	0.7
Bin No.10 :	0.0
Total	1.8

	Bin No.1		Bin No.2		Bin No.3		Bin No.4		Bin No.5		Bin No.6		Bin No.7		Bin No.8		Bin No.9		Bin No.10					
	AGGREGATE BIN FRACTIONS														**"RECYCLED MATERIALS"**										
Aggregate Source:			Limestone_Dolom		Limestone_Dolom		Gravel								RAS		Fractionated RAP				Material Type			
Aggregate Pit:															R. K. Hall Construction		R K Hall Construction				Material Source			
Aggregate Number:															Tear-off						RAS Type		27.8	
Sample ID:			Miller 7/16" rock		Miller washed coarse		Miller Dry screenings				river sand		Chemical Lime								Sample ID			

Ratio of Recycled to Total Binder, % *(based on binder percent (%) entered below in this worksheet)*

		Recycled Asphalt Binder (%)														22.1		5.0						Combined Gradation
Hydrated Lime?:												Yes		**5.0** % of Tot. Mix		**15.0** % of Tot. Mix		% of Tot. Mix		Total Bin	Lower & Upper Specification Limits		
Individual Bin (%):	0.0 Percent		**48.0** Percent		**10.6** Percent		**10.9** Percent		0.0 Percent		**10.0** Percent		**1.0** Percent		4.2 % of Aggreg		15.3 % of Aggreg		% of Aggreg		100.0%		

Sieve Size:	Cum.% Passing	Wtd Cum.%	Cum.% Passing	Wtd Cum.%	Cum.% Passing	Wtd Cum.%	Cum.% Passing	Wtd Cum.%	Cum.% Passing	Wtd Cum.%	Cum.% Passing	Wtd Cum.%	Cum.% Passing	Wtd Cum.%	Cum.% Passing	Wtd Cum.%	Cum.% Passing	Wtd Cum.%	Cum.% Passing	Wtd Cum.%	Cum.% Passing	Lower	Upper	Within Spec's
3/4"	100.0	0.0	**100.0**	48.0	**100.0**	10.6	**100.0**	10.9	100.0	0.0	**100.0**	10.0	**100.0**	1.0	100.0	4.2	100.0	15.3			**100.0**	100.0	100.0	Yes
1/2"	75.3	0.0	**100.0**	48.0	**100.0**	10.6	**100.0**	10.9	100.0	0.0	**100.0**	10.0	**100.0**	1.0	100.0	4.2	100.0	15.3			**100.0**	98.0	100.0	Yes
3/8"	8.6	0.0	**99.8**	47.9	**100.0**	10.6	**100.0**	10.9	100.0	0.0	**100.0**	10.0	**100.0**	1.0	100.0	4.2	93.5	14.3			**98.9**	85.0	100.0	Yes
No. 4	0.7	0.0	**14.8**	7.1	**99.5**	10.5	**99.9**	10.9	99.9	0.0	**100.0**	10.0	**100.0**	1.0	98.9	4.2	66.2	10.1			**53.8**	50.0	64.0	Yes
No. 8	0.6	0.0	**0.6**	0.3	**69.9**	7.4	**87.5**	9.5	92.1	0.0	**99.4**	9.9	**100.0**	1.0	97.7	4.1	46.8	7.2			**39.4**	35.0	46.0	Yes
No. 30	0.5	0.0	**0.5**	0.2	**24.1**	2.6	**45.2**	4.9	46.7	0.0	**97.0**	9.7	**100.0**	1.0	46.3	1.9	26.3	4.0			**24.4**	15.0	29.0	Yes
No. 50	0.4	0.0	**0.4**	0.2	**12.1**	1.3	**33.3**	3.6	30.9	0.0	**69.3**	6.9	**100.0**	1.0	36.6	1.5	19.4	3.0			**17.5**	7.0	20.0	Yes
No. 200	0.4	0.0	**0.3**	0.1	**2.6**	0.3	**11.0**	1.2	10.0	0.0	**7.8**	0.8	**100.0**	1.0	18.1	0.8	7.9	1.2			**5.4**	2.0	7.0	Yes

(Bold Italic) Not within specifications   *(Bold Italic)* Not within specifications- Restricted Zone   *(Italic)* Not cumulative

Lift Thickness, in:		Binder Substitution? Yes	Binder Originally Specified: PG 70-28	Substitute Binder: PG 64-22
Asphalt Source: Valero PG 64-22		Binder Percent, (%): 6.6	Asphalt Spec. Grav.: 1.030	
Antistripping Agent: lime		Percent, (%): 1		

Figure A-1. HMA Mix-Design Details for Type D Mix (Amarillo, US 54).

TEXAS DEPARTMENT OF TRANSPORTATION
WACO DISTRICT LABORATORY
HMACP MIXTURE DESIGN : COMBINED GRADATION

Refresh Workbook   File Version: 11/03/11 09:08:32

SAMPLE ID:	11TPOLANS_0073	SAMPLE DATE:	10/6/2011
LOT NUMBER:	1	LETTING DATE:	04/07/2010
SAMPLE STATUS:	COMPLETE	CONTROLLING CSJ:	0014-07-083
COUNTY:	HILL	SPEC YEAR:	2004
SAMPLED BY:		SPEC ITEM:	03462018
SAMPLE LOCATION:		SPECIAL PROVISION:	
MATERIAL CODE:	0346CM0000	MIX TYPE:	ITEM346_SMA_D_Medium
MATERIAL NAME:	ITEM 346 COMPLETE MIX QCQA ALL MIX TYPES	WMA Included in Design?	No
PRODUCER:	900003	WMA TECHNOLOGY:	
AREA ENGINEER:	TONY MORAN	PROJECT MANAGER: PATRICIA GARRISON	WMA RATE: UNITS:
COURSE\LIFT:		STATION:	DIST. FROM CL:	CONTRACTOR DESIGN # : RCW-SMADB248-J76

Recycled Binder, %

Bin No.8 :	0.7
Bin No.9 :	0.0
Bin No.10 :	0.0
Total	**0.7**

Use this value in the QC/QA template>>

Ratio of Recycled to Total Binder, %
(based on binder percent (%) entered below in this worksheet)
11.0

	AGGREGATE BIN FRACTIONS							"RECYCLED MATERIALS"			
	Bin No.1	Bin No.2	Bin No.3	Bin No.4	Bin No.5	Bin No.6	Bin No.7	Bin No.8	Bin No.9	Bin No.10	
Aggregate Source:	Limestone_Dolom	Limestone_Dolom	Limestone_Dolom	Limestone_Dolom	Limestone_Dolom			Fractionated RAP			Material Type
Aggregate Pit:	Lampasas	Perch-Hill	Perch-Hill	Lampasas	Lampasas	Franklin Materials	Chem Lime	Knife River			Material Source
Aggregate Number:	1402706	0224901	0224901	1402706	1402706						RAS Type
Sample ID:	C ROCK	3/8" BIN	C ROCK	GRADE 4	Deister Fines	Mineral Filler	Lime	RAP			Sample ID

Recycled Asphalt Binder (%)
5.5

										Combined Gradation		
Hydrated Lime?:							Yes	12.0	% of Tot. Mix		% of Tot. Mix		% of Tot. Mix	Total Bin	Lower & Upper Specification Limits
Individual Bin (%):	16.0 Percent	14.5 Percent	24.1 Percent	20.0 Percent	7.3 Percent	5.0 Percent	1.0 Percent	12.1	% of Aggreg		% of Aggreg		% of Aggreg	100.0%	

Sieve Size:	Cum.% Passing	Wtd Cum. %	Cum.% Passing	Wtd Cum. %	Cum.% Passing	Wtd Cum %	Cum.% Passing	Wtd Cum. %	Cum.% Passing	Wtd Cum. %	Cum.% Passing	Wtd Cum. %	Cum.% Passing	Wtd Cum. %	Cum.% Passing	Wtd Cum. %	Cum.% Passing	Wtd Cum. %	Cum.% Passing	Wtd Cum. %	Cum.% Passing	Lower	Upper	Within Spec's
3/4"	100.0	16.0	100.0	14.5	100.0	24.1	100.0	20.0	100.0	7.3	100.0	5.0	100.0	1.0	100.0	12.1					100.0	100.0	100.0	Yes
1/2"	66.2	10.6	99.3	14.4	67.1	16.2	98.1	19.6	100.0	7.3	100.0	5.0	100.0	1.0	99.5	12.0					86.1	85.0	99.0	Yes
3/8"	19.0	3.0	72.0	10.4	12.0	2.9	66.8	13.4	100.0	7.3	100.0	5.0	100.0	1.0	97.1	11.7					54.8	50.0	75.0	Yes
No. 4	2.8	0.4	2.8	0.4	2.6	0.6	2.5	0.5	98.3	7.2	100.0	5.0	100.0	1.0	72.6	8.8					23.9	20.0	32.0	Yes
No. 8	2.4	0.4	2.5	0.4	2.4	0.6	2.2	0.4	77.9	5.7	100.0	5.0	100.0	1.0	55.4	6.7					20.2	16.0	28.0	Yes
No. 16	2.1	0.3	2.3	0.3	2.3	0.6	2.0	0.4	61.4	4.5	100.0	5.0	100.0	1.0	45.5	5.5					17.6	8.0	28.0	Yes
No. 30	1.8	0.3	2.1	0.3	2.1	0.5	1.8	0.4	48.9	3.6	92.9	4.6	100.0	1.0	38.3	4.6					15.3	8.0	28.0	Yes
No. 50	1.6	0.3	1.9	0.3	1.9	0.5	1.6	0.3	38.7	2.8	86.3	4.3	100.0	1.0	27.7	3.4					12.8	8.0	28.0	Yes
No. 200	1.4	0.2	1.7	0.2	1.7	0.4	1.5	0.3	20.2	1.5	71.2	3.6	100.0	1.0	6.8	0.8					8.0	8.0	12.0	Yes

(Bold Italic) Not within specifications   *(Bold Italic)* Not within specifications- Restricted Zone   *(Italic)* Not cumulative

Lift Thickness, in:		Binder Substitution?	No	Binder Originally Specified:	Substitute Binder:
Asphalt Source & Grade:	JEBRO PG 76-22	Binder Percent, (%):	6.0	Asphalt Spec. Grav.: 1.030
Antistripping Agent:	HYDRATED LIME	Percent, (%):	1	Fiber Content, %: 0.30

Dry Rodded Unit Weight of Coarse Agg. (pcf)   98.900

Remarks:
VIRGIN AC ESTIMATED 5.3%

Notes:

Figure A-2. HMA Mix-Design Details for SMA Mix (Waco District, IH 35).

HMACP MIXTURE DESIGN : COMBINED GRADATION

Refresh Workbook   File Version: 06/07/10 10:24:04

SAMPLE ID:	3656000	SAMPLE DATE:	
LOT NUMBER:		LETTING DATE:	JAN. 2011
SAMPLE STATUS:		CONTROLLING CSJ:	0136-08-039
COUNTY:	LAMAR	SPEC YEAR:	2004
SAMPLED BY:		SPEC ITEM:	
SAMPLE LOCATION:		SPECIAL PROVISION:	
MATERIAL CODE:	TBPFC	MIX TYPE:	TBPFC_PG76
MATERIAL NAME:	Smith/Buster		
PRODUCER:	R.K.Hall Construction	WMA Included in Design?	No
AREA ENGINEER:	RICHARD HARPER P.E.	PROJECT MANAGER:	
COURSE/LIFT:	Surface	STATION:	DIST. FROM CL:	CONTRACTOR DESIGN #:	3656000

Recycled Binder, %	
Bin No.8 :	0.0
Bin No.9 :	0.0
Bin No.10 :	0.0
Total	0.0

AGGREGATE BIN FRACTIONS							**"RECYCLED MATERIALS"**				
	Bin No.1	Bin No.2	Bin No.3	Bin No.4	Bin No.5	Bin No.6	Bin No.7	Bin No.8	Bin No.9	Bin No.10	
Aggregate Source:	Sandstone	Sandstone									Material Type
Aggregate Pit:	Sawyer, OK	Sawyer, OK									Material Source
Aggregate Number:	0050447	0050447									RAS Type
Sample ID:	Grade 3	Grade 4	Chemical Lime								Sample ID

Ratio of Recycled to Total Binder, %
(based on binder percent (%) entered below in this worksheet)
0.0

Recycled Asphalt Binder (%)

																						Combined Gradation			
Hydrated Lime?:																		% of Tot. Mix		% of Tot. Mix		% of Tot. Mix	Total Bin	Lower & Upper Specification Limits		
Individual Bin (%):	52.0	Percent	47.0	Percent	1.0	Percent		Percent		Percent		Percent		Percent		% of Aggreg		% of Aggreg		% of Aggreg	100.0%			

Sieve Size:	Cum.% Passing	Wtd Cum. %	Cum.% Passing	Wtd Cum. %	Cum.% Passing	Wtd Cum. %	Cum.% Passing	Wtd Cum. %	Cum.% Passing	Wtd Cum. %	Cum.% Passing	Wtd Cum. %	Cum.% Passing	Wtd Cum. %	Cum.% Passing	Wtd Cum. %	Cum.% Passing	Wtd Cum. %	Cum.% Passing	Wtd Cum. %	Cum. % Passing	Lower	Upper	Within Spec's
3/4"	100.0	52.0	100.0	47.0	100.0	1.0															100.0	100.0	100.0	Yes
1/2"	73.3	38.1	98.9	46.5	100.0	1.0															85.6	80.0	100.0	Yes
3/8"	10.1	5.3	83.8	39.4	100.0	1.0															45.6	35.0	60.0	Yes
No. 4	1.9	1.0	16.4	7.7	100.0	1.0															9.7	1.0	20.0	Yes
No. 8	1.6	0.8	4.9	2.3	100.0	1.0															4.1	1.0	10.0	Yes
No. 200	1.0	0.5	2.5	1.2	100.0	1.0															2.7	1.0	4.0	Yes

(Bold Italic) Not within specifications   *(Bold Italic)* Not within specifications- Restricted Zone   *(Italic)* Not cumulative

Lift Thickness, in:		Binder Substitution?	Binder Originally Specified	Substitute Binder	
Asphalt Source & Grade:	Lion 76-22	Binder Percent, (%):	6.7	Asphalt Spec. Grav.:	1.030	Membrane Target Application Rate, gal/yd2
Antistripping Agent:	Chemical Lime	Percent, (%):	1	Fiber Content, %:	0.30	

Figure A-3. HMA Mix-Design Details for PFC Mix (Paris District, US 277).

TEXAS DEPARTMENT OF TRANSPORTATION
PARIS DISTRICT LABORATORY
HMACP MIXTURE DESIGN : COMBINED GRADATION

Refresh Workbook   File Version: 04/28/11 08:20:35

SAMPLE ID:	CAM01ABARC1101	SAMPLE DATE:	7/29/2011
LOT NUMBER:	1-11-546	LETTING DATE:	
SAMPLE STATUS:	PENA	CONTROLLING CSJ:	
COUNTY:		SPEC YEAR:	2004
SAMPLED BY:	JAMES HOPKINS JR.	SPEC ITEM:	
SAMPLE LOCATION:		SPECIAL PROVISION:	3165
MATERIAL CODE:	0344CM0000	MIX TYPE:	CAM
MATERIAL NAME:	ITEM 344 COMPLETE MIX QCQA ALL MIX TYPES	WMA Included in Design?	No
PRODUCER:	D03244001HMACP:AUSTIN BRIDGE & ROAD PLANT #2	WMA TECHNOLOGY:	
AREA ENGINEER:		PROJECT MANAGER:	WMA RATE: UNITS:
COURSE\LIFT:		STATION:	DIST. FROM CL:	CONTRACTOR DESIGN # : CECA360

Recycled Binder, %
Bin No.8 : 0.0
Bin No.9 : 0.0
Bin No.10 : 0.0
Use this value in the QC/QA template>> **Total 0.0**

AGGREGATE BIN FRACTIONS | **"RECYCLED MATERIALS"**

Ratio of Recycled to Total Binder, %
(based on binder percent (%) entered below in this worksheet)
0.0

	Bin No.1	Bin No.2	Bin No.3	Bin No.4	Bin No.5	Bin No.6	Bin No.7	Bin No.8	Bin No.9	Bin No.10	
Aggregate Source:	Igneous	Igneous	Limestone_Dolom								Material Type
Aggregate Pit:	Mill Creek (Grnt), OK.	Mill Creek (Grnt), OK.	Mill Creek, OK								Material Source
Aggregate Number:	0050433	0050433	0050445								RAS Type
Sample ID:	TY F	GRANITE SAND	MANUF. SAND								Sample ID

Recycled Asphalt Binder (%)

Combined Gradation

														% of Tot. Mix % of Aggreg		% of Tot. Mix % of Aggreg		% of Tot. Mix % of Aggreg	Total Bin	Lower & Upper Specification Limits		
Hydrated Lime?:																						
Individual Bin (%):	40.0	Percent	22.0	Percent	37.0	Percent		Percent	1.0	Percent		Percent		Percent						100.0%		

Sieve Size:	Cum.% Passing	Wtd Cum. %	Cum.% Passing	Wtd Cum. %	Cum.% Passing	Wtd Cum. %	Cum.% Passing	Wtd Cum. %	Cum.% Passing	Wtd Cum. %	Cum.% Passing	Wtd Cum. %	Cum.% Passing	Wtd Cum. %	Cum.% Passing	Wtd Cum. %	Cum.% Passing	Wtd Cum. %	Cum.% Passing	Wtd Cum. %	Cum. % Passing	Lower	Upper	Within Spec's
3/8"	99.5	39.8	100.0	22.0	100.0	37.0			100.0	1.0											99.8	98.0	100.0	Yes
No. 4	42.3	16.9	99.9	22.0	99.0	36.6			100.0	1.0											76.5	70.0	90.0	Yes
No. 8	8.1	3.2	86.8	19.1	85.0	31.5			100.0	1.0											54.8	40.0	65.0	Yes
No. 16	3.6	1.4	55.6	12.2	60.0	22.2			100.0	1.0											36.9	20.0	45.0	Yes
No. 30	2.2	0.9	29.9	6.6	40.0	14.8			100.0	1.0											23.3	10.0	30.0	Yes
No. 50	1.5	0.6	12.4	2.7	27.0	10.0			100.0	1.0											14.3	10.0	20.0	Yes
No. 200	0.9	0.4	1.7	0.4	5.0	1.9			100.0	1.0											3.6	2.0	10.0	Yes

(Bold Italic) Not within specifications   *(Bold Italic)* Not within specifications- Restricted Zone   *(Italic)* Not cumulative

Lift Thickness, in:		Binder Substitution?	No	Binder Originally Specified Substitute Binder:
Asphalt Source & Grade:	VALERO PG 76-22	Binder Percent, (%):	7.0	Asphalt Spec. Grav.: 1.025
Antistripping Agent:	LIME, CHEMICAL LIME	Percent, (%):	1	

Figure A-4. HMA Mix-Design Details for CAM Mix (Paris District, SH 121).

TEXAS DEPARTMENT OF TRANSPORTATION

HMACP MIXTURE DESIGN : COMBINED GRADATION

Refresh Workbook   File Version: 06/07/10 10:24:04

SAMPLE ID:		SAMPLE DATE:	
LOT NUMBER:		LETTING DATE:	April 2010
SAMPLE STATUS:		CONTROLLING CSJ:	0014-07-083
COUNTY:	Hill	SPEC YEAR:	2004
SAMPLED BY:		SPEC ITEM:	
SAMPLE LOCATION:		SPECIAL PROVISION:	
MATERIAL CODE:		MIX TYPE:	ITEM341_B_Fine_Base
MATERIAL NAME:			
PRODUCER:	W. W. Webber, LLC	WMA Included in Design?	
AREA ENGINEER:	Tony Moran	PROJECT MANAGER:	WMA TECHNOLOGY:
COURSE\LIFT:		STATION:	DIST. FROM CL:	CONTRACTOR DESIGN # :	0710-205-64R30

Recycled Binder, %

Bin No.8 :	1.5
Bin No.9 :	0.0
Bin No.10 :	0.0
Total	1.5

	AGGREGATE BIN FRACTIONS							"RECYCLED MATERIALS"			
	Bin No.1	Bin No.2	Bin No.3	Bin No.4	Bin No.5	Bin No.6	Bin No.7	Bin No.8	Bin No.9	Bin No.10	Material Type
Aggregate Source:		Limestone_Dolom	Limestone_Dolom	Limestone_Dolom				Unfractionated RAP			
Aggregate Pit:		Tehuacana	Tehuacana	Tehuacana				W. W. Webber, LLC			Material Source
Aggregate Number:		0914708	0914708	0914708							RAS Type
Sample ID:	Field Sand	Man. Sand	D-Rock	B-Rock	Hydrated Lime			RAP			Sample ID

Ratio of Recycled to Total Binder, %

(based on binder percent (%) entered below in this worksheet)

32.0

Recycled Asphalt Binder (%)

4.9

Combined Gradation

										Total Bin	Lower & Upper Specification Limits	
Hydrated Lime?:					Yes			30.0	% of Tot. Mix	% of Tot. Mix	% of Tot. Mix	
Individual Bin (%):	15.0 Percent	11.1 Percent	20.0 Percent	23.0 Percent	1.0 Percent	Percent	Percent	29.9 % of Aggreg.	% of Aggreg.	% of Aggreg.	100.0%	

Sieve Size:	Bin1 Cum.% Passing	Bin1 Wtd Cum. %	Bin2 Cum.% Passing	Bin2 Wtd Cum. %	Bin3 Cum.% Passing	Bin3 Wtd Cum. %	Bin4 Cum.% Passing	Bin4 Wtd Cum. %	Bin5 Cum.% Passing	Bin5 Wtd Cum. %	Bin6 Cum.% Passing	Bin6 Wtd Cum. %	Bin7 Cum.% Passing	Bin7 Wtd Cum. %	Bin8 Cum.% Passing	Bin8 Wtd Cum. %	Bin9 Cum.% Passing	Bin9 Wtd Cum. %	Bin10 Cum.% Passing	Bin10 Wtd Cum. %	Total Bin Cum. % Passing	Lower	Upper	Within Spec's
1-1/2"	100.0	15.0	100.0	11.1	100.0	20.0	100.0	23.0	100.0	1.0					100.0	29.9					100.0	100.0	100.0	Yes
1"	100.0	15.0	100.0	11.1	100.0	20.0	98.0	22.5	100.0	1.0					100.0	29.9					99.5	98.0	100.0	Yes
3/4"	100.0	15.0	100.0	11.1	100.0	20.0	73.3	16.9	100.0	1.0					98.6	29.5					93.4	84.0	98.0	Yes
3/8"	100.0	15.0	100.0	11.1	97.9	19.6	16.6	3.8	100.0	1.0					88.1	26.3					76.8	60.0	80.0	Yes
No. 4	95.7	14.4	99.2	11.0	34.5	6.9	4.0	0.9	100.0	1.0					64.2	19.2					53.4	40.0	60.0	Yes
No. 8	76.3	11.4	84.9	9.4	6.7	1.3	2.6	0.6	100.0	1.0					45.7	13.7					37.5	29.0	43.0	Yes
No. 30	48.9	7.3	55.1	6.1	3.5	0.7	2.4	0.6	100.0	1.0					30.5	9.1					24.8	13.0	28.0	Yes
No. 50	21.6	3.2	44.8	5.0	3.2	0.6	1.9	0.4	100.0	1.0					25.2	7.5					17.8	6.0	20.0	Yes
No. 200	1.2	0.2	3.7	0.4	2.0	0.4	1.3	0.3	100.0	1.0					10.6	3.2					5.5	2.0	7.0	Yes

(Bold Italic) Not within specifications   *(Bold Italic)* Not within specifications- Restricted Zone   *(Italic)* Not cumulative

Lift Thickness, in:		Binder Substitution?	No	Binder Originally Specified:	Substitute Binder:
Asphalt Source & Grade:	Valero Ardmore PG 64-22	Binder Percent, (%):	4.6	Asphalt Spec. Grav.:	1.023
Antistripping Agent:	Hydrated Lime	Percent, (%):	1		

Figure A-5. HMA Mix-Design Details for Type B Mix (Waco District, IH 35).

HMACP MIXTURE DESIGN : COMBINED GRADATION

Refresh Workbook   File Version: 10/24/07 10:53:08

SAMPLE ID:		SAMPLE DATE:	
LOT NUMBER:		LETTING DATE:	
SAMPLE STATUS:	SH 59	CONTROLLING CSJ:	0239-05-027
COUNTY:	Montague	SPEC YEAR:	2004
SAMPLED BY:		SPEC ITEM:	341
SAMPLE LOCATION:	Plant STKPL	SPECIAL PROVISION:	
MATERIAL CODE:		MIX TYPE:	ITEM341_D_Fine_Surface
MATERIAL NAME:	LIMESTONE		
PRODUCER:	SUNMOUNT CORP		
AREA ENGINEER:	Wayne Bell	PROJECT MANAGER:	

COURSE\LIFT:		STATION:		DIST. FROM CL:		CONTRACTOR DESIGN # :	

BIN FRACTIONS

	Bin No.1	Bin No.2	Bin No.3	Bin No.4	Bin No.5	Bin No.6	Bin No.7		
Aggregate Source:	HANSON	HANSON	T.X.I						
Aggregate Pit:									
Aggregate Number:	Type "D-F"	MAN_SAND	SAND						
Sample ID:									Combined Gradation
Rap?:									

Individual Bin (%):	56.0	Percent	36.0	Percent	8.0	Percent		Percent		Percent		Percent		Percent	100.0%	Total Bin	Lower & Upper Specification Limits			Restricted Zone			Individual % Retained

Sieve Size:	Cum.% Passing	Wtd Cum. %	Cum.% Passing	Wtd Cum. %	Cum.% Passing	Wtd Cum. %	Cum.% Passing	Wtd Cum. %	Cum.% Passing	Wtd Cum. %	Cum.% Passing	Wtd Cum. %	Cum.% Passing	Wtd Cum. %	Cum. % Passing	Lower	Upper	Within Spec's	Lower	Upper	Within Spec's	Individual % Retained
3/4"	100.0	56.0	100.0	36.0	100.0	8.0									100.0	100.0	100.0	Yes				0.0
1/2"	100.0	56.0	100.0	36.0	100.0	8.0									100.0	98.0	100.0	Yes				0.0
3/8"	98.7	55.3	99.9	36.0	100.0	8.0									99.2	85.0	100.0	Yes				0.8
No. 4	37.1	20.8	97.5	35.1	99.5	8.0									63.8	50.0	70.0	Yes				35.4
No. 8	5.5	3.1	75.7	27.3	98.3	7.9									38.2	35.0	46.0	Yes				25.6
No. 30	2.3	1.3	21.9	7.9	95.9	7.7									16.8	15.0	29.0	Yes				21.4
No. 50	2.0	1.1	9.2	3.3	91.0	7.3									11.7	7.0	20.0	Yes				5.1
No. 200	1.8	1.0	3.1	1.1	14.7	1.2									3.3	2.0	7.0	Yes				8.4

Not within specifications   **#** Not cumulative

Asphalt Source & Grade:	70-22 (Valero)	Binder Percent, (%):	5.0	Asphalt Spec. Grav.:	1.036

Antistripping Agent:	Arr-Maz AD-here LOF 65-00 LS.	Percent, (%):	0

Remarks:

This design was mixed at 335F. And molded at 300F.

Figure A-6. HMA Mix-Design Details for Type D Mix (Chico).

TEXAS DEPARTMENT OF TRANSPORTATION

HMACP MIXTURE DESIGN : COMBINED GRADATION

Refresh Workbook   File Version: 02/11/13 15:46:07

SAMPLE ID:	H0D12CEN081302	SAMPLE DATE:	5/10/2013
LOT NUMBER:	540004-08	LETTING DATE:	05-07-2013
SAMPLE STATUS:		CONTROLLING CSJ:	1062-02-023 ETC.
COUNTY:	Harris FM 2100	SPEC YEAR:	2004
SAMPLED BY:	Wade Cooke	SPEC ITEM:	3268
SAMPLE LOCATION:	Design	SPECIAL PROVISION:	
MATERIAL CODE:		MIX TYPE:	SS3268_D_Fine_Surface
MATERIAL NAME:	Item 3268 D LEVEL UP PG 76-22	WMA Additive in Design?	No
PRODUCER:	Century Asphalt Bender Plant	Target Discharge Temp., ºF:	325
AREA ENGINEER:		WMA TECHNOLOGY:	
		PROJECT MANAGER:	WMA RATE:	UNITS:
COURSE\LIFT:	Surface	STATION:		DIST. FROM CL:		CONTRACTOR DESIGN # :	540004-08

Maximum Allowable, %

Frac RAP:	20.0
Unfrac RAP:	10.0
RAS:	5.0
RB Ratio:	20.0

Recycled Binder, %

Bin No.8 :	0.6
Bin No.9 :	0.4
Bin No.10 :	0.0
Use this value in the QC/QA template>>	**Total** **1.0**

Ratio of Recycled to Total Binder, %
(based on binder percent (%) entered below in this worksheet)

18.9

	AGGREGATE BIN FRACTIONS							"RECYCLED MATERIALS"			
	Bin No.1	Bin No.2	Bin No.3	Bin No.4	Bin No.5	Bin No.6	Bin No.7	Bin No.8	Bin No.9	Bin No.10	
Aggregate Source:	Limestone_Dolom	Limestone_Dolom	Limestone_Dolom					Fractionated RAP	RAS		Material Type
Aggregate Pit:	Beckmann	Beckmann	Beckmann	Mega Sand				Century Asphalt Bender Plant	Century Asphalt-Melendy Plant		Material Source
Aggregate Number:	1501503	1501503	1501503								RAS Type
Sample ID:	D Rock	F Rock	Screenings	River Sand							Sample ID

								Recycled Asphalt Binder (%)				
								4.6	19.0			Combined Gradation
Hydrated Lime?:								14.0	% of Tot. Mix	2.0	% of Tot. Mix		% of Tot. Mix	Total Bin	Lower & Upper Specification Limits
Individual Bin (%):	30.0	Percent	23.2	Percent	16.0	Percent	15.0	Percent		Percent		Percent	14.1	% of Aggreg	1.7	% of Aggreg		% of Aggreg	100.0%	

Sieve Size:	Cum.% Passing	Wtd Cum. %	Cum.% Passing	Wtd Cum. %	Cum.% Passing	Wtd Cum. %	Cum.% Passing	Wtd Cum. %	Cum.% Passing	Wtd Cum. %	Cum.% Passing	Wtd Cum. %	Cum.% Passing	Wtd Cum. %	Cum.% Passing	Wtd Cum. %	Cum.% Passing	Wtd Cum. %	Cum.% Passing	Wtd Cum. %	Total Bin Cum. % Passing	Lower	Upper	Within Spec's
3/4"	100.0	30.0	100.0	23.2	100.0	16.0	100.0	15.0							100.0	14.1	100.0	1.7			100.0	100.0	100.0	Yes
1/2"	100.0	30.0	100.0	23.2	100.0	16.0	100.0	15.0							100.0	14.1	100.0	1.7			100.0	98.0	100.0	Yes
3/8"	86.0	25.8	100.0	23.2	100.0	16.0	100.0	15.0							93.1	13.1	100.0	1.7			94.8	85.0	100.0	Yes
No. 4	12.0	3.6	75.0	17.4	99.8	16.0	100.0	15.0							73.5	10.4	98.0	1.7			64.0	50.0	70.0	Yes
No. 8	6.5	2.0	12.5	2.9	85.3	13.6	100.0	15.0							57.9	8.2	92.1	1.6			43.2	35.0	46.0	Yes
No. 30	4.5	1.4	2.2	0.5	33.6	5.4	91.9	13.8							41.2	5.8	51.8	0.9			27.7	15.0	29.0	Yes
No. 50	3.0	0.9	2.1	0.5	21.9	3.5	61.5	9.2							27.5	3.9	38.0	0.6			18.6	7.0	20.0	Yes
No. 200	1.0	0.3	1.9	0.4	10.0	1.6	2.0	0.3							4.0	0.6	21.0	0.4			3.6	2.0	7.0	Yes

(Bold Italic) Not within specifications   *(Bold Italic)* Not within specificaitons- Restricted Zone   *(Italic)* Not cumulative

Lift Thickness, in:	2.00	Binder Substitution?	Yes	Binder Originally Specified:	PG 76-22	Substitute Binder:	PG 64-22
Asphalt Source:	Century Terminals LLC PG-64-22	Binder Percent, (%):	5.3	Asphalt Spec. Grav.:	1.030
Antistripping Agent:		Percent, (%):	

Figure A-7. HMA Mix-Design Details for Type D Mix (Houston District, FM 2100).

TEXAS DEPARTMENT OF TRANSPORTATION

HMACP MIXTURE DESIGN : COMBINED GRADATION

Refresh Workbook   File Version: 06/07/10 10:24:04

SAMPLE ID:	A1028	SAMPLE DATE:	RECVD. 12-6-10
LOT NUMBER:	U.S. 59	LETTING DATE:	NH 2011(399)
SAMPLE STATUS:	DESIGN	CONTROLLING CSJ:	0063-03-057
COUNTY:	PANOLA	SPEC YEAR:	2004
SAMPLED BY:	MARK DEAN	SPEC ITEM:	341-024
SAMPLE LOCATION:	STOCKPILE	SPECIAL PROVISION:	
MATERIAL CODE:		MIX TYPE:	ITEM341_D_Fine_Surface
MATERIAL NAME:	TYPE "D" HOTMIX WITH 20 % RAP		
PRODUCER:	LONGVIEW ASPHALT INC.	WMA Included in Design?	No
AREA ENGINEER:	JUNEAU	PROJECT MANAGER:	WMA TECHNOLOGY:
COURSE\LIFT:	Surface	STATION:	DIST. FROM CL:	CONTRACTOR DESIGN # : H1104

Recycled Binder, %

Bin No.8 :	0.3
Bin No.9 :	0.6
Bin No.10 :	0.0
Total	0.9

	AGGREGATE BIN FRACTIONS							"RECYCLED MATERIALS"			
	Bin No.1	Bin No.2	Bin No.3	Bin No.4	Bin No.5	Bin No.6	Bin No.7	Bin No.8	Bin No.9	Bin No.10	
Aggregate Source:	Igneous	Igneous	Igneous					Fractionated RAP	Fractionated RAP		Material Type
Aggregate Pit:	Jones Mill	Jones Mill	Jones Mill	GLOVER PIT				LAI AP 10	LAI AP 10		Material Source
Aggregate Number:	0050122	0050122	0050122								RAS Type
Sample ID:	1/2" C.A	3/8" C.A.	SCREENINGS	FIELD SAND				COARSE RAP	FINE RAP		Sample ID

Ratio of Recycled to Total Binder, %

(based on binder percent (%) entered below in this worksheet)

16.8

Recycled Asphalt Binder (%)

										3.2		5.6				**Combined Gradation**		
Hydrated Lime?:										10.0	% of Tot. Mix	9.9	% of Tot. Mix		% of Tot. Mix	Total Bin	Lower & Upper Specification Limits	
Individual Bin (%):	40.0	Percent	12.0	Percent	18.9	Percent	9.0	Percent	Percent	Percent	Percent	10.2	% of Aggreg	9.9	% of Aggreg		% of Aggreg	100.0%	

Sieve Size:	Cum.% Passing	Wtd Cum. %	Cum.% Passing	Wtd Cum. %	Cum.% Passing	Wtd Cum. %	Cum.% Passing	Wtd Cum. %	Cum.% Passing	Wtd Cum. %	Cum.% Passing	Wtd Cum. %	Cum.% Passing	Wtd Cum. %	Cum.% Passing	Wtd Cum. %	Cum.% Passing	Wtd Cum. %	Cum.% Passing	Wtd Cum. %	Cum. % Passing	Lower	Upper	Within Spec's
3/4"	100.0	40.0	100.0	12.0	100.0	18.9	100.0	9.0							100.0	10.2	100.0	9.9			100.0	100.0	100.0	Yes
1/2"	98.0	39.2	100.0	12.0	100.0	18.9	100.0	9.0							98.7	10.1	100.0	9.9			99.1	98.0	100.0	Yes
3/8"	86.3	34.5	100.0	12.0	100.0	18.9	100.0	9.0							89.0	9.1	99.9	9.9			93.4	85.0	100.0	Yes
No. 4	35.4	14.2	45.1	5.4	95.6	18.1	100.0	9.0							31.9	3.3	87.8	8.7			58.6	50.0	70.0	Yes
No. 8	9.3	3.7	14.5	1.7	75.5	14.3	100.0	9.0							20.3	2.1	60.2	6.0			36.8	35.0	46.0	Yes
No. 30	2.4	1.0	4.8	0.6	33.5	6.3	100.0	9.0							15.8	1.6	35.6	3.5			22.0	15.0	29.0	Yes
No. 50	2.0	0.8	3.9	0.5	21.8	4.1	98.9	8.9							14.3	1.5	30.3	3.0			18.7	7.0	20.0	Yes
No. 200	1.5	0.6	2.7	0.3	10.4	2.0	11.8	1.1							5.5	0.6	10.6	1.0			5.6	2.0	7.0	Yes

(Bold Italic) Not within specifications   *(Bold Italic)* Not within specificaitons- Restricted Zone   *(Italic)* Not cumulative

Lift Thickness, in:		Binder Substitution? Yes	Binder Originally Specified: PG 70-22	Substitute Binder: PG 64-22
Asphalt Source: LION PG 64-22		Binder Percent, (%): 5.2	Asphalt Spec. Grav.: 1.030
Antistripping Agent:		Percent, (%):	

Remarks:
Contractor opted to substitute PG 64-22 for PG 70-22 per special provision 341-024
Hamburg weight = 2435 grams

Notes:

Figure A-8. HMA Mix-Design Details for Type D Mix (Atlanta District, US 59).

APPENDIX B: PROPOSED MODIFICATIONS TO THE HWTT AND TEX-242-F TEST PROCEDURE

Test Procedure for

HAMBURG WHEEL TRACKING TEST

TxDOT Designation: Tex-242-F

Effective Date: _____

1.	SCOPE

1.1   Use this test method to determine the premature failure susceptibility of bituminous mixtures due to weakness in the aggregate structure, inadequate binder stiffness, or moisture damage and other factors including inadequate adhesion between the asphalt binder and aggregate. ~~This test method measures the rut depth and number of passes to failure.~~ *This test method measures the rutting susceptibility of bituminous mixtures in terms of the following rutting parameters: rut depth, number of passes to failure, normalized rutting area, and shape factor.*

1.2   The values given in parentheses (if provided) are not standard and may not be exact mathematical conversions. Use each system of units separately. Combining values from the two systems may result in nonconformance with the standard.

2.	APPARATUS

2.1   *Wheel Tracking Device,* an electrically powered device capable of moving a steel wheel with a diameter of 8 in. (203.6 mm) and width of 1.85 in. (47 mm) over a test specimen.

2.1.1   The load applied by the wheel is 158 ± 5 lb. (705 ± 22 N).

2.1.2   The wheel must reciprocate over the test specimen, with the position varying sinusoidally over time.

2.1.3   The wheel must be capable of making 50 ± 2 passes across the test specimen per minute. **Note 1**— *For mixes to be used in slow vehicle-speed areas such as intersections, urban city roads, etc., testing at lower and/or multiple HWTT wheel speeds should be considered as a supplement to the 50 ± 2 passes/minute, i.e., from 50 to as low as 35 passes/minute. In order to facilitate this, the HWTT wheel should have capabilities to run at wheel speeds ranging from 35 to 50 passes per minute.*

2.1.4   The maximum speed of the wheel must be approximately 1.1 ft./sec. (0.305 m/s) and will be reached at the midpoint of the slab.

2.2   *Temperature Control System,* a water bath capable of controlling the test temperature within $\pm 4°F$ (2°C) over a range of 77–158°F (25–70°C).

2.2.1	This water bath must have a mechanical circulating system to stabilize temperature within the specimen tank.
2.3	*Rut Depth Measurement System,* a Linear Variable Differential Transducer (LVDT) device capable of measuring the rut depth induced by the steel wheel within 0.0004 in. (0.01 mm), over a minimum range of 0.8 in. (20 mm).
2.3.1	The system should be mounted, to measure the rut depth at the midpoint of the wheel's path on the slab.
2.3.2	Take rut depth measurements at least every 100 passes of the wheel.
2.3.3	This system must be capable of measuring the rut depth without stopping the wheel. Reference this measurement to the number of wheel passes.
2.3.4	Fully automated data acquisition and test control system (computer included).
2.4	*Wheel Pass Counter,* a non-contacting solenoid that counts each wheel pass over the test specimen.
2.4.1	Couple the signal from this counter to the rut depth measurement, allowing the rut depth to be expressed as a fraction of the wheel passes.
2.5	*Specimen Mounting System,* a stainless steel tray that can be mounted rigidly to the machine in the water bath.
2.5.1	This mounting must restrict shifting of the specimen during testing.
2.5.2	The system must suspend the specimen, allowing free circulation of the water bath on all sides.
2.5.3	The mounting system must provide a minimum of 0.79 in. (2 cm) of free circulating water on all sides of the sample.

3. MATERIALS

| 3.1	*Three high-density polyethylene (HDPE) molds,* shaped according to plan view in Figure 2 to secure circular, cylindrical test specimens. Use one mold for cutting the specimen and the other two for performing the test.
3.2	*Capping compound,* able to withstand 890 N (200 lb.) load without cracking.

4. SPECIMEN

| 4.1 | *Laboratory Molded Specimen*—Prepare specimens in accordance with Tex-205-F and Tex-241-F. Specimen diameter must be 6 in. (150 mm), and specimen height must be 2.5 ± 0.1 in. (63.5 ± 2.5 mm).
Note 2— *For consistency, test all specimens within 5 days of molding.* |

Note 3—Mixtures modified with warm-mix asphalt additives or processes must be oven cured at 275°F for a maximum of 4 hours before molding.
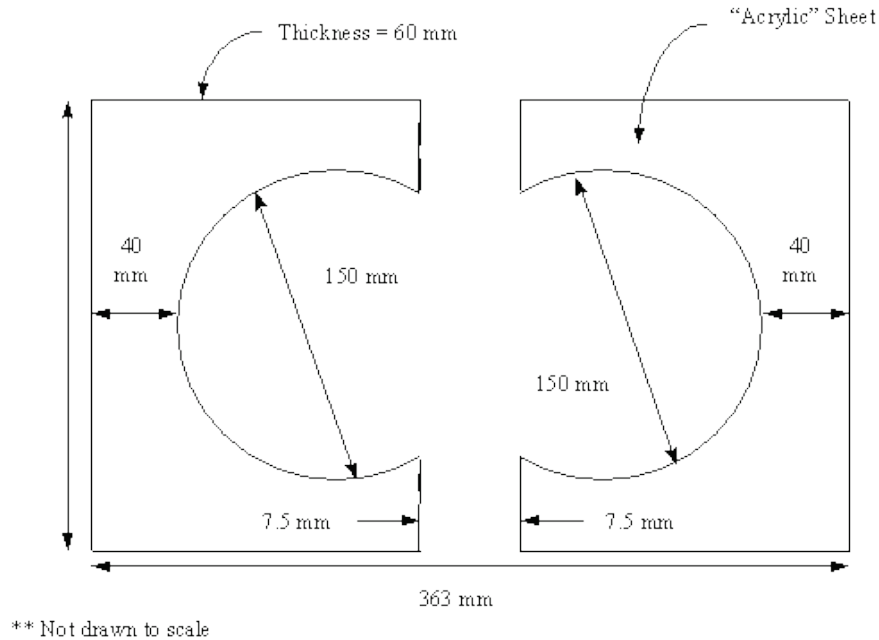
4.1.1   Density of test specimens must be 93 ± 1%.

Note 4—Mixture weights for specimens prepared in the laboratory typically vary between 2400 and 2600 g to achieve density due to different aggregate sources and mix types. *If necessary, a 'pre-molding' procedure should be conducted to systematically achieve the desired specimen density (93 ± 1%) for the laboratory-molded samples. The 'pre-molding' procedure consists of molding at least three specimens, each with a different target density varied roughly between 87% and 92%, and evaluating the resulting specimen densities for each. A "target density" versus "obtained specimen density" curve is drawn to determine the 'Optimum Molding Density' that will yield the desired specimen density (93 ± 1%); see Figure 1 below.*
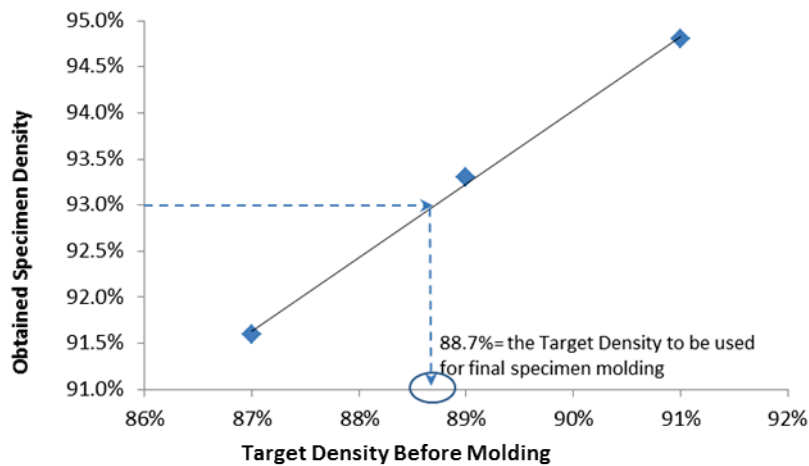
Figure 1 Pre-molding procedure: Obtained specimen density vs. target density before molding

4.2   *Core Specimen*—Specimen diameter must be 6 ± 0.1 in. (150 ± 2 mm). There is not a specific density requirement for core specimens.

Figure 2—Top View of Test Specimen Configuration for the Hamburg Wheel Tracking Device

---

5. PROCEDURE

5.1   Use two cylindrically molded specimens meeting the requirements of Section 4.

5.2   Measure the relative density of specimens in accordance with Tex-207-F and Tex-227-F.

5.3   Place a specimen in the cutting template mold and use masonry saw to cut it along the edge of the mold.

5.3.1   The cut across the specimen should be approximately 5/8 in. (16 mm) deep.

5.3.2   Cut the specimen to the dimensions shown in Figure 2 in order to fit in the molds required for performing the test.

5.4   For specimens 6 in. (150 mm) in diameter:

■   Place the HDPE molds into the mounting tray and fit specimens into each one.

■   Secure the molds into the mounting tray.

Note 5— Do not use the HDPE molds for core specimens greater than 6 in. (152 mm) in diameter.

Note 6— *Keep track of the top and bottom of the specimen according to the direction of sample compaction or trafficking in the case of field cores. Always place the specimen in the HWTT machine such that the top surface of the specimen is in contact with the wheel (i.e., direction of loading is parallel to the direction of sample compaction).*

5.5   For specimens greater than 6 in. (150 mm) in diameter:

■   Mix capping compound.

- ■ Spray the mounting tray with a light lubricant.
- ■ Place specimen in the middle of the mounting tray.
- ■ Spread the capping compound around the core specimen until level with the surface.
- ■ Allow the capping compound to dry for a minimum of 24 hours.

5.6   Fasten the mounting trays into the empty water bath.

5.7   Start the software supplied with the machine, and 'enter' the required test information into the computer.

Note 7— *For mixes to be used in slow vehicle-speed areas such as intersections, urban city roads, etc., testing at lower and/or multiple HWTT wheel speeds should be considered as a supplement to the 50 ± 2 passes/minute, i.e., from 50 to as low as 35 passes/minute. For these special slow vehicle-speed areas, any or all of the following HWTT wheel speeds can be considered: 50, 45, 40, and/or 35 passes /minute.*

5.8   Test temperature should be $122 ± 2°F$ $(50 ± 1°C)$ for all hot mix asphalt specimens.

Note 8— *For mixes to be placed in high temperature areas, high shear stress locations, and 'urban stop-go environments' (near intersections), test the samples at multiple HWTT temperatures, i.e., 50 °C, 55 °C, 60 °C, and report the test results for all tested temperatures.*

5.8.1   Fill the water bath until the water temperature is at the desired test temperature.

5.8.2   Monitor the temperature of the water on the computer screen.

5.8.3   Saturate the test specimen in the water for an additional 30 minutes once reaching the desired water temperature.

5.9   Start the test after the test specimens have been in the water for 30 minutes at the desired test temperature. The testing device automatically stops the test when the device applies the number of desired passes or when reaching the maximum allowable rut depth.

---

6.   CALCULATIONS

6.1   *From the HWTT machine, save and extract the 'Rut depth versus number of passes' data for calculation of HWTT rutting parameters.*

6.2   *Measure and record the following parameters from the 'Rut depth versus number of passes' response:*

- ▪ *Maximum Rut Depth Rut_{max} = Rutting after 20,000 load passes or 12.5 mm (whichever is smaller)*
- ▪ *Failure Cycles, N_d = Number of load passes to reach 12.5 mm rutting or 20,000 (whichever is smaller)*
- ▪ *Δ_A = Area under the Rut depth versus number of passes (Figure 3)*

Note 9— *Rut_{max} and N_d are the traditional HWTT parameters and can be obtained directly from the machine.*

Note 10— *The Area under the Rut depth versus number of passes,* Δ_A *, is calculated using the trapezoidal formula by dividing the area into **n** number of trapezoids*

$$\Delta_A = \frac{N_d}{2n}\left[f(x_o) + 2f(x_1) + 2f(x_2) + \ldots + 2f(x_{n-1}) + f(x_n)\right]$$

where, $f(x_i)$ *and* $f(x_{i+1})$ *are rut depth values at the left and right end of each trapezoid, respectively.*
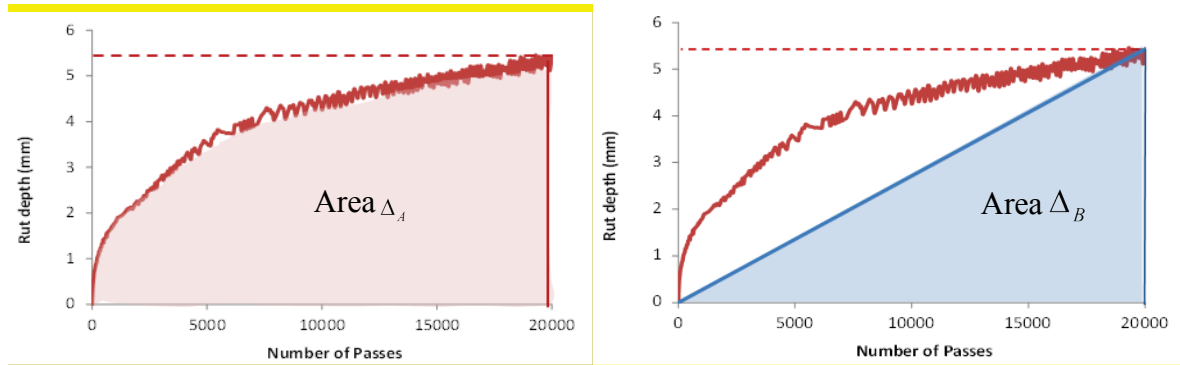
Figure 3— *HWTT Rut depth versus number of load passes curve*

6.3   *Calculate the 'Normalized Rutting Area (* Rut_Δ *)':*

$$Rut_\Delta = \frac{Area\,under\,'Rutting'\,curve}{N_d} = \frac{\Delta_A}{N_d}$$

Note 11— *the 'Normalized Rutting Area (* Rut_Δ *)' parameter accounts for the rutting path-history of the sample. Higher* Rut_Δ *indicates poor rut resistance.*

6.4   *Calculate the 'Shape Factor (SF)'*

$$SF = \frac{Area\,under\,'Rutting'\,curve}{Area\,under\,a\,triangular\,curve} = \frac{\Delta_A}{0.5 \times N_d \times Rut_{max}} = \frac{\Delta_A}{\Delta_B}$$

Note 12— *the 'Shape Factor (SF)' parameter indicates the shape of the rutting curve. SF > 1.25 indicates a convex rutting curve, which is less desirable for high temperature areas, high shear stress locations, and urban stop-go sections in terms of the early rutting life of the HMA mix.*

SF ≤ 1.25 indicates a concave rutting curve, which is more desirable for high temperature areas, high shear stress locations, and urban stop-go sections, particularly in terms of the early rutting life of the HMA mix.

7.   REPORT

7.1   *Report the following for each specimen:*

- *Trimmed specimen density,*
- *Anti-stripping additive used,*

154

- *Test temperature,*
- *Maximum Rut Depth, Rut_{max} ,*
- *Failure Cycles, N_d ,*
- *Normalized Rutting Area, Rut_Δ , and*
- *Shape Factor , SF.*

8.   ARCHIVED VERSIONS

8.1   Archived versions are available.

Test Procedure for

THE SIMPLE PUNCHING SHEAR TEST (SPST)

TxDOT Designation: Tex-2XX-F

Effective Date:

1.	**SCOPE**

1.1   This test method determines the shear properties of the compacted bituminous mixtures. The measurable and calculable shear parameters include: shear strength, shear strain, shear modulus, shear strain energy, and shear strain energy index.

1.2   The values given in parentheses (if provided) are not standard and may not be exact mathematical conversions. Use each system of units separately. Combining values from the two systems may result in nonconformance with the standard.


2.	**APPARATUS**

2.1   *Loading Press,* capable of applying a compressive load at a controlled deformation mode at the rate of 0.2 mm per second. Additionally, the device will include a controlled temperature chamber capable of maintaining a temperature of up to 60°C.

2.2   *Loading Head,* consisting of a 1.5 in. diameter cylindrical metal head to be attached to the loading shaft of the *Loading Press* (Figure 1).

2.3   *Loading Base,* consisting of a 6.0 in. diameter cylindrical metal base with a 2.5 in. diameter concentric opening. The height of the *Loading Base* is at least 2.5 in. to allow enough space for accommodating the dislodged parts of the HMA (Figure 1).

2.4   *Sample Confinement,* consisting of a cylindrical enclosure able to provide lateral confining pressure of about 20 psi to the sample (Figure 2).
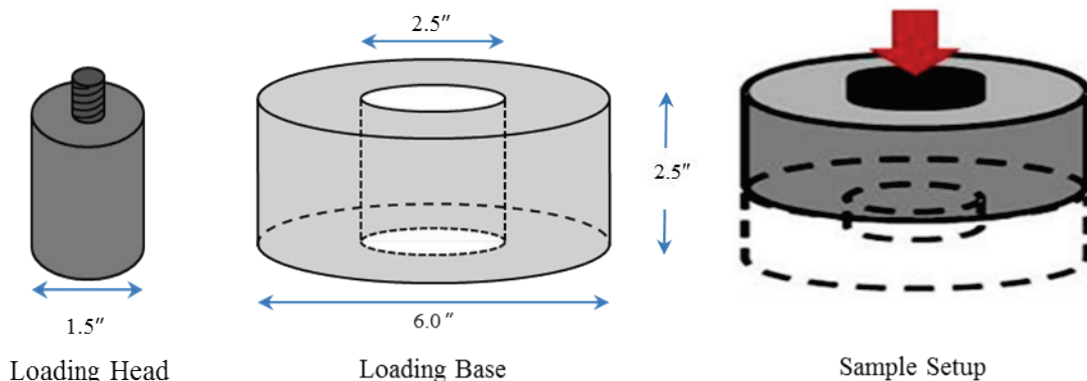
Figure 1.   Loading head, loading base, and schematic diagram of sample setup
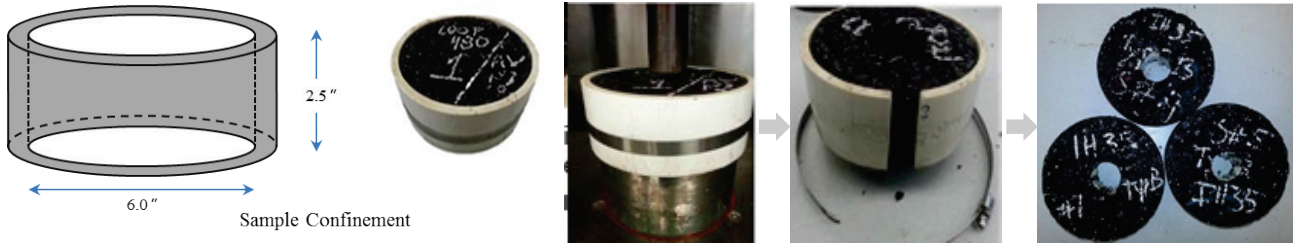
Figure 2. SPST sample confinement: schematic diagram and pictorial illustration.

2.5 *Torque Wrench,* with a torque capacity of 25 in-lb and appropriate socket drive handle.
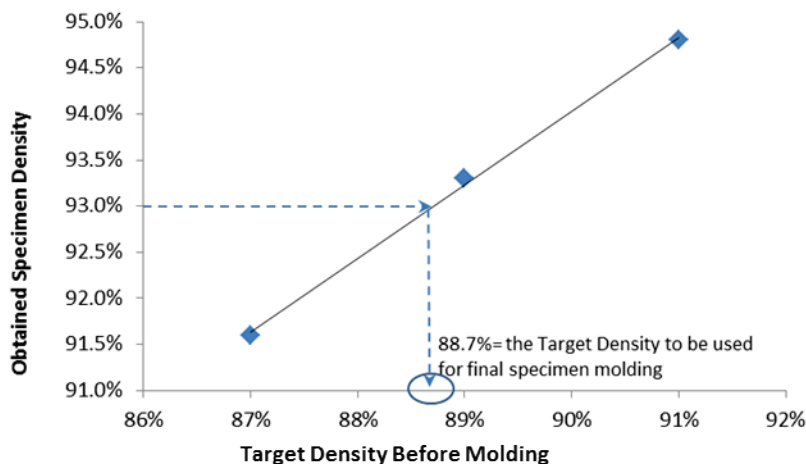
3. SPECIMENS

3.1 *Laboratory-Molded Specimens*—prepare three specimens in accordance with Tex-241-F. Specimen diameter must be 6 in. (150 mm), and height must be 2.5 ± 0.1 in. (63.5 ± 2.5 mm). For consistency, test all specimens within 5 days of molding.

3.1.1 Select curing temperature and time for WMA mixtures according to binder grade, recycled materials, and target discharge temperature. Refer to Tex-241-F to mold WMA specimens.

Note 1—Cure warm-mix asphalt (WMA) mixtures at 275°F for 4 hr. ± 5 min. before molding. WMA is defined as HMA that is produced within a target temperature discharge range of 215°F and 275°F using WMA additives or processes.

3.1.2 Density of the test specimen must be 93 ± 1%, except for Permeable Friction Course (PFC) mixtures.

Note 2— Mixture weights for specimens prepared in the laboratory typically vary between 2400 and 2600 g to achieve density due to different aggregate sources and mix types. If needed, a 'pre-molding' procedure is recommended for systematically achieving the desired specimen density (93 ± 1%) for the laboratory-molded specimens. The 'pre-molding' procedure consists of molding at least three specimens, each with a different target density varied roughly between 87% and 92%, and evaluating the resulting specimen densities for each. A "*target density*" versus "*obtained specimen density*" curve is drawn to determine the "Optimum Molding Density" that will yield the desired HMA specimen density (93 ± 1%); see Figure 3.

Figure 3 Pre-molding procedure: Obtained specimen density vs target density before molding

3.1.3   For PFC mixtures, mold test specimens to 50 gyrations (N_{design}).

Note 3— Select the mixture weight for the molded PFC specimens based on the weights used in the mix design.

3.2   *Core Specimens*—Specimen diameter must be 6 ± 0.1 in. (150 ± 2 mm), and height must be a minimum of 1.5 in. (38 mm). There is not a specific density requirement for core specimens.

---

4.   PROCEDURE

4.1   For laboratory-produced mixtures, proceed to Section 4.2. For plant-produced mixtures, proceed to Section 4.3. For roadway cores, proceed to Section 4.4.

4.2   *Laboratory-Produced Mixtures:*

4.2.1   Combine aggregates and prepare laboratory mixture as described in Tex-205-F.

4.2.2   Mold three specimens in accordance with Tex-241-F with the Superpave Gyratory Compactor (SGC).

4.2.3   Proceed to Section 4.4.

4.3   *Plant-Produced Mixtures:*

4.3.1   Sample the plant mixture in accordance with Tex-222-F.

4.3.2   Mold three specimens in accordance Tex-241-F with the Superpave Gyratory Compactor.

4.3.3   Proceed to Section 4.4.

4.4   Record the density, height, and diameter of each laboratory or plant-produced specimen or roadway core.

4.5   Place the specimens or cores, along with the testing apparatus (*loading head, loading base, sample confinement*), in the controlled temperature chamber long enough to ensure a consistent temperature of $50 \pm 1°C$ throughout.

Note 4— For mixes to be placed in high temperature areas, high shear stress locations, and 'urban stop-go environments' (near intersections), test the samples at multiple temperatures, i.e., 50°C, 55°C, 60°C, and report the test results for all tested temperatures.

4.6   Calibrate the loading press to utilize a deformation rate of 0.2 mm per second.

4.7   Attach the *Sample Confinement* to the specimen.

4.8   Carefully place the confined specimen on the *Loading Base*. Make sure the *Loading Base* and the specimen are concentrically placed below the *Loading Head.* (Figure 4)

Note 5— Keep track of the top and bottom of the specimen according to the direction of sample compaction or trafficking in the case of field cores. Always place the specimen on the *Loading Base* such that the top surface of the specimen is in contact with the *Loading Head* (i.e., direction of loading is parallel to the direction of sample compaction).

SPST Specimen Setup

**Figure 4.** SPST specimen setup: schematic diagram and pictorial illustration

4.9 Slowly lower the *Loading Head* into light contact with the specimen.

4.10 Apply the load at a controlled deformation rate of 0.2 mm per second. Capture and save the complete load versus deformation (L-D) response curve for subsequent data analysis.

---

5. CALCULATIONS

5.1 Measure and record the following parameters from the load-displacement response:

- Peak (failure) shear load, P_{max}
- Failure shear deformation at peak load, $D_{P_{max}}$
- Area under the shear load-displacement (L-D) response curve = $\int f(x)\,dx$
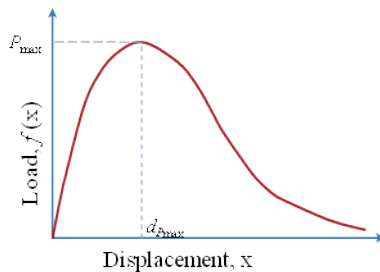
Note 6— The Area under the shear load-displacement (L-D) response curve, $\int f(x)\,dx$ is calculated using the trapezoidal formula by dividing the area into **n** number of trapezoids

$$\Delta_A = \frac{d_{max}}{2n}\left[f(x_o)+2f(x_1)+2f(x_2)+...+2f(x_{n-1})+f(x_n)\right]$$

where, d_{max} is the maximum recorded displacement and

$f(x_i)$ and $f(x_{i+1})$ are load values $\left[f(x)\right]$ at the left and right end, respectively, of each trapezoid.

5.2 Calculate the HMA shear strength:

$$\tau_s = \frac{P_{max}}{A} = \frac{P_{max}}{\pi D t}$$

where, D = Diameter of the punching (loading) head = 1.0 inch

t = Thickness of the sample

5.3   Calculate the HMA failure shear strain at peak load:

$$\gamma_s = \frac{d_{P_{max}}}{t}$$

5.4   Calculate the HMA shear modulus:

$$G_s = \frac{\tau_s}{\gamma_s} = \frac{P_{max}}{\pi D \left(d_{P_{max}} \right)}$$

5.5   Calculate the shear strain energy as the area under the L-D response curve:

$$SSE = \frac{1}{A} \int_o^\infty f(x)\, dx = \frac{1}{\pi D t} \int_o^\infty f(x)\, dx$$

5.5   Calculate the SSE Index:

$$10^3 \times SSE \frac{\gamma_s}{t\tau_s}$$

Note 7— HMA mixes with $\tau_s \geq 300\ psi$ and/or $SSE \geq 25\ kJ/m^2$ at 50°C SPST temperature have preliminarily exhibited good correlation with computational model simulations and field data. If testing at 60°C, the following should tentatively be considered as a preliminary guidance for screening mixes: $\tau_s \geq 200\ psi$, and $SSE \geq 17\ kJ/m^2$.

---

6.   REPORT

6.1   Report the following for each specimen:

- Trimmed specimen density,
- Peak shear (failure) load,
- Failure shear deformation at peak load,
- HMA shear strength,
- HMA failure shear strain at peak load,
- HMA shear modulus,
- Shear strain energy,
- Shear strain energy Index, and
- Additional comments.

---

7.   ARCHIVED VERSIONS

7.1   Archived versions are available.